SIGNALING MECHANISMS FOR GENE REGULATION BY METALS AND METAL MIXTURES

by

Antonia A. Nemec

B.S., Lebanon Valley College, 2002

Submitted to the Graduate Faculty of

the Graduate School of Public Health in partial fulfillment

of the requirements for the degree of

Doctor of Philosophy

University of Pittsburgh

2009

UNIVERSITY OF PITTSBURGH

GRADUATE SCHOOL OF PUBLIC HEALTH

This dissertation was presented

by

Antonia A. Nemec

It was defended on

April 24th, 2009

and approved by

Chairperson: Bruce R. Pitt, Ph.D., Professor, Department of Environmental and Occupational Health, Graduate School of Public Health, University of Pittsburgh

George D. Leikauf, Ph.D., Professor, Department of Environmental and Occupational Health, Graduate School of Public Health, University of Pittsburgh

Patricia L. Opresko, Ph.D., Assistant Professor, Department of Environmental and Occupational Health, Graduate School of Public Health, University of Pittsburgh

Thomas E. Smithgall, Ph.D., Professor, Department of Microbiology and Molecular Genetics, School of Medicine, University of Pittsburgh

Dissertation Advisor: Aaron Barchowsky, Ph.D., Associate Professor, Department of Environmental and Occupational Health, Graduate School of Public Health, University of Pittsburgh

SIGNALING MECHANISMS FOR GENE REGULATION BY METALS AND METAL MIXTURES

Antonia A. Nemec, Ph.D.

University of Pittsburgh, 2009

Numerous epidemiological studies associate chronic inhalation of metal mixtures with increased risk of pulmonary diseases. Although exposure to metal mixtures is of great public health relevance, the integration of cellular responses to metals within these mixtures that promote disease is poorly understood. This dissertation investigated the hypothesis that chromium (VI) (Cr(VI)) stimulates signaling that alters transcriptional complexes to silence protective gene induction by nickel (Ni). In airway epithelial (BEAS-2B) cells, Cr(VI) activated signal transducer and activator of transcription 1 (STAT1)-dependent signaling within 1 h of exposure. This activation was dependent on Src family kinases (SFKs) since inhibiting SFKs prevented Cr(VI)-stimulated STAT1 signaling. Moreover, Cr(VI) activated STAT1 in wild-type mouse embryonic fibroblast (MEF) cells, but no response was observed in MEF cells null for the SFKs, Src, Yes, and Fyn. However, reconstituting human Fyn in the deficient MEF cells restored the Cr(VI) response. These data indicate that Cr(VI)-activated STAT1 is mediated by Fyn. This signaling may be detrimental as STAT1 has been implicated as an inflammatory mediator in asthma patients that is specifically activated in bronchial epithelial cells (1). Metallothionein (MT) and vascular endothelial growth factor A (VEGFA) are involved in protecting the lung from injury by sequestering metals and promoting wound repair, respectively. Ni-induced *MT2A*, the most abundant human isoform, required zinc (Zn) redistribution which directly

activated metal transcription factor-1 (MTF-1). A prolonged induction was mediated by secondary signaling pathways. Cr(VI) negatively regulated the secondary pathway and had no effect on Zn mobilization. For *VEGFA* induction, Ni activated a complex signaling cascade involving ERK. Ni-stimulated ERK was upstream of hypoxia-inducible factor-1α (HIF-1α) and Src-mediated Sp1 transactivation. Cr(VI) inhibited Ni-activated ERK, HIF-1α stabilization, Src phosphorylation, and *VEGFA* induction. The current study demonstrated that Cr(VI)-activated STAT1 is responsible for the silencing of inducible genes. In BEAS-2B cells stably expressing STAT1 shRNA, Cr(VI) no longer had an inhibitory effect on Ni-induced MT or VEGFA mRNA expression and positively interacted with Ni to induce both genes. These data indicate that Cr(VI)-activated STAT1 may play a role in the pathogenesis of Cr(VI)-induced pulmonary diseases by silencing the protective gene transcription in the airway epithelium.

TABLE OF CONTENTS

LIST OF TABLES

LIST OF FIGURES

ACKNOWLEDGEMENTS

I would first like to thank Dr. Aaron Barchowsky for his unwavering guidance and support through my graduate studies. His door was always open and he was eager to give encouragement when unexpected and unwanted results were realized. I will forever be grateful to the mentorship he provided.

I would like to thank my committee members Drs. George Leikauf, Bruce Pitt, Patty Opresko, and Tom Smithgall for their support, suggestions, and criticisms that have helped to make me a better scientist.

I would like to thank my father Michael Nemec for always encouraging me, insisting that I could do whatever I put my mind to, and never allowing me to quit anything because it was getting too difficult. I dedicate my thesis to him. I also thank my sister, Desiree Nemec, and brother, Daryl Muromoto, for pretending to understand what I do.

I thank the past and current members of the Barchowsky laboratory especially Dr. Kimberley O'Hara. Kim trained and mentored me as a technician and I am most indebted to her for choosing to attend graduate school. I also thank Adam Straub and Linda Klei for their technical support. I would also like to thank all the people in the department of Environmental and Occupational Health and all the friends I have made along the way and who have supported me over the years.

I lastly wish to thank my boyfriend, Robert Tomko, Jr. As a chemist, he was always eager to draw me a mechanism of how some chemical functioned (even though I never asked nor cared). As a friend and boyfriend, he always listened as I told him I was never going to graduate because an experiment failed or a paper got rejected. None of this work would have been accomplished without his daily support.

ABBREVIATIONS

A549	human lung carcinoma cell line
AA	ascorbic acid
ALI	acute lung injury
ARDS	acute respiratory distress syndrome
BEAS-2B	human bronchial epithelial cell line
Cd	cadmium
Cr	chromium
Csk	c-Src kinase
DMSO	dimethylsulfoxide
ERK	extracellular signal-regulated kinase
FBS	fetal bovine serum
GAS	gamma interferon activation site
GFP	green fluorescent protein
HBSS	Hank's buffered saline solution
HDAC	histone deacetylase
HIF-1α	hypoxia-inducible factor 1α
HRE	hypoxic response element
IFN	interferon
IFNAR	interferon α/β receptor
IRF	interferon regulatory factor
ISGF3	interferon-stimulated growth factor 3
ISRE	interferon-stimulated response element
JAK	Janus kinase
JNK	cJun N-terminal kinase
LPS	lipopolysaccharide
Keap1	Kelch-like ECH-associated protein 1
MAPK	mitogen-activated protein kinase
MEF	mouse embryonic fibroblast
MRE	metal response element
MT	Metallothionein
MTF-1	metal transcription factor-1
NAC	N-acetyl-L-cysteine
NaB	sodium butyrate
Ni	nickel
NPL	national priority list
Nrf2	nuclear E2 related factor 2

NRTK	non-receptor tyrosine kinase
PAH	polycyclic aromatic hydrocarbon
PHD	prolyl hydroxylase domain
PI3K	phosphoinositide 3-kinase
PKC	protein kinase C
PlGF	placenta growth factor
PP	protein phosphatase
PTK	protein tyrosine kinase
ROS	reactive oxygen species
RPL13A	ribosomal protein L13A
RPTK	receptor protein tyrosine kinase
SFK	Src family kinase
SH	Src homology domain
STAT	signal transducer and activator of transcription
SYF	MEF cells null for Src, Yes, and Fyn
TPEN	*N*,*N*,*N*',*N*'-Tetrakis(2-pyridylmethyl)ethylenediamine
UV	ultraviolet
VEGF	vascular endothelial growth factor
VHL	von-Hippel Lindau
VPF	vascular permeability factor
Zn	zinc

1.0 INTRODUCTION

1.1 CHROMIUM OVERVIEW

Chromium (Cr) is the 21st most abundant metal and the 24th element on the periodic table (2). Cr is naturally occurring in the environment and is found in rocks, animals, plants, and the soil (3,4). It is a transition metal existing predominantly in three valence states: Cr(VI), Cr(III), Cr(0) (reviewed in (5)). Cr(0) is typically present in its metallic form and is oxidized to Cr(III) and Cr(VI) during processes such as welding (6). Cr(III) is a nutrient that regulates insulin and cholesterol homeostasis through altering membrane trafficking (7,8). Cr(VI) exists as a chromate oxyanion under physiological conditions and, unlike Cr(III), can readily enter the cell through sulfate and phosphate anion channels due to its structural similarity to these anions (5,9). Once Cr(VI) enters the cell, greater than 90% is reduced by ascorbate or glutathione to Cr(III) within one hour (9,10). Cr(VI) is reduced through a series of one electron reductions generating Cr(V) and Cr(IV) intermediates. Cr(VI) can also be reduced to Cr(IV) through a two electron reduction when high levels of reducing agents are present (5) (Figure 1). Cr(III) is the final oxidized form of Cr found in all biological systems (6). Cr(VI) itself is not reactive, but Cr(III) and the short-lived intermediates produced through the reduction reaction can directly bind to proteins and DNA causing deleterious effects (10-12). Reactive oxygen species (ROS) are also

produced during the reduction of Cr(VI) and can react with macromolecules to cause adverse effects (5).

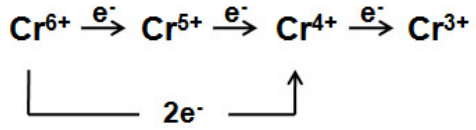

Figure 1. Reduction reaction of Cr(VI).

Reprinted from Mutation Research Volume 533. O'Brien, T. J., Ceryak, S., and Patierno, S. R. Compexities of chromium carcinogenesis: role of cellular response, repair, and recovery mechanisms, 3-36: 2003 with permission from Elsevier.

1.1.1 Sources of Chromium

Cr was initially discovered in Siberia in the 1700s as lead chromate and was used as a pigment (2). Natural sources of Cr include continental dust flux and volcanic dust. However, most of the Cr found in the environment is a result of its industrial use. Cr(VI) is primarily found as chromates or dichromates generated by oxidizing chromite in molten alkali followed by extraction into water and acidification (3). Due to its chemical properties, Cr(VI) is widely used in industries (2) with the main applications of use including metallurgical applications, chemical manufacturing, and refractory processes (2). Chromates are used in various industries including textiles, tanning, dyeing, welding, chrome manufacturing, and wood preservation (3,4) (Figure 2).

Combustion of coal and oil and Cr processing industries accounts for most of the Cr emitted into the atmosphere (13). Cr deposited in lakes and rivers eventually settles into sediments (13). Because of the widespread use of Cr, it is present in over half of the National Priority List (NPL) waste sites (Figures 3-4) (3,4,13).

Use	1996 Western world	1996 United States	1951 United States
Wood preservation	15%	52%	2%
Leather tanning	40%	13%	20%
Metals finishing	17%	13%	25%
Pigments	15%	12%	35%
Refractory	3%	3%	1%
Other	10%	7%	17%

Souce: Barnhart 1997

Figure 2. Historical uses of Cr in the United States and the western world.

1.1.2 Human Exposures

Several million people worldwide are estimated to be exposed to Cr or Cr-containing compounds (6). Exposure to Cr most commonly occurs through inhalation, ingestion, or dermal contact although inhalation of Cr poses the greatest risk. Environmental exposure to Cr arises from urban particulate matter and exhaust, proximity to industrial sites and toxic waste sites (6), from cigarette smoke, and as a soil and water contaminant (13). In the United States, Cr is found in soil at an average of 40 ppm (2). Cr concentrations in fresh water range from 1 to 10 ppb (14). The concentration of Cr in the air ranges from 0.001 to 0.01 $\mu g/m^3$, but urban areas have higher levels with an estimated concentration of 0.03 $\mu g/m^3$ (13). Exposure to high levels of Cr is more likely in the occupational setting, specifically for workers in the stainless steel welding, chromate production, chrome plating, ferrochrome industry, chrome pigments industries (13). Depending on the industry, exposures can be higher than 100 mg/m^3 (5). Occupational exposures of Cr(VI) are of greater concern than Cr(III) since Cr(VI) readily enters the epithelial cells lining the

respiratory tract (11,13). Exposure to Cr can be monitored in blood, urine, hair, and nails, but it is difficult to differentiate between species of Cr (13).

The guidelines set by the environmental protection agency (EPA) for safe levels of Cr(VI) in the drinking water are 100 µg/L per day. The Occupational Safety and Health Administration (OSHA) set a legal limit of 0.005 mg/m^3 in the air for a 8 hour workday, 40 hour workweek for Cr(VI) (13).

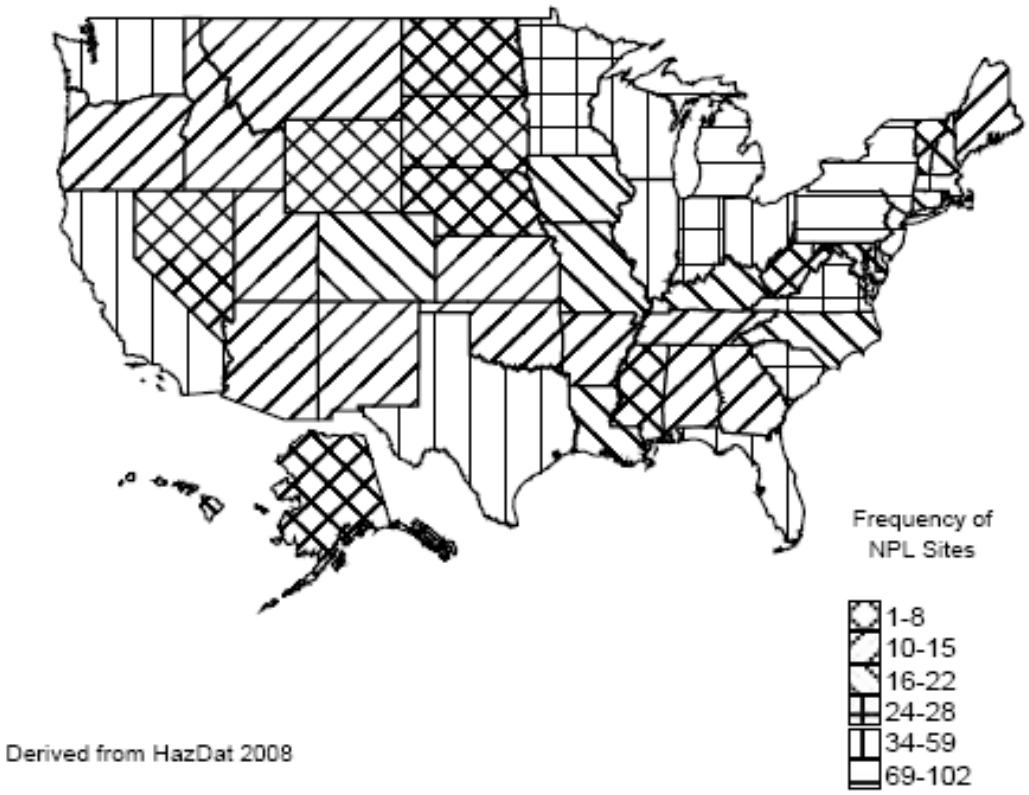

Figure 3. Frequency of NPL sites with Cr contamination.

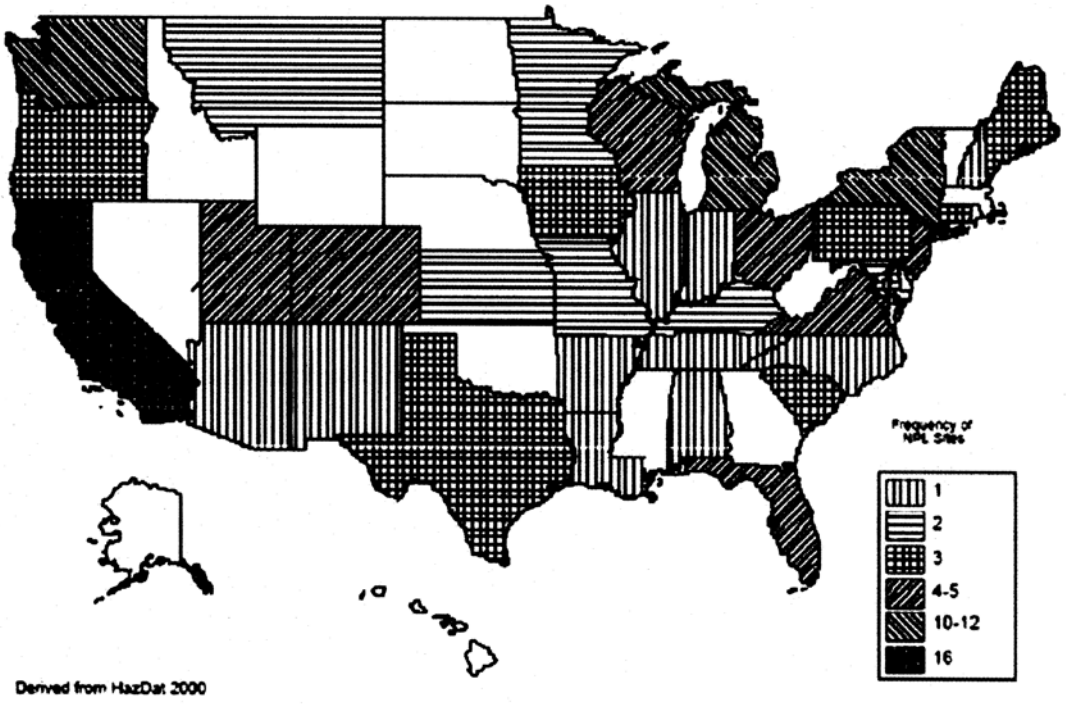

Figure 4. Frequency of NPL sites with Cr(VI) contamination.

1.1.3 Adverse Health Effects

The primary route of Cr(VI) exposure is through inhalation. Due to the rapid reduction of Cr(VI) to Cr(III), the main target of Cr(VI) exposure is the respiratory tract and airway epithelium (11). Exposure to Cr(VI) results in airway irritation, airway obstruction, and lung cancer (13). Chronic inhalation of chromate dust leads to chronic irritation of the airway, polyps of the upper respiratory tract, emphysema, and chronic bronchitis (13). Pulmonary sensitization has also been reported to result in an asthmatic response (13). However, the severity of the disease state varies greatly and depends on the dose, length of exposure, and Cr species (5).

1.1.4 Cr(VI) Effects on Gene Expression

Cr(VI) rarely affects constitutive gene expression (15,16) but differentially affects inducible genes *in vivo* and *in vitro* (16-19). The traditional view for how Cr(VI) inhibits inducible gene expression is through genotoxic mechanisms. Exposure to Cr(VI) causes DNA damage including formation of DNA adducts, single strand breaks, DNA-protein cross-links and DNA interstrand crosslinks (5,20). The type of damage is dependent upon the Cr species generated from Cr(VI) metabolism (Figure 5). Cr(III), the short-lived and unstable Cr(IV) and Cr(V) intermediates, and ROS produced through the reduction reaction are all highly reactive with DNA (5). Cr(V) and Cr(IV) can catalyze ROS through Fenton-like reactions with hydrogen peroxide (21). The role of ROS in the deleterious effects of Cr(VI) remains controversial. The amount of ROS produced depend largely on the concentrations of Cr(VI) used. Low level, non-cytotoxic concentrations of Cr(VI) produce detectable amounts of ROS, however, it is not required for Cr(VI) effects on cell

signaling (22). Exposure to Cr(VI) may result in the direct binding to the chromatin which is exists in a more open state in inducible genes compared to constitutive gene (16,17). Moreover, exposure to Cr(VI) also suppresses RNA synthesis likely by creating lesions in GC-rich regions of DNA that prevents RNA polymerase from elongating the nascent RNA chain (5).

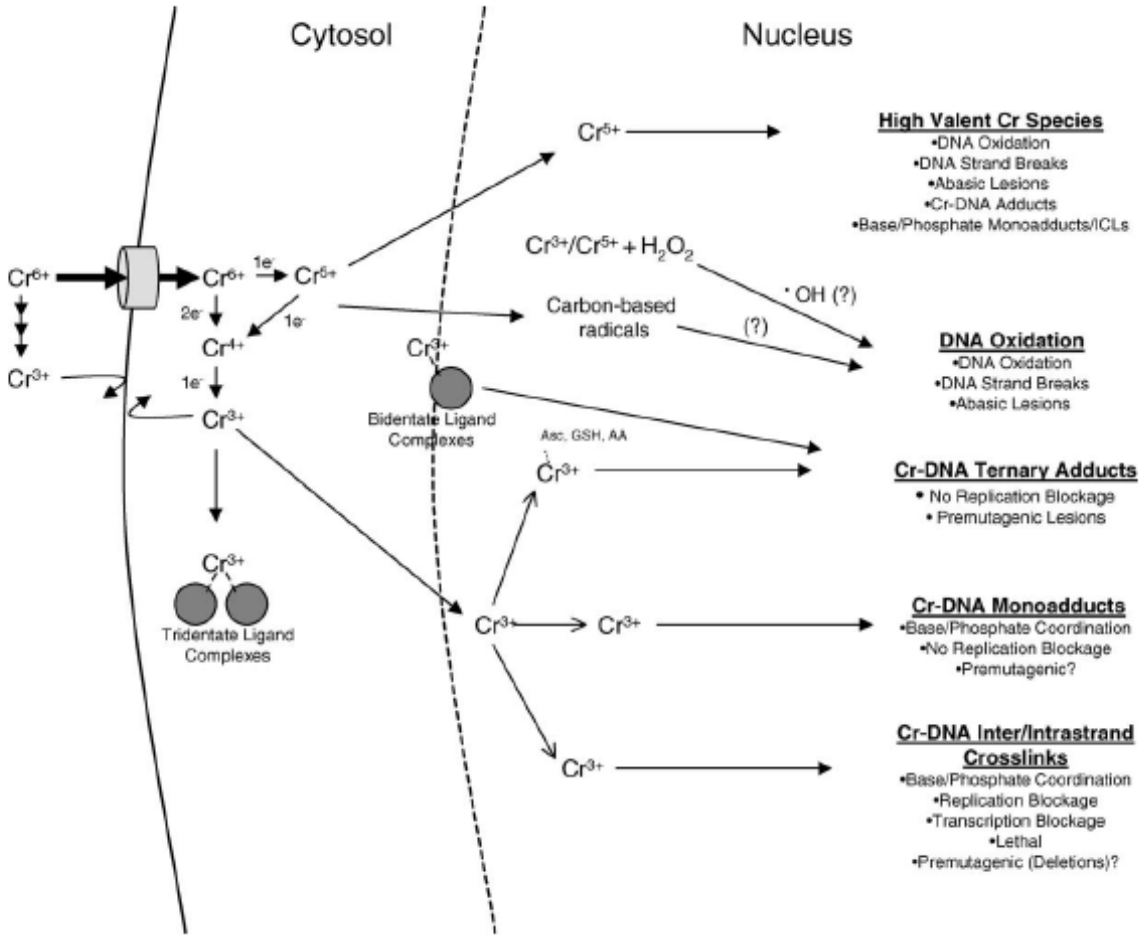

Figure 5. Major pathways involved in the formation of genetic lesions by Cr.

Schematic illustrates the interrelationships between Cr metabolism and genotoxicity (5).

Reprinted from Mutation Research Volume 533. O'Brien, T. J., Ceryak, S., and Patierno, S. R. Compexities of chromium carcinogenesis: role of cellular response, repair, and recovery mechanisms, 3-36: 2003 with permission from Elsevier.

However, there is emerging evidence indicating epigenetic mechanisms by which Cr(VI) alters transcriptional activation and complex formation (19,23-25). Our laboratory has demonstrated that Cr(VI) inhibits basal and arsenic-stimulated heme oxygenase 1, a key cytoprotective gene, *in vivo* and *in vitro* (19) through the sequestering the critical transcription factor, nuclear E2 related factor 2 (Nrf2), in the cytosol. In its inactive state, Nrf2 remains bound to kelch-like ECH-associated protein 1 (Keap1) in the cytosol and Cr(VI) may prevent the release of Nrf2 from this complex. Cr(VI) prevents zinc (Zn)- and cadmium (Cd)-induced metallothionein (MT) expression by disrupting the essential transcription factor, metal transcription factor-1 (MTF-1), from binding to the *MT* promoter (23). Although the precise mechanism in not known, Cr(VI) interferes with the recruitment RNA polymerase II to the *MT* promoter (25). TNFα-induction of *IL-8* is prevented by preincubation with Cr(VI) which inhibits the interaction between NF-κB and co-activators (26). Cr(VI) silences polycyclic aromatic hydrocarbon (PAH)-induced gene expression by preventing the liberation of histone deacetylase 1 (HDAC1) from the promoters, thereby interfering with the recruitment of co-activators (24). Interestingly, this effect was not gene-specific; instead having a global effect on PAH-induced genes (24). Together these studies reveal a possible mechanism that Cr(VI) may activate cell signaling to repress gene expression since the repression is not specific to the stimulus or the gene endpoint. Furthermore, the negative regulation of gene induction by Cr(VI) occurs independent of cell type as these effects are found in airway epithelial cells and type II cells, as well as other non-lung cell types. Cr(VI) also induces numerous stress responses including cell cycle arrest, DNA damage, and apoptosis (5,27-29) that may play a role in repressing gene expression.

1.2 NICKEL OVERVIEW

Nickel (Ni) is a naturally occurring metal; the 24th most abundant element. Ni is widely used in industry due to its resistance to corrosion and heat, strength, and conductivity (30). Although Ni can be found in several oxidation states, Ni(II) is the most prevalent species (30). Ni compounds are separated into two groups based on their solubility in water. Ni carbonates ($NiCO_3$), sulfides (Ni_3S_2), and oxides (NiO) are insoluble; Ni chlorides ($NiCl_2$), sulfates ($NiSO_4$), and nitrates ($Ni(NO_3)_2$) are soluble. Soluble Ni readily enters the cell through calcium and magnesium channels and the similarity in structure to these essential metals and other divalent cations may contribute to Ni toxicity (30,31). Since Ni sulfate is the major species found in the ambient air (32), it is the species used in this thesis research.

1.2.1 Sources of Ni

The majority of Ni mining occurs in Canada and Russia. Most Ni is combined with other metals such as Cr, copper (Cu), cobalt (Co), iron (Fe), and Zn to manufacture alloys because of its corrosion and heat resistance, hardness, and strength (Table 1) (30). Ni is also used to produce jewelry, coins, and in nickel plating and manufacturing (6). Nil salts are used in electroplating, ceramics, pigments, and as catalysts (30). Although the Ni from these industries is released into the air, Ni is also found in industrial waste waters and in the soil and sediments (30). Currently, Ni is found in over half of the NPL waste sites (Figure 6) (30). In the United States, a large portion of Ni is released into the atmosphere primarily from coal and oil combustion and from industries that make or use Ni or Ni-containing compounds.

Table 1. Ni consumption by use in 2002.

Use	Percentage
Stainless and heat-resistant steel	61%
Ni-Cu and Cu-Ni alloys	4%
Other Ni alloys	13%
Electroplating	6%
Superalloys	9%
Other	7%

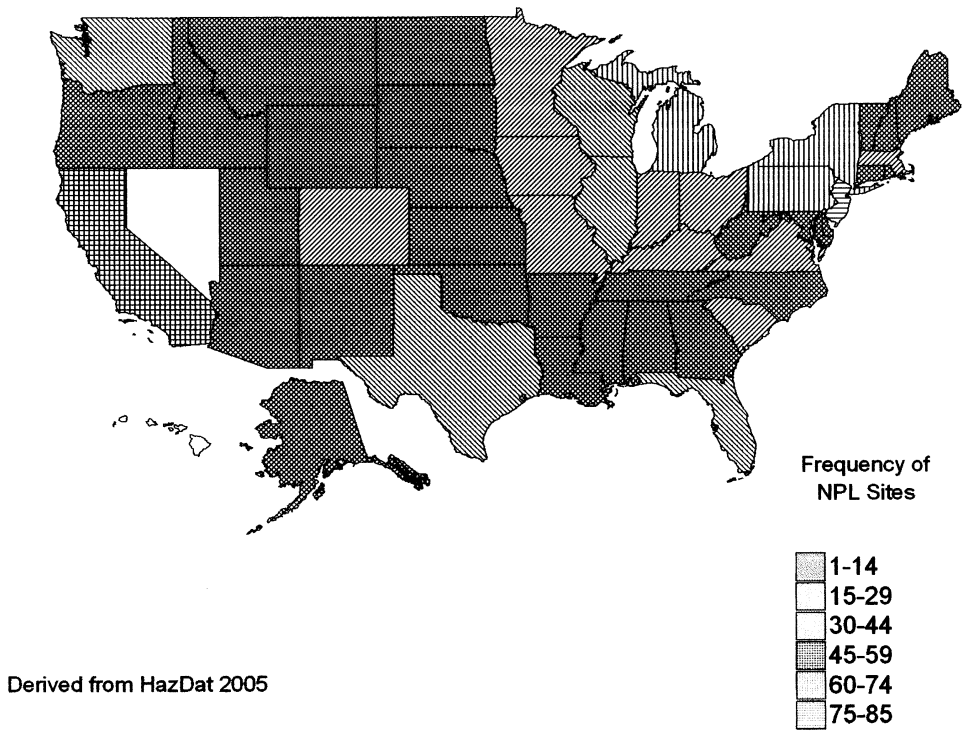

Figure 6. Frequency of NPL sites with Ni contamination.

1.2.2 Human Exposures

Ni is a main component of air pollution (33,34), cigarette smoke (35), diesel exhaust (36), and welding fumes (37,38). The major route of exposure is through inhalation, but Ni can also be ingested from contaminated water and food, and through skin contact (30,32). The guidelines set by the EPA for safe levels of Ni in the drinking water are 0.1 mg/L per day. OSHA set a legal limit of 1.0 mg/m^3 for a 8 hour workday, 40 hour workweek for Ni (30). However, the EPA estimates the average Ni concentration is 2.2 ng/m^3 in ambient air and 2-4.3 ppb in water (30). Exposures are greater to workers in Ni industries that result from breathing Ni-containing fumes (30) and levels in Ni refineries have been estimated at 1-5 mg/m^3 for soluble Ni (32). The amount of Ni found in ambient air is variable with the highest concentrations found near Ni industries and in urban areas (39) and absorption of Ni depends on the route of exposure (Table 2) (32). Despite the route of exposure, Ni is excreted in urine (30).

Table 2. Levels of daily Ni intake by humans from different types/routes of exposure.

Type/Route of Exposure	Daily Ni Intake (µg)	Absorption
Foodstuffs	<300	<15%
Drinking water	<20	<15%
Ambient air (urban dweller)	<0.8	50%
Ambient air (smoker)	<23	50%

1.2.3 Adverse Health Effects

Chronic inhalation of soluble Ni causes non-cancer pulmonary diseases; whereas insoluble Ni is more carcinogenic due to it prolonged retention in the lung (6). 50% of Ni is retained in lungs and the respiratory tract is a major target organ (Table 2) (30,32). High levels of Ni were found in the urine of automobile spot welders and this exposure was associated with pulmonary diseases including airway irritation (38). Ni can cause inappropriate immune responses (40,41), asthma (42,43), acute lung injury (ALI) (37,44,45), and cardiopulmonary diseases (33,38). However, the pathogenesis of these diseases remains unknown. Also, chronic dermal contact with Ni results in hypoallergic responsiveness with 10-20% of the country's population being sensitive to nickel (30).

1.3 MIXED EXPOSURES

Cr(VI) and Ni are found together in over half of the NPL waste sites. Exposures to these metals often occur in industries (e.g. electroplating and stainless steel welding) and are also components of coal and oil combustion. Epidemiological studies associate exposure to metal mixtures with exacerbated pulmonary diseases. A metal plating worker exposed to Cr and Ni experienced airway reactivity and developed asthma (46). In a study from Japan, lung tissues were analyzed to determine if metals correlated to emphysema. It was concluded that the detected levels of Cr, Ni, and lead represented environmental exposures that increased with age and the severity of emphysema (47). Workers who were chronically exposed to Cr(VI) and Ni fumes from electroplating developed asthma. Bronchial challenge tests revealed that the fumes from these

metals are a significant cause of occupational asthma (42). A case-controlled study in Taiwan examined the metal concentrations in lung tumors to determine if the metals, either independently or through the production of ROS, contributed to tumorigenesis (48). A significant increase in Cr and Ni levels were observed in lung tumors compared to non-cancer controls suggesting that exposure to these metals may contribute to lung cancer (48). Painters using a high-temperature spray paint were diagnosed with interstitial pneumonia caused by inhalation of nickel and chrome fumes (49). Although these studies reveal that exposures to metal mixtures are common and may increase the risk of pulmonary diseases, little is known about the mechanisms of the individual metals or how they can possibly interact to promote diseases.

1.4 STAT FAMILY OF TRANSCRIPTION FACTORS

Signal transducers and activators of transcription (STAT) are a family of latent cytoplasmic transcription factors. There are seven members (STATs 1, 2, 3, 4, 5A, 5B, and 6) that all contain a N-terminal domain, coiled-coil domain, DNA binding domain, a linker domain, Src homology 2 (SH2) domain, and a C-terminal transactivation domain (Figure 7) (51). The conserved N-terminal domain and coiled-coil domain facilitate protein interactions with non-STAT proteins such as co-activators or other transcription factors (50).

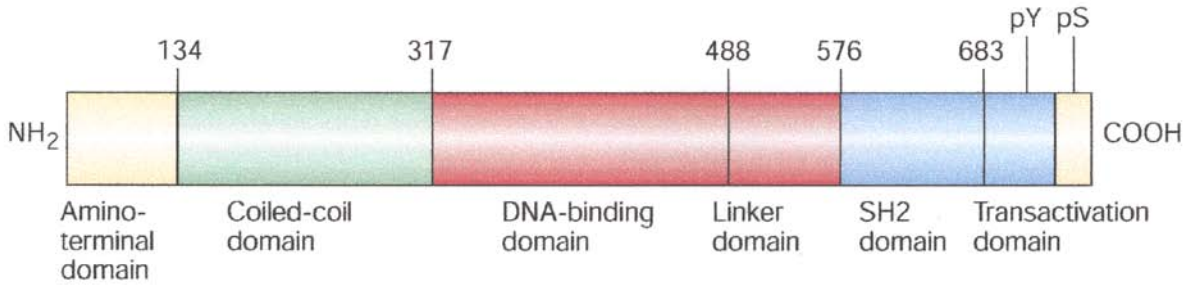

Figure 7. Structure of STAT proteins.

Reprinted with permission from Macmillian Publishers Ltd: Nat. Rev. Mol Cell Biol 3, 651-662, 2002.

Extracellular stimuli or cytokines interact with cell surface receptors or non-receptor tyrosine kinases that activate the STATs through phosphorylation on a conserved tyrosine residue located in the C-terminus. The SH2 domain regulates the tyrosine phosphorylation of the STATs and also promotes STAT dimerization and translocation into the nucleus to initiate gene expression (52). The Janus kinase (JAK) protein tyrosine kinase family was initially identified as the critical kinases in the activation of the STATs (53). However, STATs can be directly activated by receptors with intrinsic kinase activity or indirectly through the recruitment of non-receptor tyrosine kinases (NRTKs). The NRTKs include the Src family kinases (SFKs) which can initiate the STAT signaling pathway (Figure 8) (51,54-56). Although there is great homology between the family members, the STAT proteins are selectively activated by various stimuli resulting in diverse biological effects (52).

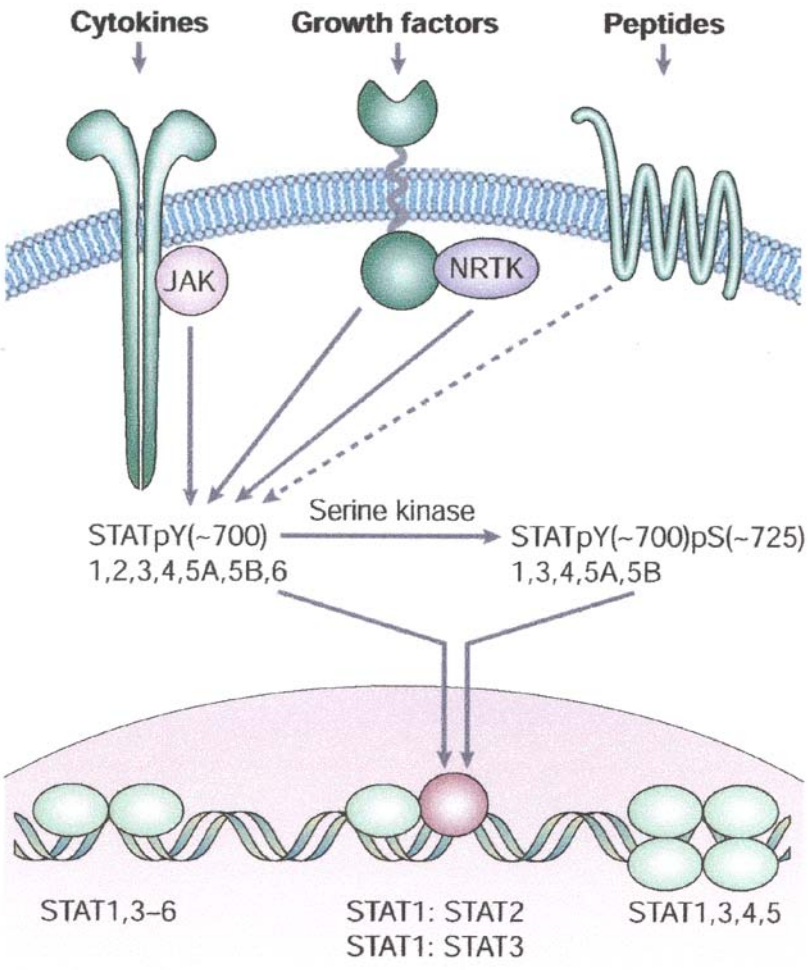

Figure 8. Mechanisms of STAT signaling.

Reprinted with permission from Macmillian Publishers Ltd: Nat. Rev. Mol Cell Biol 3, 651-662, 2002.

1.4.1 STAT1

STAT1 was the first of the STAT proteins discovered. It was originally identified as a downstream effector of type I interferon (IFN) (e.g. IFN-α) and type II IFN (e.g. IFN-γ) stimulation (57). Through deletional and mutational analysis, the DNA sequences responsible for IFN-α and IFN-γ transcription were identified as interferon-stimulated response element (ISRE) and IFN-γ activation site (GAS), respectively (reviewed in (57)). Type I IFNs bind to the interferon α/β receptor (IFNAR), stimulating STAT1 and STAT2 tyrosine phosphorylation and subsequent dimerization. A heterotrimeric complex, interferon-stimulated gene factor 3 (ISGF3), is formed after interferon regulatory factor 9 (IRF9) binds the STAT1/STAT2 heterodimer. Following the translocation of this complex to the nucleus, it binds to ISRE elements to drive transcription of certain genes (e.g. IRF7). The interaction of STAT1 and STAT2 with IRF9 is required for optimal binding to the ISRE (52,58). Type I IFNs can also activate STAT1 homodimers which bind to GAS elements to transactivate GAS-driven genes (e.g. IRF1). In contrast, type II IFNs can only induce STAT1 homodimers (reviewed in (59)). Type I IFN-stimulated gene transcription also requires HDAC1 to interact with both STAT1 and STAT2 (60). HDAC activity does not affect the activation of STAT1 or 2, the dimerization, or the nuclear translocation of the ISGF3 complex. Instead, HDAC recruits RNA polymerase II to the promoter to initiate transcription of ISRE-driven genes (60,61).

Recently, the ISGF3 complex has emerged as having an important role in mediating cellular responses. All three protein components of this complex are required for the inhibition of *MMP9* (62) and *IL-8* (63) induced by IFN-β. Surprisingly, this inhibition does not occur through direct binding to the promoter of these genes, nor does it affect the activation of

upstream proteins in the signaling pathway (62,63). Instead, this complex interferes with the recruitment of transcription factors and co-activators to the promoter through an unknown mechanism (62). The activation of ISGF3 may induce other proteins that directly interfere with these inducible genes or that there is competition with co-activators (e.g. CBP/p300) that may prevent the gene induction (62).

1.4.2 Pathophysiological Role of STAT1

STAT pathways can be activated in response to exogenous stresses (64-66) including metals (55). STAT1 is required to induce antiviral and antiproliferative responses (67,68). It promotes apoptosis in cardiac myocytes after ischemia and reperfusion by inducing pro-apoptotic genes (64). It can also interact with and increase the transcriptional activity of p53 (64,69). Moreover, STAT1 has been implicated in the pathogenesis of lung diseases (70) where it is selectively activated in the airway epithelial cells of asthmatic patients leading to the transcription the STAT1-dependent genes (1). STAT1 activation is independent of IFN and this inflammatory process was specific to STAT1 and not other inflammatory transcription factors (e.g. NF-κB). These data suggest that inappropriate STAT1 signaling contributes to the development of pulmonary inflammatory diseases (1). Moreover, aberrant expression of STAT1 in the airway may be a precursor to disease.

1.5 SRC FAMILY KINASES

Src family kinases (SFK) are cytoplasmic NRTKs involved in diverse biological functions including cell proliferation, migration, differentiation, and survival (71). There are 11 known members of which 8 are well-characterized (72). Src, Yes, and Fyn are ubiquitously expressed, while the other family members are more cell-type specific (71). These kinases contain 6 functional domains, as depicted in Figure 9 (71). The SH4 domain is responsible for lipid modification that is aided by a myristoylation at the glycine at position 2. Palmitoylation can occur in this domain, as well (73). These modifications are required to recruit the SFK to the cellular membrane. The SH4 domain is followed by a unique domain. This domain, although its function remains unclear, is proposed to be responsible for interactions or signaling that is specific to each family member. The SH3 domain is composed of 50 amino acids that bind to proline-rich residues and is essential for negative regulation of catalytic activity, localization, and substrate recruitment (71). The SH2 domain also regulates the catalytic activity and localization of SFK through phosphotyrosine-containing sequences.

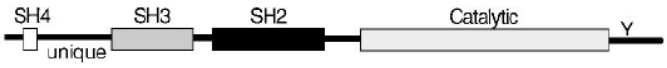

Figure 9. Structure of SFKs.

Reprinted, with permission, from the *Annual Review of Cell and Developmental Biology*, Volume 13 © 1997 by Annual Reviews www.annualreviews.org .

The SH2 and SH3 domains regulate the kinase activity of SFKs. As shown in Figure 10 (71), there is an inhibitory tyrosine residue 527 in the C-terminal tail that is phosphorylated by

C-terminal Src kinase (Csk). The SH2 domain interacts with this residue to inhibit SFK kinase activity (71). The SH3 domain binds with sequences in the catalytic domain and linker region thereby connecting the SH2 and catalytic domains (73). These interactions keep the kinase in a closed and inactive conformation. SFKs are activated by the dephosphorylation of tyrosine 527 by a protein tyrosine phosphatase, followed by the autophosphorylation of tyrosine 416 located in the C-lobe of the catalytic domain and the disruption of the interactions between the SH2 and SH3 domains. Once activated, SFKs facilitate downstream signaling by transferring the phosphate to substrate proteins (71).

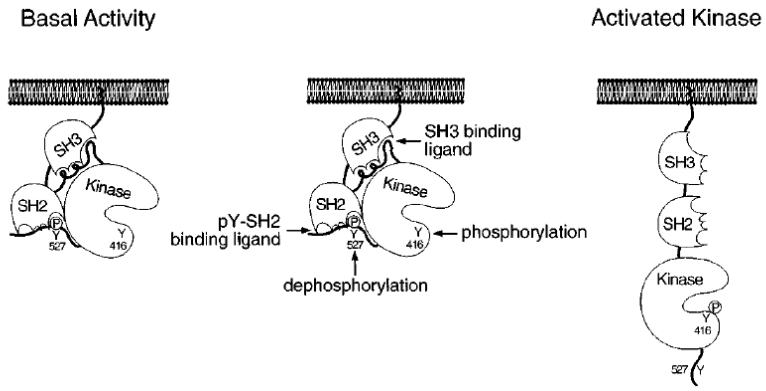

Figure 10. Conformations of SFKs.

Reprinted, with permission, from the *Annual Review of Cell and Developmental Biology*, Volume 13 © 1997 by Annual Reviews www.annualreviews.org .

SFKs can be activated through interactions with receptors (e.g. G protein-coupled receptors (GPCRs) or receptor protein tyrosine kinases (RPTK)), ligand activation of these receptors, or by stress responses (71). Metals, including Ni, Cd, arsenic, and cobalt have been shown *in vitro* to directly bind to the C-lobe of the catalytic domain of protein tyrosine kinases (PTKs) (74). Only PTKs containing cysteines in the C-lobe (e.g. Src, Fyn) are conformationally changed in response to incubation with metals (74). Cr(VI) directly activated Fyn *in vitro* and incubation of A549 cells with Cr(VI) activated Fyn and Lck, but had no, or even an inhibitory,

effect on Src and Yes (22). This activation did not require ROS production. However, increasing the thiol pool in the cells through the addition of *N*-acetyl-*L*-cysteine (NAC) prevented Cr(VI) activation of SFKs suggesting that Cr(VI) directly binds to the thiol containing regulatory domain of SFKs (22).

1.6 PROTECTIVE MECHANISMS IN THE LUNG

1.6.1 METALLOTHIONEIN

Metallothioneins (MT) are low molecular weight, highly conserved, intracellular proteins. There are 4 isoforms of mouse MT: MT1-4; and 10 functional isoforms of human MT including multiple isoforms of MT1 (reviewed in (75,76)). MT1 and MT2 are the most commonly expressed in mammals with *MT2A* being the most abundantly expressed gene isoform in human tissues (75). MT3 is expressed mostly in the brain (77) and MT4 is only detected in certain tissues, specifically the squamous epithelium (78).

The main function of MT is maintaining metal homeostasis. Due to the unique thiol-rich structure of MT, it is able to sequester heavy metals and plays an important role in protecting the cells from heavy metal toxicities and in maintaining Zn homeostasis (76,79,80). MT is induced by and can bind 18 different metals, including Ni (81,82). The cysteine residues of MT can interact with up to 7 divalent or 14 monovalent metals per molecule with varying affinities (76). MT can also be induced by inflammatory mediators (83) and environmental insults such as ROS, nitric oxide, and ultraviolet light (UV) (76,84).

1.6.1.1 MT Expression in the lung

Tissue expression of MT is the highest in the liver, pancreas, kidney, and intestine (76), but is also expressed in the lung. MT levels are dramatically increased in the lungs of mice exposed to Ni (82), diesel exhaust particles and lipopolysaccharide (LPS) (85), during hyperoxia (86), and during inflammation (87). Furthermore, the role of MT in protecting the lung from various stressors was elucidated by utilizing *Mt*-transgenic mice that express two times the basal MT protein expression in the lung and *Mt1/2*$^{(-/-)}$ mice that are null for Mt1 and Mt2. Compared to wild-type mice, *Mt1/2*$^{(-/-)}$ mice exposed to Ni had increased inflammation, permeability, and death (44). Other studies demonstrated that *Mt1/2*$^{(-/-)}$ mice had increased inflammatory cell recruitment, cytokine expression, and oxidative damage induced by an antigen-related inflammation model (87). Furthermore, the *MT*-transgenic mice are resistant to Ni- (44) and Cd- (75) induced injury. MT was also protective against LPS-induced injury by enhancing pulmonary integrity and scavenging free radicals (83). Overall, these studies support the notion that MT plays a crucial role in protecting the lung against damage and promoting survival.

1.6.1.2 Mechanisms of MT induction

MT is primarily transcriptionally regulated (75). The *MT* promoter contains numerous *cis* elements, but the main transcription factor involved in its induction is MTF-1. MTF-1 contains six zinc fingers of the C_2H_2-type, is highly conserved, and ubiquitously expressed in the cytosol. MTF-1 is required for embryogenesis, since mice lacking MTF-1 die *in utero* from liver degeneration (88). The embryonic lethality is not a result of the lack of MT transcription, as *Mt1/2*$^{(-/-)}$ mice are viable. MTF-1 regulates other genes included enzymes needed for glutathione biosynthesis that may be essential for liver function and cell proliferation (88). The embryonic

fibroblasts isolated from these mice are more sensitive to metal and free radical-induced insults (88).

MTF-1 acts like an intracellular Zn sensor and rapidly translocates to the nucleus upon activation to bind metal response elements (MRE) and initiate gene transcription (89,90). MTF-1 is required for both basal and metal-induced MT (90). Although there are many agents known to induce MT, the mechanism of its induction is only known for Zn. Zn directly and reversibly binds to MTF-1 leading to its activation (90). Large concentrations of Cd are able to activate MTF-1, but this is not from Cd activating MTF-1 directly. Instead, this may be through the redistribution of Zn (89). It is likely that other transition metals stimulate MT through indirect mechanisms (91). The activation of upstream kinases, such as c-Jun-N-terminal kinase (JNK) and protein kinase C (PKC), can phosphorylate and activate MTF-1 (90-92). MTF-1 also cooperates with other transcription factors, such as hypoxia-inducible factor-1 α (HIF-1α) (93,94) and Sp1 (95,96), that may affect MT expression.

1.6.2 Vascular endothelial growth factor A

The vascular endothelial growth factor (VEGF) family contains five members in mammals: VEGFA, B, C, D, and placenta growth factor (PLGF). These proteins are secreted, mitogenic, glycoproteins. The expression of each family member is tissue-specific and dependent on the stimulating factor (reviewed in (97)). VEGFA is the predominant and most studied family member. VEGFA was initially named vascular permeability factor (VPF) as it was discovered for its role in the induction vascular permeability (97). VEGFA is alternatively spliced producing six isoforms, 121, 145, 165, 183, 189, and 206, which only differ by the presence or absence of exons 6 and 7 (98). $VEGFA_{121}$, $VEGFA_{165}$, and $VEGFA_{183}$ are preferentially

expressed whereas $VEGFA_{145}$ and $VEGFA_{206}$ are rare isoforms (98). $VEGFA_{165}$ is the most abundant and will be referred to simply as VEGF or VEGFA throughout this dissertation.

1.6.2.1 VEGFA expression in the lung

VEGFA is most abundantly expressed in the lung, kidney, and spleen. VEGFA is important for lung development (99) and deletion of a single allele in a mouse model is embryonic lethal (97). There is an intricate balance of expression of VEGFA required for normal lung development; overexpression of VEGFA in a transgenic mouse model disrupts lung morphogenesis and causes inappropriate vessel development (100). However, less is known of its role in the airway epithelium and lung injury repair. The bronchial epithelial cells and alveolar epithelial cells are the major source of VEGFA in the lung (99,101) and it is necessary for airway cell proliferation (102). In specific lung-targeted VEGFA knockout mice, an emphysema-like phenotype is observed (103). VEGFA is elevated in patients with inflammatory pulmonary diseases, such as asthma, chronic bronchitis (104,105), ALI, and acute respiratory distress syndrome (ARDS) (105,106). It is decreased in patients developing bronchopulmonary dysplasia (107), in emphysema (105), and during ischemia and reperfusion (108). Furthermore, VEGFA overexpression protects against pulmonary hypertension in rats (109) and during hyperoxia in mice overexpressing IL-13 (106).

It is hypothesized that the varying levels of VEGFA during lung injury (ALI or ARDS) are due, in part, to the different stages of the disease process (106). When the injury initially occurs, the epithelial cells and certain inflammatory cells (e.g. neutrophils and macrophages) secrete VEGFA. The high levels of VEGFA cross the endothelial barrier and increase permeability of endothelium to promote edema, leading to epithelial cell damage and death. The loss of epithelial cells leads to a decrease in VEGFA secretion. However, as the epithelial cells

recover, VEGFA can be secreted to promote angiogenesis and lung repair (106,110,111). This hypothesis is substantiated by the observation that decreased VEGFA protein observed during ischemia and reperfusion is associated with epithelial cell damage (108). Furthermore, VEGFA secreted by bronchial epithelial cells promotes endothelial repair in the lung (112) and promotes wound repair while preventing apoptosis (113). Also, increasing VEGFA levels is associated with the resolution of ARDS (114) and is upregulated during the wound healing *in vivo* (115).

1.6.2.2 Mechanisms of VEGFA induction

HIF-1α is the major stimulus for *VEGFA* induction. HIF-1α is a heterodimeric basic-helix-loop-helix-PAS transcription factor (116). The main inducer of HIF-1α is molecular oxygen (117). In the presence of oxygen, prolyl hydroxylases post-transcriptionally modify HIF-1α leading to its interaction with the von-Hippel Lindau (VHL) complex. The VHL complex mediates the ubiquination of HIF-1α. In the absence of oxygen, prolyl hydroxylases cannot modify HIF-1α and it is stabilized. Once stabilized, HIF-1α can translocate into the nucleus and bind to hypoxia-responsive elements (HRE) and activate transcription of its target genes (116). Metals, including Ni, stabilize and transactivate HIF-1α in the presence of oxygen (118-121); although the exact mechanism remains unknown. It may result from a direct inhibitory effect on the prolyl hydroxylases marking the protein for degradation (122). The prolyl hydroxylases contain an iron moiety that Ni has been predicted to displace (122) resulting in the inactivation of the enzyme.

VEGFA expression and HIF-1α stabilization have been shown to be upregulated through the activation of kinases including SFKs, phosphoinositide 3-kinases (PI3K), and mitogen-activated protein kinases (MAPKs) (118,120,121,123). Also, HIF-1α cooperates with other transcription factors (e.g. Sp1, activator protein 1 (AP-1), STAT3) to induce *VEGFA* (124-126);

although there is evidence of HIF-1α-independent mechanisms of *VEGFA* induction (127,128). Furthermore, phosphorylation of Sp1 is required for full induction of *VEGFA* (129,130). Sp1 is one of 4 members of zinc finger transcription factors, is widely expressed, and binds to GC motifs in promoters producing broad and diverse biological responses (131). Sp1 has three major functions: DNA binding, promoter activation, and protein-protein interactions. There are 5 different phosphorylation sites (Ser59, Ser131, Thr453, Thr579, and Thr739) that contribute to the function and activity of Sp1. The two serine sites and Thr453 are located in the transactivation domains in the N terminus and are involved in promoter activation. Phosphorylation of Thr579 has been correlated with DNA binding and Thr739 is important for facilitating protein interactions (131). Sp1 is phosphorylated by various kinases including ERK, cyclin-dependent kinases, and DNA-PK. ERK has been implicated in the phosphorylation of Thr453 and Thr739 resulting in decreased activation of the *VEGFA* promoter (131). The phosphorylation of Sp1 conveys both positive and negative effects on the regulation of the target genes. The dephosphorylation of Sp1 through the activation of the serine/threonine phosphatases, protein phosphatases 1 and 2A (PP1 and PP2), also has a crucial role in Sp1-dependent gene induction. Thus, activation of both kinases and phosphatases can regulate Sp1-dependent *VEGFA* induction.

1.7 STATEMENT OF THE PROBLEM AND HYPOTHESIS

Cr(VI) and Ni are well-established environmental and occupational hazards that are often found together in industry and in over half of the NPL toxic waste sites. Chronic exposure to each metal alone promotes pulmonary diseases. However, it is likely that humans are exposed to

metal mixtures. Epidemiological studies have associated exposure to metal mixtures to increased risk and exacerbated pulmonary diseases and *in vivo* studies in rats have shown that exposure to welding fumes particles containing a complex of Cr and Ni represses lung defense mechanisms (132-134). However, there are few studies that have addressed how metals may interact to worsen these diseases.

Cr(VI) silences inducible gene expression *in vivo* and *in vitro* (19,24) without affecting constitutive gene expression (15,24). While the canonical belief is that Cr(VI) affects the inducibility of gene expression by directly binding to the chromatin in the promoter region, recent evidence suggest that Cr(VI) exerts epigenetic effects to silence gene induction by altering transcriptional complexes (19,23,24). Cr(VI) activates select SFKs directly, leading to the phosphorylation of downstream effectors including members of the STAT family (22,55). STAT1 is the primary regulator of antiproliferative and apoptotic effects in response to IFNs (135,136) and also opposes other transcription factors capable of promoting protective and repair responses, such as HIF-1α, Sp1, and STAT3 (62,137,138).

The objective of this research was to investigate the potential mechanisms for Cr(VI)-induced pulmonary disease by defining how Cr(VI) alters transcriptional activity to repress gene expression. The central hypothesis is that Cr(VI) activates STAT1-dependent signaling to silence protective gene induction by Ni in human airway epithelial cells. Thus, the specific aims of this dissertation were to 1) probe the upstream kinases mediating Cr(VI)-activated STAT1, 2) identify the mechanism for Ni induction of the protective genes, *MT and VEGFA*, 3) determine the effect of Cr(VI)-stimulated STAT1 on Ni-induced *MT and VEGFA*. Identifying these molecular mechanisms will advance the understanding of the pathogenesis of Cr(VI)-related

diseases and elucidate how signaling pathways induced by metals may interact to worsen pulmonary diseases.

2.0 MATERIALS AND METHODS

2.1 CELL CULTURE

2.1.1 BEAS-2B Cells

Human bronchial epithelial cells (BEAS-2B) (ATCC, Manassas, VA) and the stable BEAS-2B cell lines expressing random negative control (shNC) or STAT1 (shSTAT1) shRNA were cultured on a matrix of 0.01 mg/ml of human fibronectin (Invitrogen, Carlsbad, CA), 0.029 mg/ml Vitrogen 100 (COHESION Inc, Palo Alto, CA), and 0.01 mg/ml bovine serum albumin (Invitrogen) in LHC-9 medium (Invitrogen). The parental BEAS-2B cells were cultured in LHC-9 media and the stably transfected cell lines were cultured in the same medium supplemented with 75 μg/ml G418 (Sigma-Aldrich, St. Louis, MO). The cells were maintained at 37ºC under an atmosphere of 5% CO_2. Experiments were performed on 1-day postconfluent cells unless otherwise indicated. Medium was changed 12-16 h prior to all experiments.

2.1.2 Generation of the shNC and shSTAT1 Stable Cell Lines

Human STAT1 shRNA sequences were designed using the Insert Design Tool for pSilencer™ Vectors at www.ambion.com and were subcloned into the pSilencer™ 4.1-CMV neo vector (Applied Biosystems, Foster City, CA) using BamHI and HindIII sites according to the

manufacturer's instructions. The resultant clones were sequenced at the Genomics and Proteomics Core Laboratories at the University of Pittsburgh to verify the presence of the shRNA. A negative control expressing random shRNA in the pSilencer™ 4.1-CMV neo vector was purchased from Applied Biosystems. BEAS-2B cells were transfected with either the random shRNA or the STAT1 shRNA using Lipofectamine and PLUS reagents (Invitrogen) according to the manufacturer's instructions. Transfected cells were selected with G418 (75 µg/ml) (Sigma-Aldrich) and three cell lines were generated for each shRNA. STAT1 knockdown was confirmed by western analysis.

2.1.3 Mouse Embryonic Fibroblasts

Mouse embryonic fibroblasts (MEF) were grown at 37°C under an atmosphere of 5% CO_2 in Dulbecco's Modified Eagle Medium (DMEM) (Invitrogen) supplemented with 10% fetal bovine serum (FBS) (Thermo Fisher Scientific, Pittsburgh, PA), 4 mM L-glutamine (Invitrogen), and 1% penicillin/streptomycin (Invitrogen). The media was changed 12-16 h prior to the experiment to media containing 0.1% BSA in replacement of FBS to arrest cell growth. All MEF cell lines are SV-40 immortalized. Dko7 cells are derived from MTF-1 double knockout embryonic stem cells, SYF cells are derived from mouse embryos with functionally null mutations in Src, Yes, and Fyn, and Src++ cells are deficient in Yes and Fyn, but express endogenous Src. Wild-type MEF cells are used as the control cells in these experiments. Wild-type, SYF, and Src++ MEF cells were purchased from ATCC. Dko7 were kindly provided by Dr. Elias Aizenman from the University of Pittsburgh.

2.1.4 Cell Maintenance and Storage

All cells were passaged by rinsing once with Ca^{2+}/Mg^{2+}-free Hank's Buffered Salt Solution (HBSS) (Invitrogen). The cells were incubated for 5 min at room temperature with the second rinse of HBSS. Cells were incubated for 2-3 min with trypsin/EDTA solution (Lonza Group Ltd., Basel, Switzerland) and an equal volume of trypsin neutralizing solution (TNS) (Lonza Group Ltd.) was added. BEAS-2B cells were dislodged by gentle scraping with a rubber policeman and MEF cells were dislodged by gently tapping the flask. Cells were pelleted by centrifugation at 1000 rpm for 10 min. BEAS-2B cells were passaged at a 1:4 ratio and MEF cells were passaged at a 1:10 ratio.

For long-term storage, BEAS-2B cells were frozen in LHC-9 media containing 10% FBS, 7.5% dimethylsulfoxide (DMSO) (Sigma-Aldrich), and 1% polyvinyl pyrrolidine (PVP) (Sigma-Aldrich). MEF cells were frozen in the serum-containing DMEM with 10% DMSO.

2.2 TREATMENTS

2.2.1 Metals

Cr(VI), $NiSO_4$ (Ni), and $ZnCl_2$ (Zn) solutions were prepared fresh from potassium dichromate, nickel(II) sulfate hexahydrate, and zinc chloride (Sigma-Aldrich), respectively. Unless otherwise noted, cells were exposed to 5 µM Cr(VI), 200 µM Ni, or 100 µM Zn. These exposure levels are relevant to occupational exposures and are based on our previous demonstration of effective increases in cell signaling for gene expression changes without cytotoxicity.

2.2.2 Other reagents and chemicals

IFN-α2 (100 U/ml) (PBL Biomedical Laboratories, New Brunswick, NJ) and IFN-γ (100 ng/ml) (R&D Systems, Minneapolis, MN) were used as positive controls for ISRE and GAS activation, respectively. The ionophore, 2-mercaptopyridine-*N*-oxide sodium salt (pyrithione) (5 µM) (Sigma-Aldrich), was added to facilitate the entry of Ni and Zn into the cell. U0126 (10 µM), SB203580 (20 µM), PP2 (10 µM), and wortmannin (1 µM) (EMD Biosciences, San Diego, CA) were used to inhibit ERK, p38, SFK, and PI3K, respectively. Sodium butyrate (NaB) (2 mM) (Sigma-Aldrich) was used to inhibit HDAC activity. *N*-acetyl-*L*-cysteine (NAC) (2 mM) (Sigma-Aldrich) was added to increase intracellular pools of thiols. *L*-ascorbic acid (AA) (2 mM) (Sigma-Aldrich) was used as an antioxidant. *N*,*N*,*N*',*N*'-Tetrakis(2-pyridylmethyl)ethylenediamine (TPEN) (5 µM) (Sigma-Aldrich) was added to chelate Zn. Mouse monoclonal antibody against human IFNα/β receptor chain 2 (IFNAR) (1 µg/ml) (PBL Laboratories) was used to neutralize the human IFN-α receptor.

2.3 DETERMINATION OF PROTEIN LEVELS AND LOCALIZATION

2.3.1 Total Protein Isolation

For analysis of HIF-1α and total STAT1, cells were rinsed twice with stop buffer and lysed in boiling lysis buffer (Table 3). Lysates were boiled for an additional 5 minutes. For analysis of MT, after the lysate was boiled for 5 min, it was incubated with *tris*(2-carboxyethyl)phosine (Sigma-Aldrich) (1 mM) for 15 min at 37°C followed by a 30 min incubation with 20 mM

iodoacetamide (Sigma-Aldrich) at 37°C. For analysis of ERK, cells were rinsed twice in stop buffer and lysed in modified RIPA buffer (Table 3) supplemented with sodium orthovanadate and protease inhibitors. Lysates were incubated on ice for 30 min and centrifuged at 13,000*g* for 15 min at 4°C.

2.3.2 Nuclear and Cytosolic Protein Isolation

Nuclear protein was isolated by rinsing twice in stop buffer and scraping in stop buffer (Table 3). Lysates were centrifuged at 400*g* for 10 min at 4°C. The pellet was resuspended in 100 µl of buffer A, incubated on ice for 10 min, and centrifuged at 13,000*g* for 2 min at 4°C. The supernatant (cytosolic fraction) was transferred to a new tube. The pellet was rinsed with 100 µl buffer A and centrifuged at 13,000*g* for 2 min at 4°C. The pellet was resuspended in 15 µl of buffer C, vigorously shook for 15 min at 4°C, and centrifuged at 13,000*g* for 5 min at 4°C. The supernatant (nuclear fraction) (15 µl) was transferred to a new tube and 22.5 µl of buffer D was added. Protein concentrations were determined by measuring the absorbance (595 nm) after the addition of Coomassie blue dye (Thermo-Fisher Scientific) using BSA as a reference standard.

Table 3. Buffers

Buffer	Formulation	Purpose
Stop buffer	10 mM Tris-HCl, pH 7.4, 10 mM EDTA, 5 mM EGTA, 0.1 M NaF, 0.2 M sucrose, 100 µM sodium orthovanadate	Protein isolation
Buffer A	10 mM HEPES, pH 7.9, 0.1 mM EDTA, 0.1 mM EGTA, 10 mM KCl, 1 mM DTT, 0.1% NP-40, 100 µM sodium orthovanadate	Nuclear protein isolation
Buffer C	20 mM HEPES, pH 7.9, 0.4 M NaCl, 1 mM EDTA, 0.1 mM EGTA, 1 mM DTT, 100 µM sodium orthovanadate	Nuclear protein isolation
Buffer D	20 mM HEPES, pH 7.9, 20% glycerol, 0.1 M KCl, 1 mM EDTA, 0.1 mM EGTA, 0.1% NP-40, 1 mM DTT, 100 µl sodium orthovanadate	Nuclear protein isolation
SDS Lysis buffer	20 mM Tris, pH 7.5, 1% SDS	Protein isolation
Modified RIPA buffer	50 mM Tris, pH 7.6, 150 mM NaCl, 1 mM EDTA, 10 mM NaF, 1% Triton X-100, 0.1% SDS	Protein isolation
Luciferase assay lysis buffer	25 mM glycylglycine, 4 mM EGTA, 15 mM $MgSO_4$, 1% Triton X-100, 1 mM DTT	Luciferase assay
Luciferase assay buffer	25 mM glycylglycine, 15 mM KH_2PO_4, 15 mM $MgSO_4$, 4 mM EGTA, 2 mM ATP, 1 mM DTT	Luciferase assay
TTBS	10 mM Tris-HCl. pH 8.0, 150 mM NaCl, 0.05% Tween-20	Washing membranes and diluting antibodies
Towbin's Transfer Buffer	25 mM Tris, 192 mM glycine, 20% methanol, 0.01% SDS	Westerns
SDS sample buffer	62.5 mM Tris-HCl, pH 6.8, 10% glycerol, 2% SDS, 5% β-mercaptoethanol, 0.05% bromophenol blue	Westerns
PBS	0.136 M NaCl, 3 mM K Cl, 8 mM Na_2HPO_4, 2 mM KH_2PO_4	Rinsing cells
LB Broth	170 mM NaCl, 1% (w/v) Peptone 140, 0.5% (w/v) yeast extract	Plasmid Preparations

2.3.3 Western Blotting

To determine specific protein abundance, cell lysates were resolved by SDS-PAGE and transferred to PVDF membranes (Millipore, Billerica, MA). Membranes were blocked in either 5% non-fat milk or 5% BSA for 1 h at room temperature and incubated overnight at 4°C with the primary antibodies (Table 4) diluted in TTBS (Table 3). To determine MT protein abundance, after the transfer to the PVDF membrane, the membrane was fixed in 2% glutaraldehyde (Sigma-Aldrich) before incubating with the primary antibody overnight. After washing the membranes three times for 10 min with TTBS, horseradish peroxidase-conjugated secondary antibodies (GE Healthcare, Piscataway, NJ) were added for one hour before 3 additional TTBS washes. The proteins were visualized using enhanced chemiluminescence (Perkin-Elmer, Boston, MA) and quantification was performed using Image J.

Table 4. Antibodies

Antibody	Supplier	Dilution	Purpose
β-actin	Sigma-Aldrich (A5441)	1:10,000	Western
ERK	Cell Signaling Technology (CST) (Danvers, MA) (9101)	1:2000	Western
Fyn	Santa Cruz (sc-434)	1:200; 1:1000	IP; western (human)
Fyn	Millipore (06-133)	1:1000	Western (mouse)
HIF-1α	BD Biosciences (610958)	1:500	Western
MT	Dako Cytomation (M0639)	1:500	Western
pERK	CST (9101)	1:2000	Western
pSFK (Tyr416)	CST (2101)	1:1000	Western
pYSTAT1	Millipore (07-307)	1:1000	Western
Src	CST (2110)	1:200; 1:1000	IP; western
STAT1	CST (9176)	1:1000	Western (human)
STAT1	Santa Cruz (sc-346)	1:2000	Western (mouse)

2.3.4 Immunoprecipitation

Cells were rinsed twice in stop buffer and scraped in modified RIPA buffer supplemented with sodium orthovanadate and protease inhibitors. Lysates were incubated for 30 min on ice and then sonicated 3 times at 5 sec intervals. Lysates were centrifuged at 13,000*g* for 15 min at 4°C and the supernatants were collected. Equal amounts of protein were incubated with the antibody against either total Src or total Fyn overnight at 4°C on a rotating platform. Protein A/G beads (Thermo-Fisher Scientific) were added and incubated for an additional 3 h at 4°C. The beads were collected by centrifugation at 13,000*g* for 1 min, rinsed 3 times with modified RIPA buffer supplemented with sodium orthovanadate and protease inhibitors, suspended in 2X sample buffer, and boiled for 5 min.

2.3.5 MTF-1 Localization

Cells were transiently transfected with eGFP-MTF-1 and after twenty-four hours, cells were trypsinized, replated on chamber well slides, and allowed to attach overnight. Cells were exposed to Ni (200 µM; 30 min to 4 h) and Zn (100 µM; 2 h). Cells were fixed with 4% paraformaldehyde (Sigma-Aldrich) and nuclei were stained with DRAQ5™ (Biostatus Limited, Leicestershire, UK). Images were taken at 60X magnification with an Olympus Fluoview 500 confocal microscope in the University of Pittsburgh Center for Biological Imaging. Images were quantified by dividing the total number of eGFP-MTF1 positive nuclei by the total number of nuclei in each image.

2.3.6 Enzyme Linked Immunosorbant Assay

Conditioned medium was collected and stored at -80°C until use. VEGFA($_{165 \text{ and } 121}$) content in the medium was analyzed using Quantikine® VEGFA Immunoassay (R&D Biosystems) according to the manufacturer's instructions. VEGFA protein release was normalized to total cellular protein from each individual sample.

2.4 RNA ISOLATION AND QUANTIFICATION

Total RNA was isolated using TRIzol® reagent (Invitrogen) according to manufacturer's instructions. Briefly, cells were lysed in TRIzol® reagent and incubated for 5 min at room temperature. After transferring the sample to a tube, chloroform was added and samples were mixed vigorously for 15 s. Samples were incubated at room temperature for 2-3 min before centrifuging at 11,000*g* for 15 min at 4°C. The aqueous layer was transferred to a new tube, isopropanol was added, and samples were incubated for 10 min at room temperature before centrifuging at 11,000*g* for 15 min at 4°C. The supernatant was discarded and the pellet was washed with 75% ethanol and centrifuged at 7,500*g* for 5 min at 4°C. The pellet was dried and resuspended in RNAse- and DNAse-free water. The RNA was quantified by measuring absorbance (260 nm) and was reverse transcribed to cDNA.

VEGFA, MT2A, Mt1, IRF1, ribosomal protein L13A (RPL13A), and β-actin cDNA levels were amplified by real-time PCR using the MJ Research Opticon 2 (Bio-Rad Laboratories, Hercules, CA)) with specific primers (Table 5). Each PCR reaction contained 1X SYBR GreenER™ qPCR Supermix (Invitrogen) and 0.4125 pmol each of forward and reverse primers.

Thermal cycling was performed by incubating at 50°C for 2 min and 95°C 10 min followed by 40 cycles of 95°C for 15 s and 57°C for 1 min. Gene expression was quantified using standard curves for both the mRNAs of interest as well the housekeeping genes, RPL13A or β-actin for human or mouse cDNA, respectively.

IRF7 and Irf7 cDNA levels were amplified by conventional PCR using the MJ Research PTC-100 Thermocycler (Bio-Rad Laboratories) with specific primers (Table 5). Thermocycling was performed using the following conditions: 95°C for 5 min; 25 cycles or 20 cycles of 94°C 20 s, 55°C for 30 s, and 72°C for 30 s for IRF7 or Irf7, respectively; and 72°C for 5 min. PCR products were run on 2% agarose gels stained with ethidium bromide. Densitometry was performed on the gels using Image J. The mRNAs of interest were normalized to the housekeeping genes.

Table 5. Primers

Gene	**Forward Primer (5'-3')**	**Reverse Primer (5'-3')**
VEGFA	CTTGCCTTGCTGCTCTACCT	GCAAGGCCCACAGGGATTTT
MT2A	CAACCTGTCCCGACTCTAGC	TGGAAGTCGCGTTCTTTACAT
Mt1	CACCAGATCTCGGAATGGAC	AGGAGCAGCAGCTCTTCTTG
RPL13A	CGAGGTTGGCTGGAAGTACC	ATTCCAGGGCAACAATGGAG
β-actin	GGGACCTGACCGACTACCTC	GGGCGATGATCTTGATCTTC
IRF7	TGTGGACACCTGTGACACCT	GTTATCTCGCAGCATCACGA
IRF1	TGCTAAGAGCAAGGCCAAGAG	CGACTGCTCCAAGAGCTTCAT
Irf7	CAGTTGATCCGCATAAGGTGT	CTCGTAAACACGGTCTTGCTC

2.5 TRANSFECTIONS AND LUCIFERASE ASSAYS

2.5.1 Transformation of DH5α™ competent cells and plasmid preparation

The plasmid was mixed with 50 µl of DH5α competent cells and incubated on ice for 30 min. The mixture was heat shocked for 45 s at 42°C to allow the plasmid to enter the bacteria. The cells were incubated on ice for 2 min before 900 µl of LB Broth (Table 3) was added. The cells were shaken at 37°C for 1 h and cultured on plates containing the specific antibiotic to which the plasmid conferred resistance. After incubating overnight at 37°C, one colony was selected and allowed to grow in LB broth containing the specific antibiotic for the plasmid. DNA was isolated using either QIAGEN Plasmid Mini Kit or EndoFree Plasmid Maxi Kit (Qiagen Inc., Valencia, CA).

2.5.2 Transient Transfection

2.5.2.1 BEAS-2B Cell Transfection

BEAS-2B cells (70-80% confluence) were transfected with the luciferase reporter constructs (Table 6) using Lipofectamine and PLUS reagents (Invitrogen) in 12-well plates. Briefly, 1 µg of plasmid DNA was incubated with 4.2 µl of PLUS reagent in 100 µl of LHC-9 media for each well for 15 min at room temperature. After the incubation period, 2.8 µl of lipofectamine reagent diluted in 100 µl of LHC-9 media per well was added to the plasmid DNA mixture and incubated for an additional 15 min. 200 µl of the transfection reagent was added to each well containing 300 µl of fresh LHC-9 medium. 3-4 h after the transfection, an additional 500 µl of LHC-9 medium was added to each well. After an overnight recovery period, cells were treated.

Cells were co-transfected with pRL-TK or eGFP plasmids for normalizing transfection efficiency.

2.5.2.2 MEF Cell Transfection

MEF cells were transiently transfected as described above with the BEAS-2B cells except for the following adjustments. Cells were transfected with the control or Fyn-Myc expression plasmid (Table 6) in 12-well plates for RNA and total protein or 6-well plates for nuclear protein. 2 µg or 4 µg of plasmid DNA was incubated with PLUS reagent in 100 or 250 µl of Opti-MEM® I Reduced-Serum Medium (Invitrogen) for 12-well or 6-well plates, respectively. The transfection reagent was added to each well containing fresh DMEM supplemented with 10% FBS, 4 mM L-glutamine, and 1% penicillin/streptomycin. The next day the medium was replaced with DMEM supplemented with 0.1% BSA instead of 10% FBS. Cells were treated 48 h after the transfection for optimal expression of the plasmid.

2.5.3 Luciferase Assay

Luciferase assays were performed using the Dual-Luciferase® Reporter Assay System (Promega, Madison, WI) in experiments that were co-transfected with pRL-TK. Briefly, cells were rinsed twice and scraped in 1 ml of cold PBS and centrifuged at 13,000*g* for 3 min at 4°C. The pellet was resuspended in 50 µl of the lysis buffer provided and centrifuged at 13,000*g* for 5 min at 4°C. The supernatant was transferred to 12 X 50 polypropylene tubes (Turner Designs, Sunnyvale, CA) and 50 µl of Luciferase Assay Reagent II was added and firefly luciferase activity was determined. 50 µl of Stop & Glo® Reagent was added to quench the firefly

luciferase signal and initiate *Renilla* luciferase activity. Results are expressed as a ratio of firefly luciferase activity to *Renilla* luciferase activity.

Cells co-transfected with eGFP were harvested in 80 µl of lysis buffer (Table 3) and centrifuged at 13,000*g* for 5 min at 4°C. The supernatant was transferred to 12 X 50 polypropylene tubes and 120 µl of luciferase assay buffer was added. The tube was placed in a TD-20/20 luminometer (Turner Designs) and 50 µl of luciferin was added. The RLU were determined for 20 s. RLU were normalized to GFP fluorescence measured using a fluorescent plate reader (ex 485 nm, em 508 nm).

2.6 REACTIVE OXYGEN SPECIES (ROS) MEASUREMENTS

ROS were detected using 5-(and-6)-chloromethyl-2'7'-dichlorodihydrofluorescein diacetate, acetyl ester (CM-H_2DCFDA) (Invitrogen). Cells were seeded in a 24 well plate and preincubated with NAC or AA. Cells were incubated (37°C; 10 min) with CM-H_2DCFDA (20 µM) and exposed to Ni (10 min). Fluorescence was read using a fluorescent plate reader (excitation (485 nm) emission (530 nm)).

Table 6. Plasmids

Plasmid	Description	Origin
eGFP-MTF-1	enhanced green fluorescent protein (eGFP) fused to the N-terminus of MTF-1	B.R. Pitt (139)
pLucMRE	luciferase reporter construct driven by 4 MRE tandem repeats	D. Giedroc (140)
pRL-TK	*Renilla* luciferase reporter construct containing the herpes simplex virus thymidine kinase promoter region	Promega (Madison, WI)
HRE-luc	Luciferase reporter construct driven by 3 HRE tandem repeats	K. Salnikow (141)
Sp1-luc	Luciferase reporter construct driven by Sp1	K. Salnikow (141)
eGFP-N2	Enhanced green fluorescent protein	BD Biosciences
ISRE-luc	luciferase reporter construct driven by ISRE	Mercury™ JAK/STAT Pathway Profiling System, BD Biosciences
GAS-luc	luciferase reporter construct driven by GAS	Mercury™ JAK/STAT Pathway Profiling System, BD Biosciences
Fyn-myc	Fyn expression vector	L.M. Zubritsky and A.A. Nemec
pcDNA™ 3.1/*myc*-His(-) C	Expression vector	Invitrogen

2.7 FLOW CYTOMETRY

Cells were incubated (37°C; 1 h) with 5 µM free Zn fluorophore FluoZin-3™ AM ester (Invitrogen) with Pluronic F-127 (equal volume) (Invitrogen) in HBSS containing calcium and magnesium (Invitrogen). Cells were then rinsed with HBSS and treated (30 min) with pyrithione in the presence or absence of either 20 µM Ni or 10 µM Zn. TPEN (50 µM) was added (5 min)

to chelate the free Zn. Cells were rinsed in PBS, trypsinized, and centrifuged at 1000*g* for 10 min. The pellet was resuspended with PBS containing 100 µg/ml propidium iodide (Sigma-Aldrich) and incubated (37°C; 1 h) in the dark to stain dead cells. Flow cytometry was performed using a FACSCanto (BD Biosciences, San Jose, CA).

2.8 CONSTRUCTION OF THE FYN EXPRESSION VECTOR (FYN-MYC)

The c-Fyn cDNA from pRK5 c-Fyn (Addgene, Inc, Cambridge, MA) was subcloned into pcDNA 3.1/*myc*-His(-)C (Invitrogen) using BamHI and HindIII sites. The insert was separated on a 1% agarose gel stained with ethidium bromide and the DNA was isolated using the QIAquick Gel Extraction Kit (Qiagen Inc.). The c-Fyn cDNA was ligated with the linearized pcDNA 3.1/*myc*-His(-)C using T4 DNA ligase (Stratagene La Jolla, CA). The ligation was transformed and the resultant clones were sequenced at the Genomics and Proteomics Core Laboratories at the University of Pittsburgh to verify the presence of c-Fyn cDNA.

2.9 LENTIVIRAL SHRNA TRANSDUCTION

BEAS-2B cells were seeded at 50% confluence in 6 well plates. After the cells were allowed to attach overnight, they were transduced with GFP-expression control and Fyn shRNAs. The GFP-expression control and 5 Fyn shRNAs were designed and prepared by the Lentiviral Core Facility at the University of Pittsburgh Cancer Institute. Briefly, 1 ml of LHC-9 media was combined with 1 ml of the specific virus (10^6 infectious units per ml) and 2 µl polybrene and was

added to each individual well. Cells were incubated overnight and fresh media was given the following day. The cells were analyzed for GFP expression and protein knockdown 3 days after transduction.

2.10 CELL VIABILITY ASSAY

The viability of cells following experimental exposures was examined using the Alamar Blue™ assay (Alamar Biosciences, Inc., Sacramento, CA) according to manufacturer's instructions. Following exposure, 50 µl of alamar blue was added to each well of a 24-well plate and incubated at 37°C for an additional 3 h. Absorbance was measured at 570 nm and 600 nm in a microplate reader.

2.11 STATISTICS

One-way analysis of variance (ANOVA) or two-way ANOVA were used as appropriate to determine whether the mean of each treatment was different from the untreated cells. Dunnett's or Tukey's Multiple Comparisons post hoc tests were used to determine significant differences between the means of each group. Linear trend analysis was performed to determine if there was a time-dependent response. All statistics were performed using GraphPad Prism version 5 (GraphPad Software, San Diego, CA). Data are represented as mean ± SEM or as fold control.

3.0 CHROMIUM(VI)-ACTIVATED SIGNAL TRANSDUCER AND ACTIVATOR OF TRANSCRIPTION 1 (STAT1) SIGNALING IS MEDIATED BY FYN

3.1 ABSTRACT

Mechanisms for metal signaling in the molecular pathogenesis of airway injury or diseases are poorly understood. We previously reported that chromium (Cr(VI)) represses induction of repair genes by activating signal transducer and activator of transcription 1 (STAT1). In the current study, we investigated the hypothesis that Cr(VI) activates the Src family kinase (SFK), Fyn, to activate STAT1 and stimulate STAT1-dependent gene induction in human airway epithelial (BEAS-2B) cells. Cr(VI) selectively stimulated transactivation of STAT1 responsive interferon-stimulated response element (ISRE) and induced ISRE-driven interferon regulatory factor 7 (IRF7), without affecting the gamma interferon-activated site (GAS)-driven IRF1. Cr(VI)-induced IRF7 was absent in cells stably expressing STAT1 shRNA or cells treated with sodium butyrate indicating requirements for both STAT1 and histone deacetylase (HDAC) activity. In contrast, Cr(VI)-activated ISRE was not blocked in cells incubated with a neutralizing antibody to interferon α/β receptor indicating that Cr(VI) signaling was independent of interferon signaling. Cr(VI) activation of STAT1 signaling was diminished in mouse embryonic fibroblasts null for the SFKs, Src, Yes, and Fyn. However, expressing Fyn, but not Src in these deficient cells restored the Cr(VI) response indicating that Fyn was required for Cr(VI)-stimulated

STAT1. Cr(VI) activated Fyn in BEAS-2B cells and the activation of STAT1-dependent signaling was abrogated in cells expressing Fyn shRNA These data presents a novel mechanism through which Cr(VI) initiates interferon-like signaling by activating Fyn to stimulate STAT1-dependent transactivation and repression of airway epithelial cell genes.

3.2 INTRODUCTION

Chromium is a well-known environmental pollutant known to promote airway diseases. Several million people world-wide are exposed to Cr(VI) and Cr(VI)-containing compounds (6). Chronic inhalation of Cr(VI) causes pulmonary diseases such as chronic bronchitis, asthma, emphysema, and cancers through poorly defined mechanisms (13,42,47). Cr(VI) exists as a chromate oxyanion under physiological conditions and, unlike Cr(III), can readily enter the cell through anion channels (5,9). Once Cr(VI) enters an airway cell, greater than 90% is trapped within the cell through reduction by ascorbate or glutathione to Cr(III) (9,10). These one-way kinetics reduce Cr clearance and make the epithelium lining of the airways the main target of inhaled Cr(VI) (11).

Signal transducers and activators of transcription (STAT) are a family of latent cytoplasmic transcription factors. There are seven different members that are activated by exogenous stresses (64-66), including metals (55), to produce diverse biological responses. STAT proteins are activated through phosphorylation on a conserved tyrosine residue in the C-terminus, followed by dimerization, and translocation into the nucleus (52). Non-receptor tyrosine kinases (NRTKs) such as Janus kinases (JAKs) and Src family kinases

(SFKs) are involved in phosphorylating the STAT proteins to initiate STAT-dependent signaling (52,55,142,143). We have previously shown that Cr(VI)-activates both STAT1 and STAT3 in airway epithelium and that prolonged STAT3 activation required the SFK, Lck (55).

STAT1 was originally identified as a downstream effector of interferon (IFN) signaling (57) and is required to induce antiviral and antiproliferative responses (67,68). Once phosphorylated, STAT1 forms either a homodimer that binds to IFNγ activation sites (GAS) to transcribe GAS-driven genes (e.g. interferon regulatory factor (IRF 1)) or a heterotrimeric complex, interferon-stimulated gene factor 3 (ISGF3), with STAT2 and IRF9 and bind to interferon-stimulated response elements to transcribe ISRE-driven genes (e.g. IRF7) (57). Type I IFNs (e.g. IFN-α2) and type II IFNs (e.g. IFN-γ) signal through cell surface receptors to activate STAT1. Type I IFNs induce the formation of STAT1 homodimers and STAT1 and STAT2 heterodimers, whereas type II IFNs induce only the formation of STAT1 homodimers (144). Histone deacetylase (HDAC) binding to the ISGF3 complexes and its enzymatic activity are required to recruit RNA polymerase II to the promoter for STAT1 activation of ISRE-, but not GAS-, driven genes (61,145).

STAT1 activation promotes apoptosis in cardiac myocytes after ischemia and reperfusion (64) and has also been implicated in the pathogenesis of lung diseases (70). STAT1 activation was localized to the bronchial epithelial cells in asthmatic patients (1) suggesting that aberrant expression of STAT1 may be a precursor to disease. In addition, type II IFN therapies to kill tumor cells fail in cancers that lack STAT1 (67,146) demonstrating the important suppressive role of the transcription factor. We have previously reported that Cr(VI) stimulated the acute activation of STAT1 in human airway epithelial cells and STAT1-dependent repression of inducible genes. In the current study, we sought to determine the mechanism through which

Cr(VI) initiated STAT1 signaling to provide insight into how Cr(VI) exerts pathological effects on the airway epithelium.

3.3 RESULTS

3.3.1 Cr(VI) selectively activates ISRE-dependent STAT1 signaling.

We have previously reported that Cr(VI) induces the tyrosine phosphorylation and nuclear translocation of STAT1 within 4 h in BEAS-2B cells (55). Upon activation, STAT1 can form homodimers or heterodimers that bind to GAS and ISRE consensus sequences, respectively, to induce gene transcription (57). Using luciferase constructs driven by these sequences, it was determined that exposure to Cr(VI) results in ISRE, but not GAS transactivation (Fig. 11 and data not shown). Similarly, Cr(VI) induced the ISRE-driven gene, IRF7, and had no effect on GAS-driven IRF1 (Fig. 11).

3.3.2 STAT1 is required for Cr(VI) activation of ISRE.

To confirm the requirement for STAT1 in the Cr(VI)-stimulated ISRE transactivation, BEAS-2B cells stably expressing random (shNC) or STAT1-specific (shSTAT1) shRNA were exposed to Cr(VI). Western analysis verifies the knockdown of STAT1 in the shSTAT1 cells compared to shNC cells (Fig 12A). Cr(VI) activated ISRE and induction of IRF7 mRNA expression in the shNC cells. However, this response was lost in the shSTAT1 cells (Fig. 12B-C) indicating the necessity of STAT1 in the response to Cr(VI).

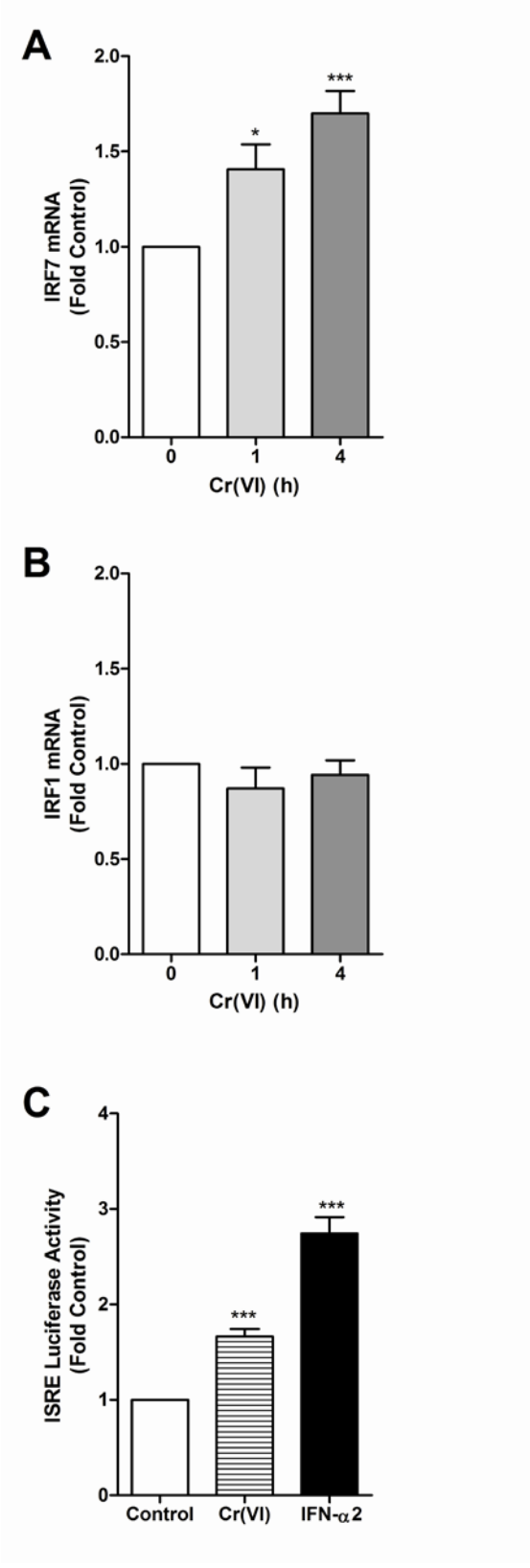

Figure 11. Cr(VI) stimulates ISRE-, but not GAS-dependent transactivation.

A-B. BEAS-2B cells were exposed to Cr(VI) for indicated times and total RNA was isolated. IRF7 and IRF1 mRNA levels were measured by RT-PCR and real-time PCR, respectively, and normalized against the housekeeping gene, RPL13A. **C.** BEAS-2B cells were transfected with the ISRE-luc reporter construct. After 24 h, cells were treated with 5 μM Cr(VI) or 100 U/ml IFN-α2 for 4h. Cell lysates were analyzed for luciferase activity. Data are presented as mean ± SEM of fold control (n=3). * and *** designate $p<0.05$ and $p<0.001$, respectively.

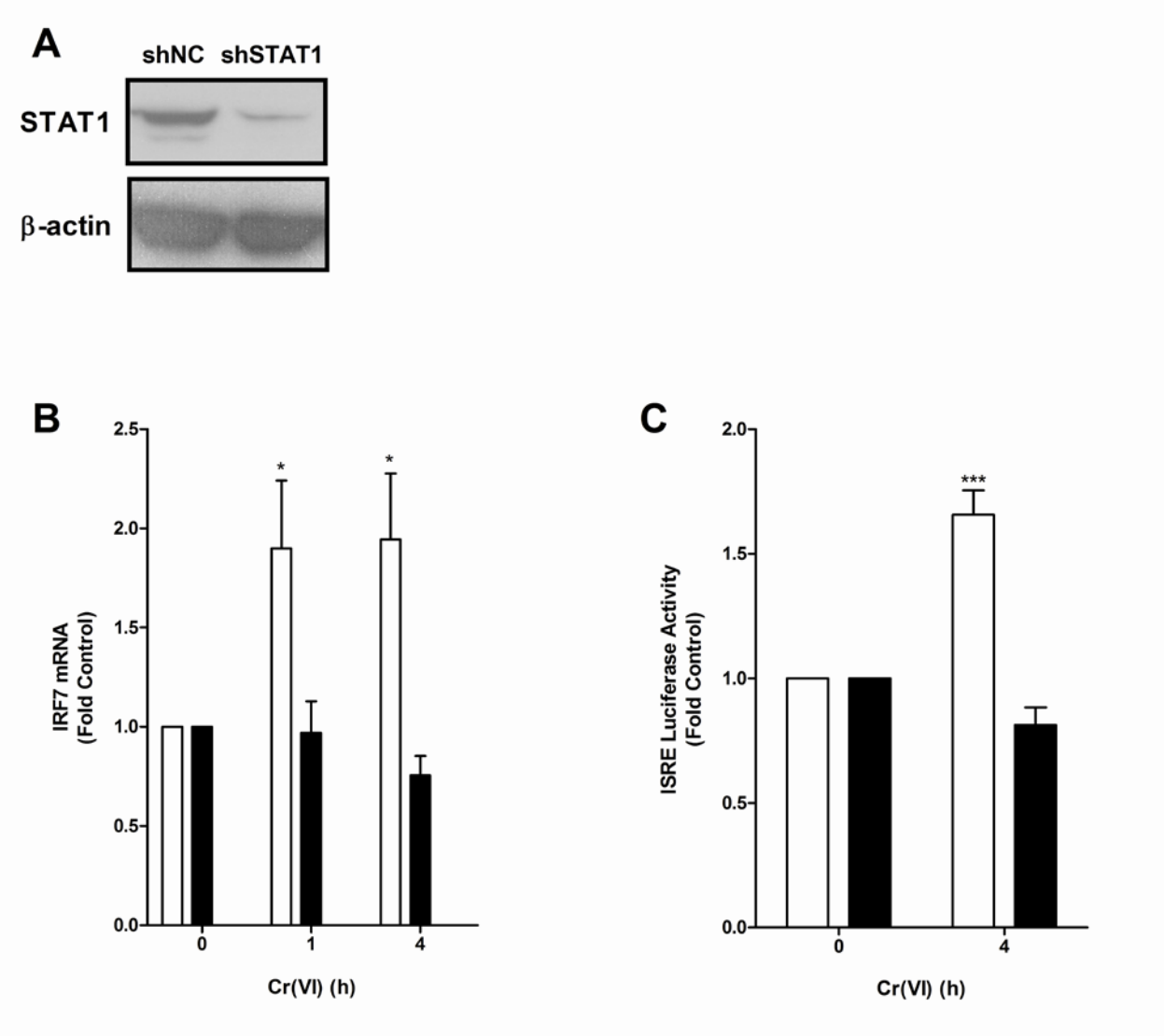

Figure 12. Cr(VI) induction of IRF7 mRNA requires STAT1.

A. Total protein was isolated from BEAS-2B cell lines stably expressing either random (shNC) or STAT1 (shSTAT1) shRNA and total STAT1 and β-actin protein levels were determined by western analysis. **B.** shNC

(open bars) and shSTAT1 (closed bars) cells were exposed to 5 µM Cr(VI) for 0, 1, and 4 h. Total RNA was isolated and IRF7 mRNA was measured by RT-PCR and normalized to the housekeeping gene, RPL13A. **C.** shNC (open bars) and shSTAT1 (close bars) cells were transiently transfected with the ISRE-luc reporter construct. After 24 h, cells were exposed to 5 µM Cr(VI) for 4 h and luciferase activity was measured. Data are presented as mean ± SEM of fold control (n=3). * and *** designate $p<0.05$ and $p<0.001$, respectively, compared to untreated (control) cells. ^ and ^^^ designate $p<0.05$ and $p<0.001$, respectively, compared to the shNC cells at the same time point.

3.3.3 HDAC activity is required for Cr(VI) induction of IRF7.

Cr(VI) inhibits polycyclic aromatic hydrocarbon (PAH)-induced gene induction by retaining HDAC in their proximal promoters (24). In contrast, HDAC activity is required to recruit RNA polymerase to the promoter of ISRE-driven genes (61). To examine the necessity of HDAC for Cr(VI) induction of IRF7, BEAS-2B cells were pretreated with the global HDAC inhibitor, sodium butyrate (NaB), before exposure to Cr(VI). Cr(VI) had no effect on ISRE transactivation levels in cells pretreated with NaB compared to vehicle-treated cells (Fig. 13) suggesting that HDAC activity is essential for Cr(VI) activation of ISRE and IRF7 induction.

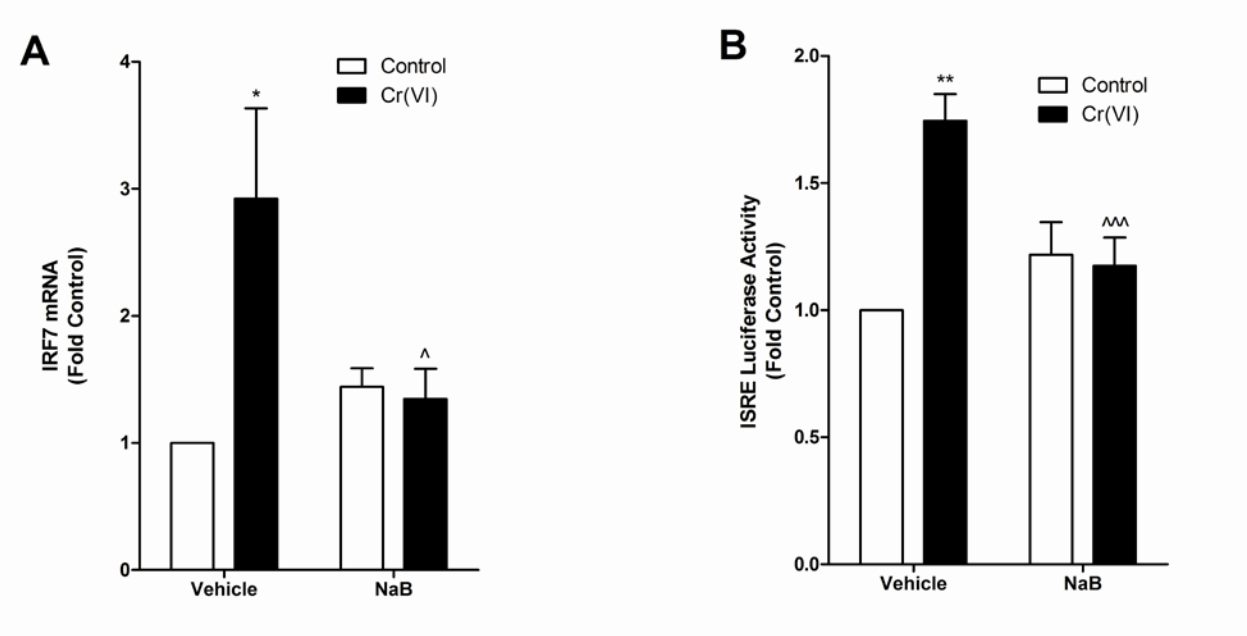

Figure 13. H DAC ac tivity i s n ecessary f or C r(VI)-stimulated I SRE t ransactivation an d I RF7 induction.

A. BEAS-2B cells were exposed to 5 μM Cr(VI) for 4 h after a 16 h pretreatment with 2 mM NaB and total RNA was isolated. IRF7 mRNA levels were measured by RT-PCR and normalized against the housekeeping gene, RPL13A. **B.** BEAS-2B cells were transfected with the ISRE-luc reporter construct. After 24 h, cells were pretreated with 2 mM sodium butyrate for 16 h followed by treatment with 5 μM Cr(VI) for 4 h. Cell lysates were analyzed for luciferase activity. Data is presented as mean ± SEM of fold control (n=3). * and ** designate $p<0.05$ and $p<0.01$, respectively, compared to untreated (control) cells. ^ and ^^^ designate $p<0.05$ and $p<0.001$, respectively, compared to cells treated with Cr(VI) alone.

3.3.4 Cr(VI) transactivation of ISRE is independent of type I interferon signaling.

Type I IFNs bind to the type I IFN receptor to stimulate STAT1 and STAT2 tyrosine phosphorylation and subsequent dimerization (52,59). To determine if Cr(VI) was also signaling through this receptor, a neutralizing antibody against one of the 2 subunits of the receptor (IFNAR) was added to cells prior to Cr(VI) treatment. Whereas the IFN-α2 induction of IRF7

was abrogated in cells treated with the neutralizing antibody, no effect was observed in the Cr(VI)-treated cells (Fig. 14). These data indicate that Cr(VI) signaling for IRF7 induction is independent of type I IFN signaling.

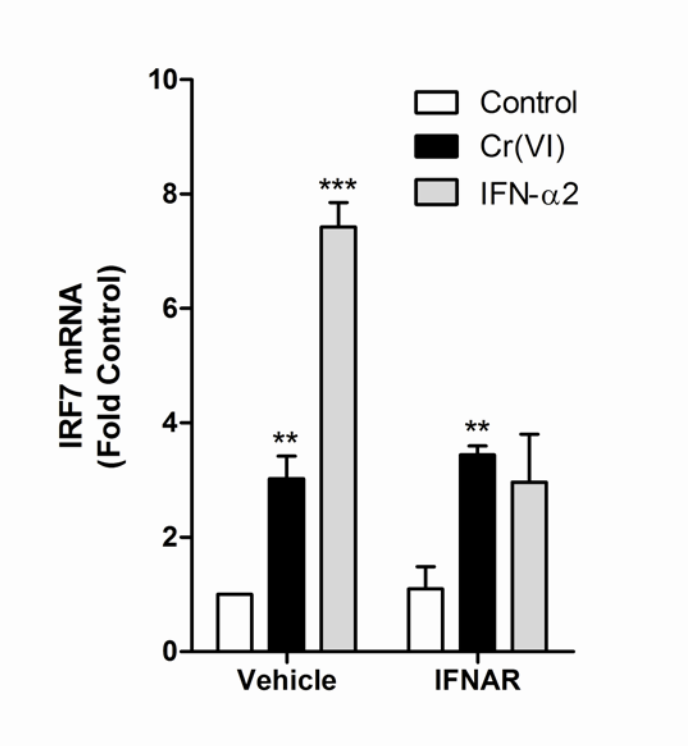

Figure 14. Cr(VI) induction of IRF7 mRNA is independent of type I IFN signaling.

BEAS-2B cells were treated with IFNAR, a neutralizing antibody for the IFN-α/β receptor, for 30 min prior to treatment with 5 μM Cr(VI) or 100 U/ml IFN-α2. Total RNA was isolated and IRF7 mRNA levels were measured by RT-PCR and normalized against the housekeeping gene, RPL13A. Data is presented as means ± SEM of fold control. ** and *** designate $p<0.01$ and $p<0.001$, respectively, compared to the respective untreated (control) cells. ^^^ designates $p<0.001$ compared to cells treated with IFN-α2 alone.

3.3.5 Cr(VI)-activated STAT1 signaling requires Fyn.

We previously reported that Cr(VI) activates both Fyn and Lck, but not Src or Yes in airway cells (22). In addition, we demonstrated that Cr(VI)-stimulated STAT3 translocation and induction of interleukin-6 (IL-6) mRNA transcription required Lck activity (55). In keeping with the previous observation made in A549 cells, Cr(VI) activated Fyn within 15 min of exposure in the BEAS-2B cells (Fig. 17A-B). Incubating the BEAS-2B cells with the global SFK inhibitor PP2 blocked Cr(VI)-activated STAT1 and the induction of IRF7 transcription (Fig. 15A-C) indicating a role for SFK in the STAT1-dependent response. STAT1 was activated by Cr(VI) in wildtype MEF cells (Fig 15D-F). However, there was no Cr(VI) response in Src, Yes, and Fyn (SYF) null MEF cells or in (Src++) MEF cells lacking only Yes and Fyn (Fig. 15D-F). In contrast, transiently transfecting SYF cells with human Fyn restored Cr(VI)-stimulated STAT1 signaling (Fig. 16). The overexpression of Fyn was verified by western analysis and it should be noted that the antibody used only recognized human Fyn (Fig. 16A). In reciprocal experiments, BEAS-2B cells were transduced with GFP-expression control and Fyn lentiviral shRNA. The knockdown of Fyn was verified by western analysis (Fig. 17C). Cr(VI)-activated STAT1 and induction of IRF7 was inhibited in BEAS-2B cells expressing Fyn shRNA compared to the control shRNA cells (Fig. 17D-F). These data indicate that Cr(VI)-activated Fyn mediates the phosphorylation of STAT1 and induction of IRF7 mRNA expression.

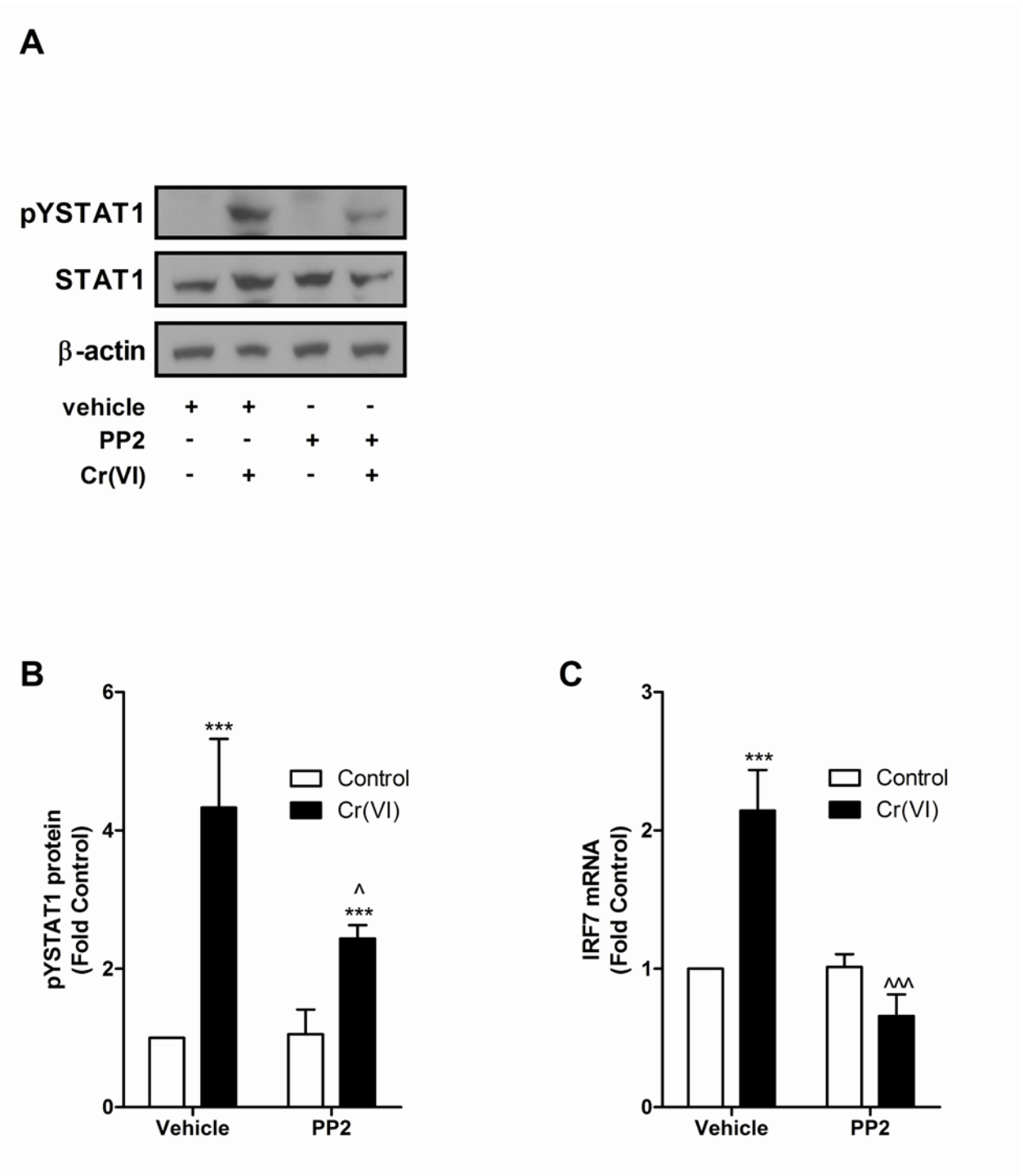

Figure 15 continued below.

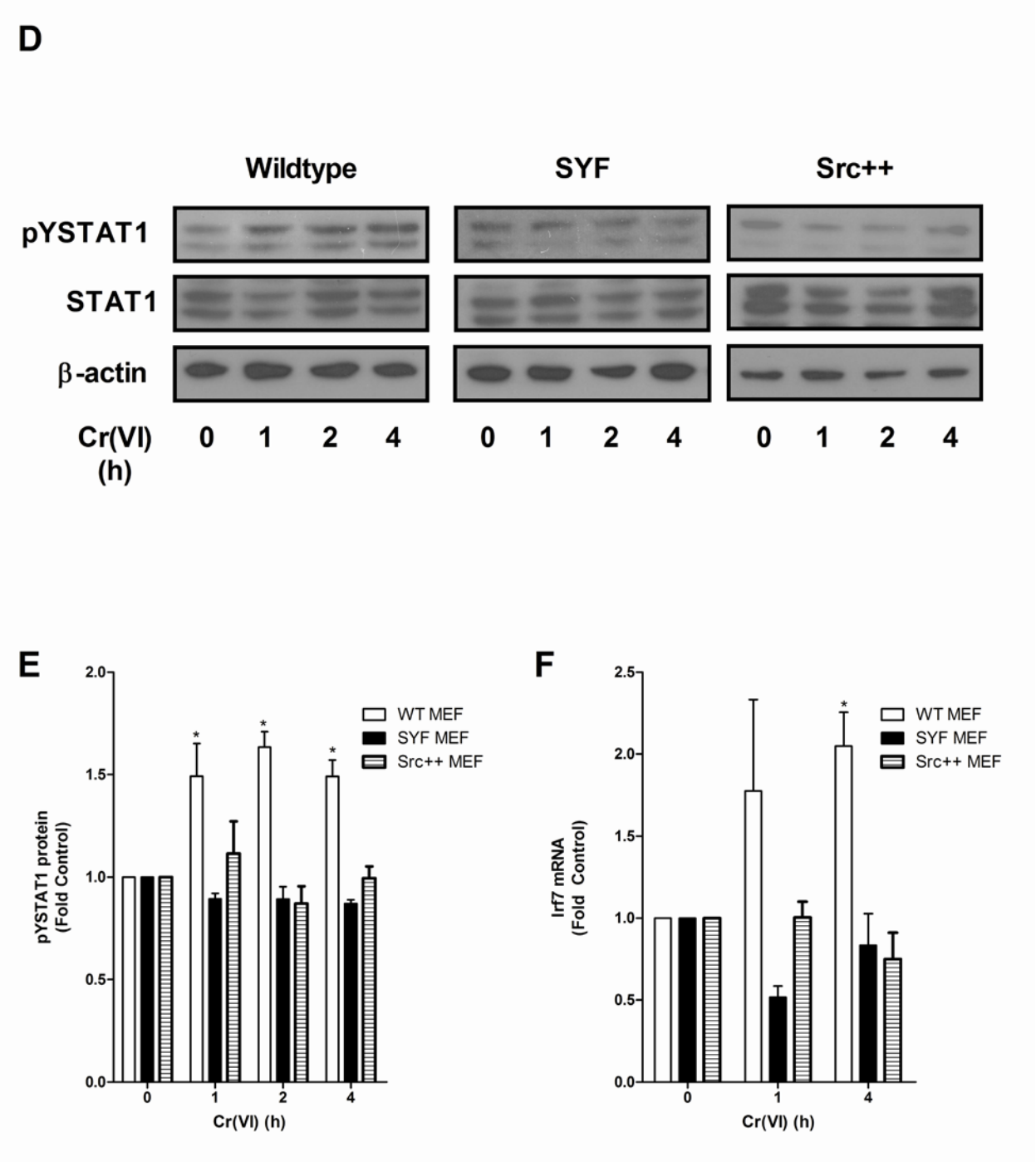

Figure 15. Cr(VI) activation of STAT1 requires Src family kinases.

A. BEAS-2B cells were pretreated with PP2 for 30 min prior to the addition of 5 µM Cr(VI) for 1 h. pYSTAT1, STAT1, and β-actin levels were determined by western analysis and a representative blot from a single experiment is shown. **B.** Density of the protein bands from three separate experiments were quantified with ImageJ software. **C.** BEAS-2B cells were pretreated with PP2 for 30 min prior to the addition of 5 µM Cr(VI) for 4 h.

Total RNA was isolated and IRF7 mRNA levels were measured by RT-PCR and normalized against the housekeeping gene, RPL13A. **D.** Wild-type (WT), SYF, and Src++ MEF cells were incubated with 5 μM Cr(VI) for the indicated times and nuclear protein was isolated. pYSTAT1, total STAT1, and β-actin levels were determined by western analysis and a representative blot from a single experiment is shown. **E.** Density of the protein bands from three separate experiments were quantified with ImageJ software. **F.** WT, SYF, and Src++ MEF cells were exposed to 5 μM Cr(VI) for the indicated times and total RNA was isolated. Irf7 mRNA levels were measured by RT-PCR and normalized to the housekeeping gene, β-actin. Data is presented as mean ± SEM of fold control (n=3). * and *** designate $p<0.05$ and $p<0.001$, respectively, compared to untreated (control) cells. ^ and ^^^ designate $p<0.05$ and $p<0.001$, respectively, compared to cells treated with Cr(VI) alone.

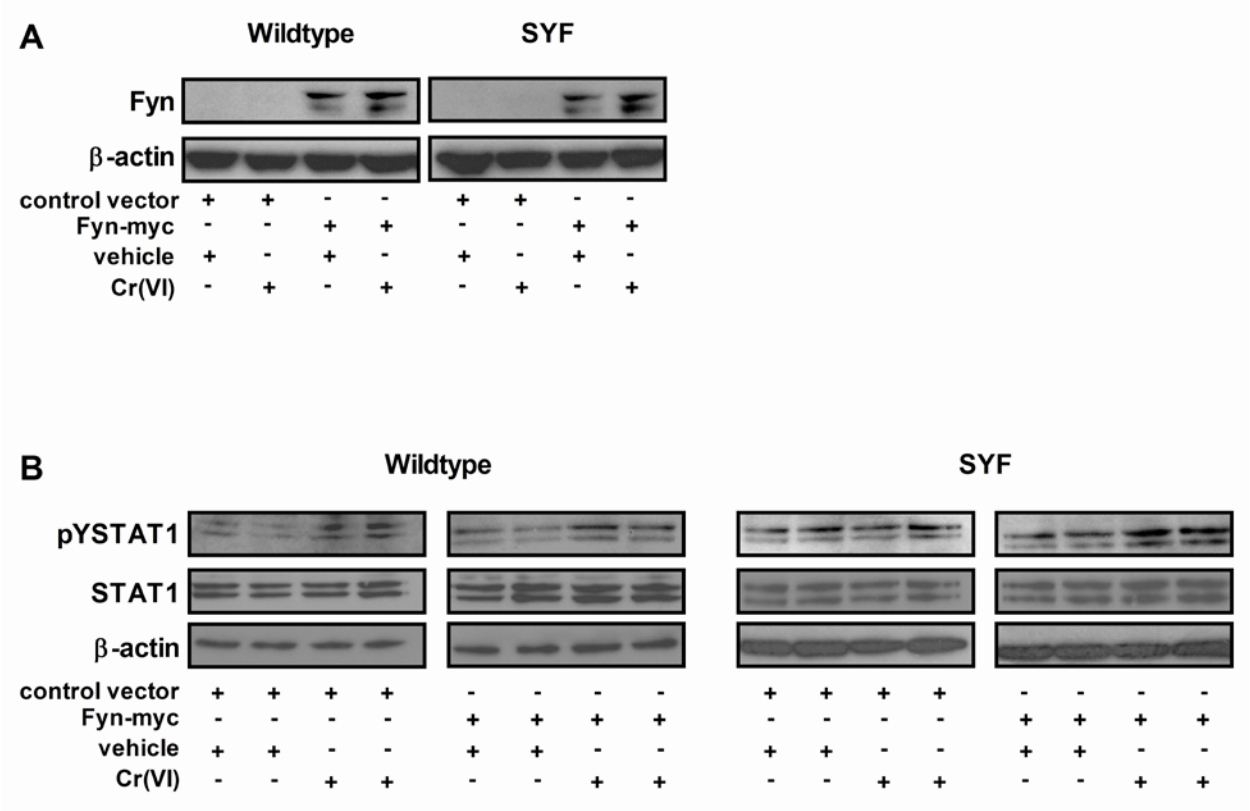

Figure 16 continued below.

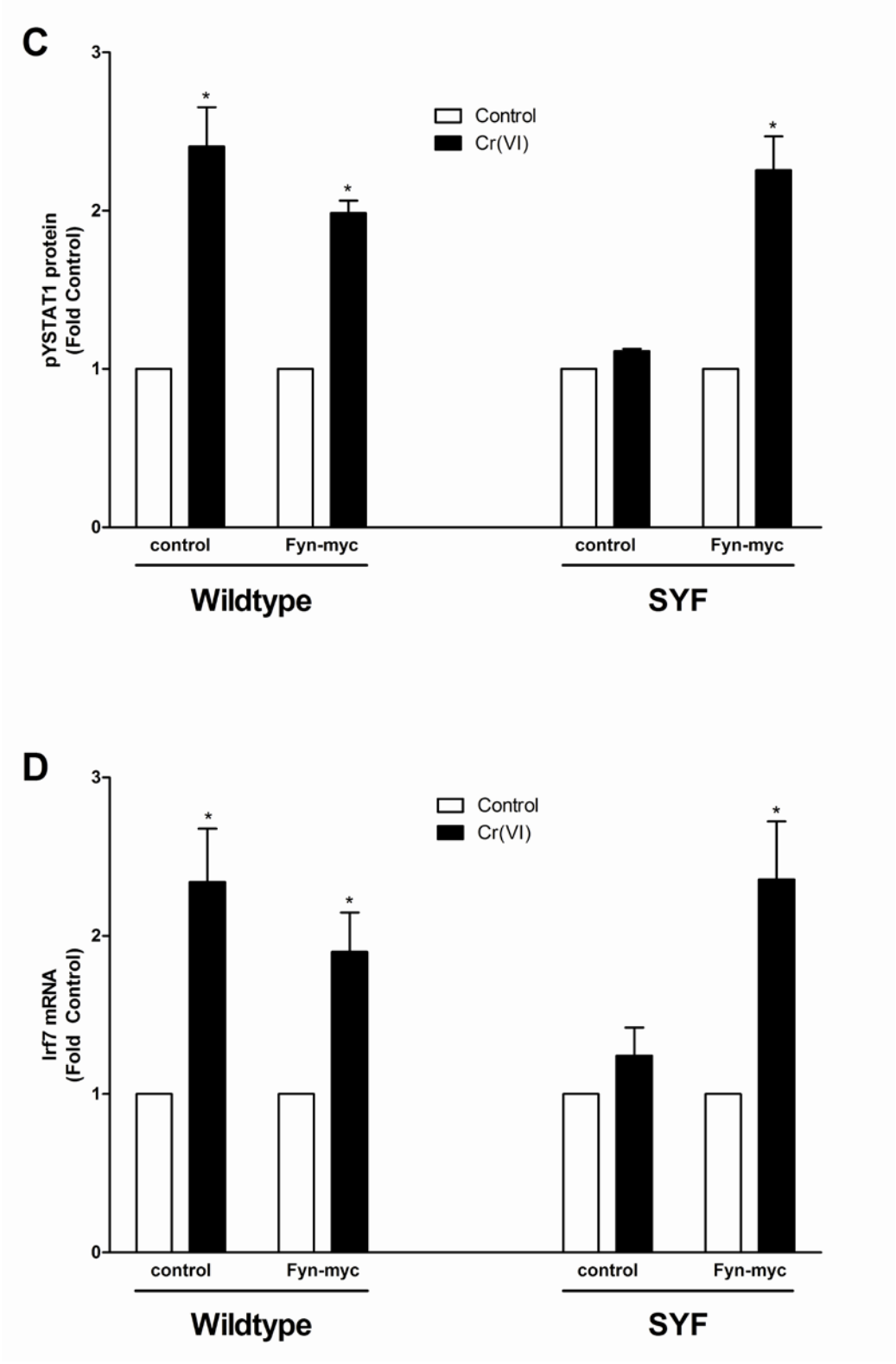

Figure 16. Fyn mediates Cr(VI)-activated STAT1 signaling in MEF cells.

Wildtype and SYF MEF cells were transiently transfected with either the control vector or the Fyn-myc expression vector. **A.** Total protein was isolated and Fyn and β-actin protein levels were determined by western analysis. **B.** Cells were treated with 5 μM Cr(VI) for 2 h and nuclear protein was isolated. pYSTAT1, total STAT1, and β-actin levels were determined by western analysis and a representative blot from a single experiment is shown. **C.** Density of the protein bands from three separate experiments were quantified with ImageJ software. **D.** Cells were treated with 5 μM Cr(VI) for 4 h and total RNA was isolated and Irf7 mRNA levels were measured by RT-PCR and normalized to the housekeeping gene, β-actin. Data is presented as mean ± SEM of fold control. * designates $p<0.05$ compared to respective untreated (control) cells.

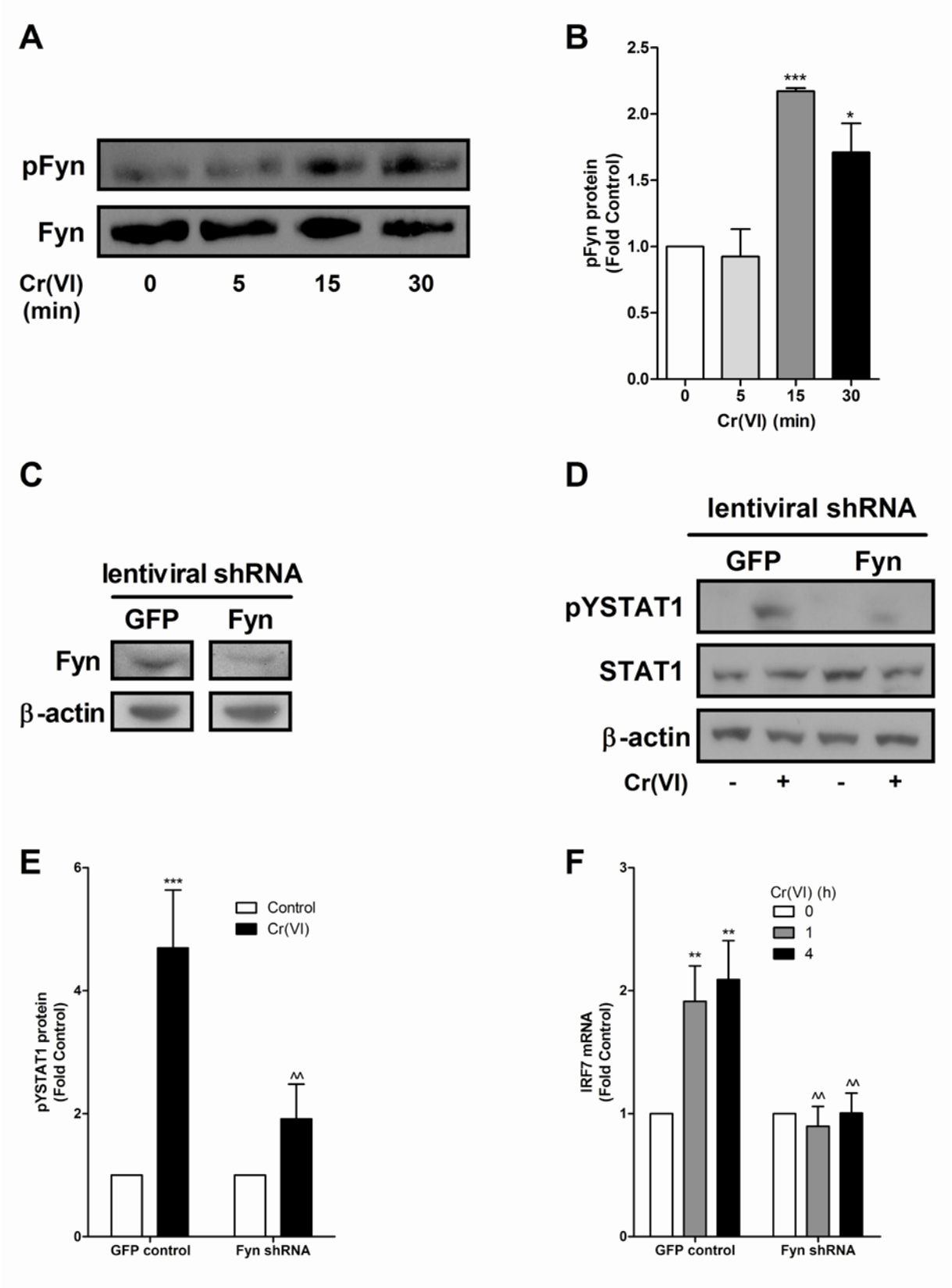

Figure 17. Fyn is required for Cr(VI) activation of STAT1 in BEAS-2B cells.

A. BEAS-2B cells were exposed to 5 μM Cr(VI) and total Fyn was immunoprecipitated from whole cell lysates and immunoblotted for pFyn and total Fyn. A representative blot from a single experiment is shown. **B.** Density of the protein bands from three separate experiments were quantified with ImageJ software. **C-F.** BEAS-2B cells were transduced with GFP-expression control or Fyn shRNA. **C.** Total protein was isolated and Fyn and β-actin protein levels were determined by western analysis. **D.** Cells were exposed to 5 μM Cr(VI) for 1 h and nuclear protein was isolated. pYSTAT1, total STAT1, and β-actin levels were determined by western analysis and a representative blot from a single experiment is shown. **E.** Density of the protein bands from three separate experiments were quantified with ImageJ software. **F.** Cells were exposed to 5 μM Cr(VI) for 4 h and total RNA was isolated and Irf7 mRNA levels were measured by RT-PCR and normalized to the housekeeping gene, RPL13A. Data is presented as mean ± SEM of fold control. *, **, and *** designate $p<0.05$, $p<0.01$, and $p<0.001$, respectively, compared to respective untreated (control) cells. ^^ designates $p<0.01$ compared to GFP-expression control-transfected cells.

3.4 DISCUSSION

Cr(VI) is a well known environmental and occupational hazard known to promote pulmonary diseases (6,13,42,47). However, the mechanisms of Cr(VI)-induced pulmonary diseases remain unresolved. The data in this study demonstrated that non-cytotoxic concentrations of Cr(VI) activated STAT1-dependent gene signaling and transactivation in airway epithelial cells. In addition, the SFK, Fyn, was identified as mediating Cr(VI)-stimulated STAT1. STAT1 activation can contribute to the development of pulmonary inflammatory diseases and its actions are localized to the airway epithelium (1), a target of Cr(VI) toxicity (11). Thus these novel findings may reveal mechanistic understanding of the molecular pathogenesis of Cr(VI)-induced lung diseases.

The current data and our previous report (55), demonstrate that airway epithelial cell exposure to Cr(VI) increases the transcriptional activation of members of the STAT family, including STAT1 and STAT3. STATs are activated through the phosphorylation of a conserved tyrosine residue in the C-terminus by JAKs or SFKs (52,55,142,143). We have previously demonstrated that the prolonged stimulation of STAT3 was mediated by the SFK, Lck (55). SFK activity was also involved in Cr(VI)-activated STAT1 signaling since pretreatment of cells with the SFK, PP2, prevented STAT1 activation and *IRF7* induction (Fig. 5A-C). Cr(VI) stimulation of STAT1 was attenuated in MEF cells null for Src, Yes, and Fyn (SYF) suggesting that Cr(VI) was activating one or more of these kinases (Fig. 5D-F). However, Cr(VI) only stimulated Fyn, and not Src or Yes, in A549 cells and directly activated affinity purified Fyn *in vitro* (22). Similarly, Cr(VI) stimulated the phosphorylation of Fyn in BEAS-2B cells (Fig. 7A-B). Furthermore, Cr(VI)-activated STAT1 and induction of Irf7 mRNA expression in SYF cells transiently transfected with human Fyn cDNA (Fig. 6B-D) indicating that Cr(VI) stimulates STAT1-dependent signaling through the activation of Fyn. Moreover, the Cr(VI) was lost in BEAS-2B cells transduced with Fyn shRNA compared to control cells (Fig. 7D-F). However, the mechanism for the increase in the catalytic activity of Fyn is unclear. There are 2 critical cysteine residues flanking 10 amino acids in the C-terminal lobe of several members of the SFKs that can bind metals to induce a conformational change (74). The effect of Cr(VI) on the binding to these cysteines has not been investigated, but remains an area of interest. Also, Fyn may not be directly activating STAT1 since both Fyn and Src phosphorylate another NRTK, c-Abl (147), which has been demonstrated to phosphorylate STAT1 (148,149) and is an indirect target of PP2. However, despite a possible intermediate step, the data indicate that activation of Fyn is the initial target of Cr(VI) signaling.

Activated STAT1 forms homodimers or heterotrimers with STAT2 and IRF9 in the ISGF3 complex to bind to GAS or ISRE consensus sequences, respectively (57). Cr(VI) selectively activated ISRE-driven transcription and had no effect on GAS transactivation (Fig. 1). Cr(VI)-stimulated ISRE transactivation and IRF7 mRNA induction was attenuated in BEAS-2B cells stably expressing STAT1 shRNA (Fig. 2), thus confirming the requirement of STAT1. IFN-mediated signaling is the most characterized pathway for STAT1 activation. Type I IFNs, such as IFN-α2, bind the cell surface type I IFN receptor to activate kinases to phosphorylate STAT1 (52,59). However, the signaling events activated by Cr(VI) are independent of type I IFN signaling since blocking IFNAR subunit of the receptor with a neutralizing antibody did not affect Cr(VI)-induced IRF7, but did prevent the IFN-α2 induction of the gene (Fig. 4). The negative control, normal mouse IgG antibody, had no effect indicating that the results observed were due to interfering with type I IFN-mediated signaling and not a nonspecific response (data not shown).

Although histone deacetylation is correlated with gene repression, HDAC activity is required for induction of ISRE-driven genes by facilitating the recruitment of RNA polymerase II to the promoter (61). HDAC activity is required for Cr(VI)-induced IRF7 transcripts since pre-incubating cells with NaB, a HDAC inhibitor, prevented both ISRE transactivation and *IRF7* induction (Fig. 3). Interestingly, Cr(VI) suppresses the induction of AHR receptor-transactivated genes by preventing HDAC release from their proximal promoters and interfering with the assembly of the transcriptional machinery (24).

In summary, the present study demonstrated that Cr(VI) activates STAT1 to form the ISGF3 complex and induce IRF7 mRNA expression. This activation is independent of type I interferon signaling, but is mediated by Fyn. STAT1 is a primary regulator of antiproliferative

and apoptotic responses (67,68) and plays a role in the pathogenesis of inflammatory lung diseases (1). Thus, these findings may provide critical insight into the mechanism of the development of Cr(VI)-related pulmonary diseases.

4.0 SIGNAL TRANSDUCER AND ACTIVATOR OF TRANSCRIPTION 1 (STAT1) IS ESSENTIAL FOR CHROMIUM SILENCING OF GENE INDUCTION IN HUMAN AIRWAY EPITHELIAL CELLS

The data presented in this chapter is published in *Toxicol Sci* 2009 Apr 29 [Epub ahead of print].

Antonia A. Nemec and Aaron Barchowsky

Department of Environmental and Occupational Health

University of Pittsburgh

Bridgeside Point Building

100 Technology Dr., Ste. 350

Pittsburgh, PA 15219

4.1 ABSTRACT

Cr(VI) promotes lung injury and pulmonary diseases through poorly defined mechanisms that may involve the silencing of inducible protective genes. The current study investigated the hypothesis that Cr(VI) actively signals through a STAT1-dependent pathway to silence Ni-induced expression of VEGFA, an important mediator of lung injury and repair. In human bronchial airway epithelial (BEAS-2B) cells, Ni induced *VEGFA* transcription by stimulating an ERK signaling cascade that involved Src kinase-activated Sp1 transactivation, as well as increased HIF-1α stabilization and DNA binding. Ni-stimulated ERK, Src, and HIF-1α activities, as well as Ni-induced VEGFA transcript levels were inhibited in Cr(VI) exposed cells. We previously demonstrated that Cr(VI) stimulates STAT1 to suppress VEGFA expression. In BEAS-2B cells stably expressing STAT1 shRNA, Cr(VI) increased VEGFA transcript levels and Sp1 transactivation. Moreover, in the absence of STAT1, Cr(VI) and Ni co-exposures positively interacted to further increase VEGFA transcripts. This study demonstrates that metal-stimulated signaling cascades interact to regulate transcription and induction of adaptive or repair responses in airway cells. In addition, the data implicate STAT1 as a rate limiting mediator of Cr(VI)-stimulated gene regulation and suggest that cells lacking STAT1, such as many tumor cell lines, have opposite responses to Cr(VI) relative to normal cells.

4.2 INTRODUCTION

Chronic inhalation of Cr(VI) and Ni are well known environmental and occupational hazards that promote pulmonary diseases (42,43,150). Mixed exposures are common in metal industries (37,42,47) and human epidemiological studies have associated mixed exposures with increased risks of lung diseases compared to exposure to the individual metals (37,42,47-49). However, there is limited mechanistic understanding of the cellular and molecular pathogenic actions of the individual metals or their interactions in airway epithelial cell injury and repair processes.

VEGFA expression is well-established in vascular biology for its role in angiogenesis and vascularization. However, its role in the airway epithelium and lung injury repair remains unclear. Epithelial cells are the major source of VEGFA in the lung (99) and VEGFA is crucial for normal lung development (99) and airway epithelial cell proliferation (102). Yet, its role in lung injuries and disease remains controversial (106). Elevated VEGFA promotes pulmonary edema in the initial phase of inflammatory diseases, such as asthma, chronic bronchitis, and ALI (105,106). However, in later phases, increased VEGFA levels are associated with the resolution of ALI (114). VEGFA levels are decreased in patients with bronchopulmonary dysplasia, emphysema, and during ischemia and reperfusion correlating to epithelial cell damage (105,108). Moreover, in both *in vivo* skin and *in vitro* lung epithelial cell models, VEGFA promotes wound repair and elicits anti-apoptotic responses (113,115).

The main inducers of VEGFA expression are hypoxia (151) and other stimuli that stabilize HIF-1α, which transactivates the *VEGFA* promoter (116). These stimuli include a variety of metals, including Ni (118,119,122,141). Ni stabilizes HIF-1α primarily by direct inhibition of the prolyl hydroxylases that mark HIF-1α for proteosomal degradation (122). However, Ni can also signal through ERK and PI3K to increase both HIF-1α stability and its

transactivation of genes (118,119). HIF-1α cooperates with other transcription factors (e.g. Sp1, activator protein 1 (AP-1), STAT3) (124-126) and Sp1 transactivation is required for full induction of the *VEGFA* promoter (129). Unlike STAT3, STAT1, stimulated by IFN, is a negative regulator of VEGFA (68) and the loss of STAT1 results in IFN stimulating transcriptional activation of the *VEGFA* promoter (146,152). Once STAT1 is activated, it forms the complex, ISGF3 which inhibits IFN-β-stimulated genes by interfering with the assembly of the transcriptional machinery on the promoters (62,63).

Exposure to Cr(VI) silences the induction of protective genes induced by polycyclic aromatic hydrocarbons and metals by activating signaling pathways that alter transcriptional activity (19,24). We previously reported that Cr(VI) stimulates STAT1 phosphorylation and nuclear translocation in human airway epithelial cells (55). Therefore, the current studies examined the hypothesis that Cr(VI) suppresses Ni-induced VEGFA expression by stimulating STAT1-dependent gene repression.

4.3 RESULTS

4.3.1 Cr(VI) inhibits Ni-induced VEGFA mRNA and protein release

Cr(VI) often suppresses gene inducibility, including induction of protective genes in the lung and metal-stimulated gene induction in cultured lung cells (19). The data in Figure 18 are consistent with this observation and confirm that Cr(VI) represses both Ni-induced VEGFA mRNA and protein release in BEAS-2B cells, but has no effect on basal expression.

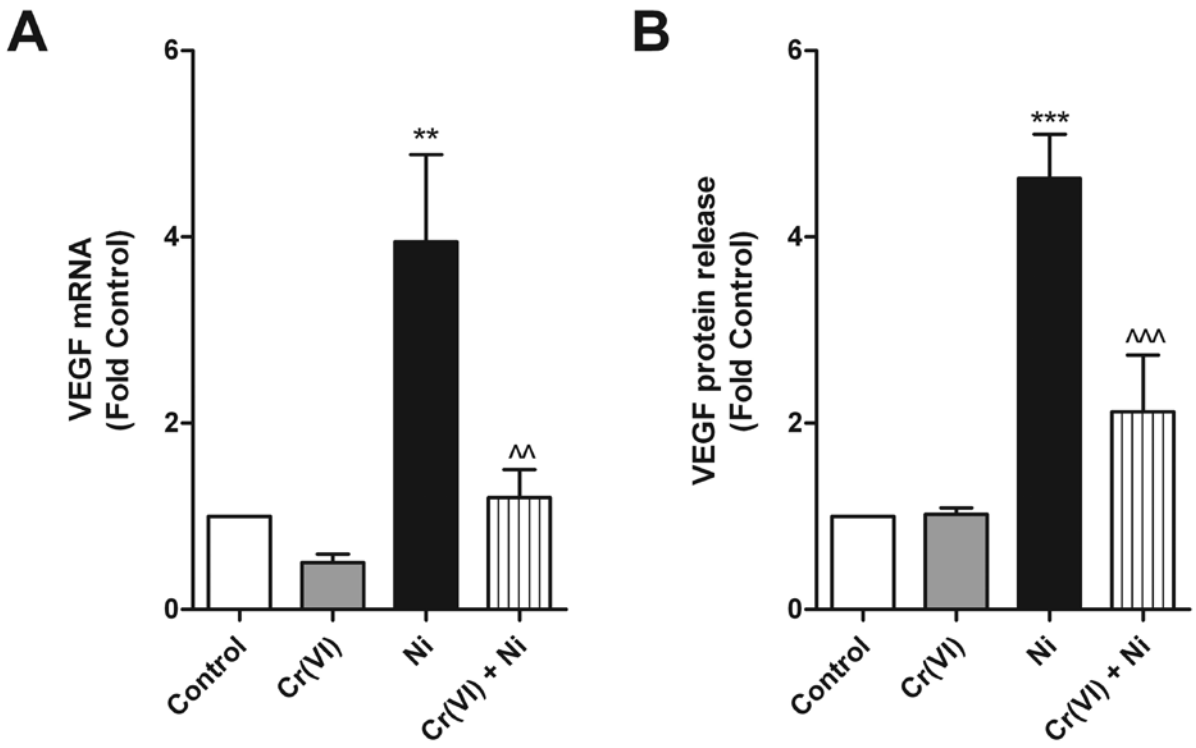

Figure 18. Cr(VI) inhibits Ni-induced VEGFA mRNA and protein levels.

BEAS-2B cells were exposed to 5 µM Cr(VI), 200 µM Ni, or Cr(VI) for 2 h prior to adding 200 µM Ni for **A.** 24 h and **B.** 48 h. **A.** VEGFA mRNA levels were measured by real-time PCR. **B.** Conditioned medium was collected and VEGF protein release was measured by ELISA. Data represent means ± SEM of fold control (n=3). ** and *** designate $p<0.01$ and $p<0.001$, respectively compared to untreated cells (control); ^^ and ^^^ designate $p<0.01$ and $p<0.001$, respectively compared to cells treated with Ni alone.

4.3.2 Ni induction of VEGFA mRNA requires ERK-dependent Src and HIF-1α activation

To identify the mechanism for the negative interaction between Cr(VI) and Ni in the induction of VEGFA, we first characterized the Ni-stimulated signaling cascades leading to this induction. Ni activates both ERK- and HIF-1α signaling pathways in BEAS-2B cells (119) and both pathways are implicated in VEGFA transactivation (118,121,153). To identify the role of the ERK relative to other kinases in Ni-induced VEGFA expression, BEAS-2B cells were pretreated with inhibitors of ERK (U0126), p38 (SB203580), PI3K (wortmannin), or SFK (PP2) prior to exposure to Ni. Inhibition of ERK and SFK prevented Ni-induced VEGFA mRNA level whereas inhibiting p38 and PI3K had no effect (Figure 19A-B). Note that there is no statistical difference between VEGFA transcript levels in the presence of Ni plus U0126 or PP2 relative to U0126 or PP2 alone. This would suggest that the two inhibitors are equally effective in providing a complete or at least equal block of Ni-induced VEGFA. ERK appeared to be upstream of SFK activation, since Ni-stimulated Src phosphorylation was absent in cells pretreated with U0126 (Figure 19C). As demonstrated for Ni-induction of the *SERPIN1* promoter (119), ERK was required for maximal Ni-stimulated HIF-1α stabilization and transactivation of *VEGFA* (Figure 20A). In addition, Src was also found to be essential for Ni-induction of the gene (Figure 19B), but not for Ni-stimulated HIF-1α stabilization (Figure 20B). These data indicate that both HIF-1α and Src are required for Ni-induced VEGFA mRNA expression and that they are divergent pathways downstream of ERK. The *VEGFA* promoter contains numerous response elements that might be targets of ERK signaling, including Sp1 (129,154,155). A role for Sp1 in Ni-induced transactivation was demonstrated by Ni stimulating

the activity of a Sp1-driven luciferase reporter construct by 3.764 ± 0.6853 fold compared to untreated cells. Together, these data suggest that the ERK-regulated pathways activated by Ni are both capable of functional gene activation that converge to induce the *VEGFA* promoter.

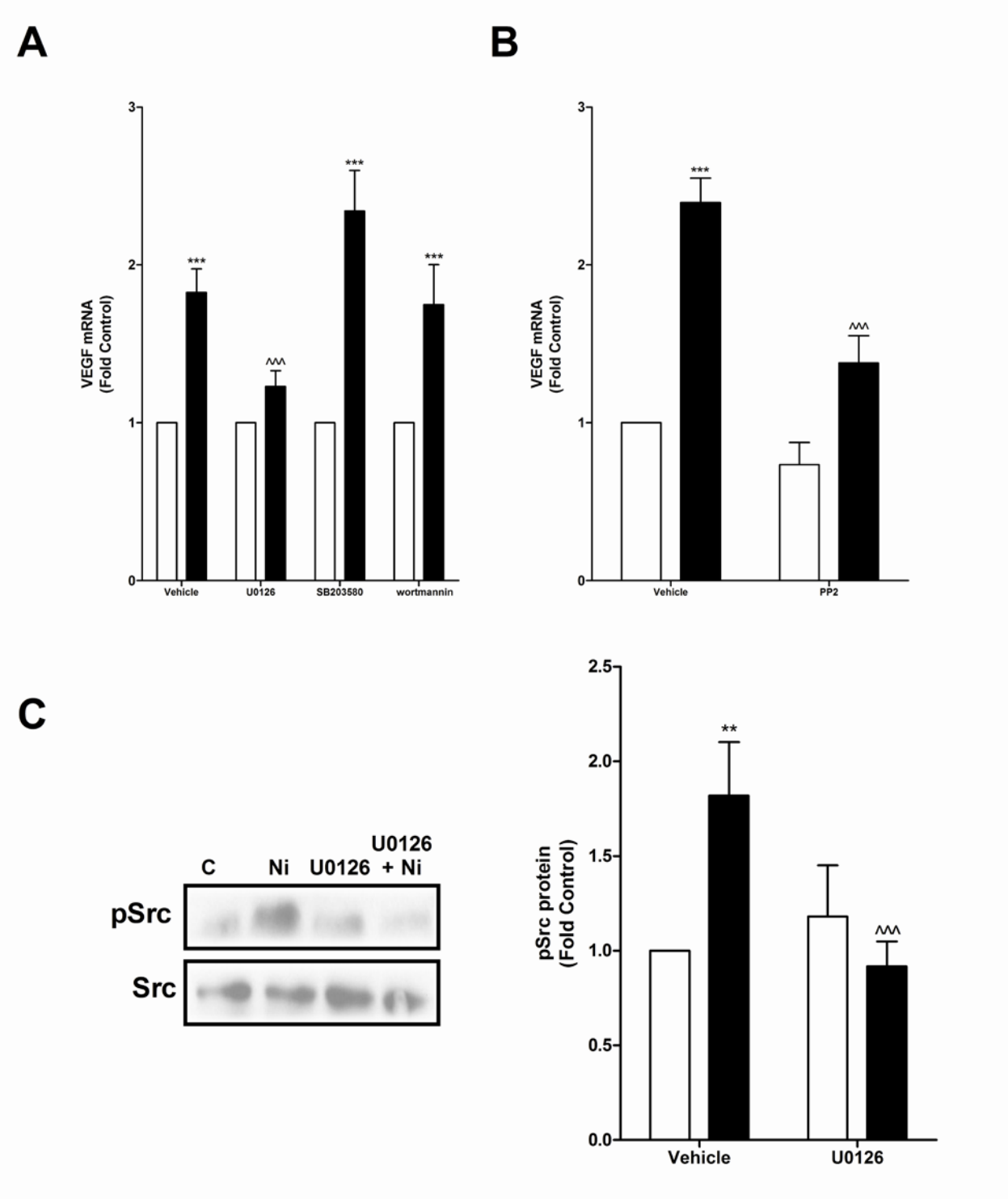

Figure 19. ERK mediates Ni-induced VEGFA mRNA levels.

BEAS-2B cells were pretreated with **A.** 10 µM U0126, 20 µM SB203580, or 1 µM wortmannin or **B.** 10 µM PP2 prior to adding vehicle (white bars) or 200 µM Ni (black bars) for 24 h. VEGFA mRNA levels were

measured by real-time PCR. Data represent means ± SEM of fold control (n=3). **C.** BEAS-2B cells were pretreated with 10 μM U0126 prior to adding vehicle (white bars) or 200 μM Ni (black bars) for 30 min. Total Src was immunoprecipitated from whole cell lysates and immunoblotted for pSrc. ImageJ software was used to quantify the intensity of the bands and data represent means ± SEM of fold control (n=3). ** and *** designate $p<0.001$ and $p<0.001$, respectively compared to untreated cells (control). ^^^ designates $p<0.001$ compared to cells treated with Ni alone.

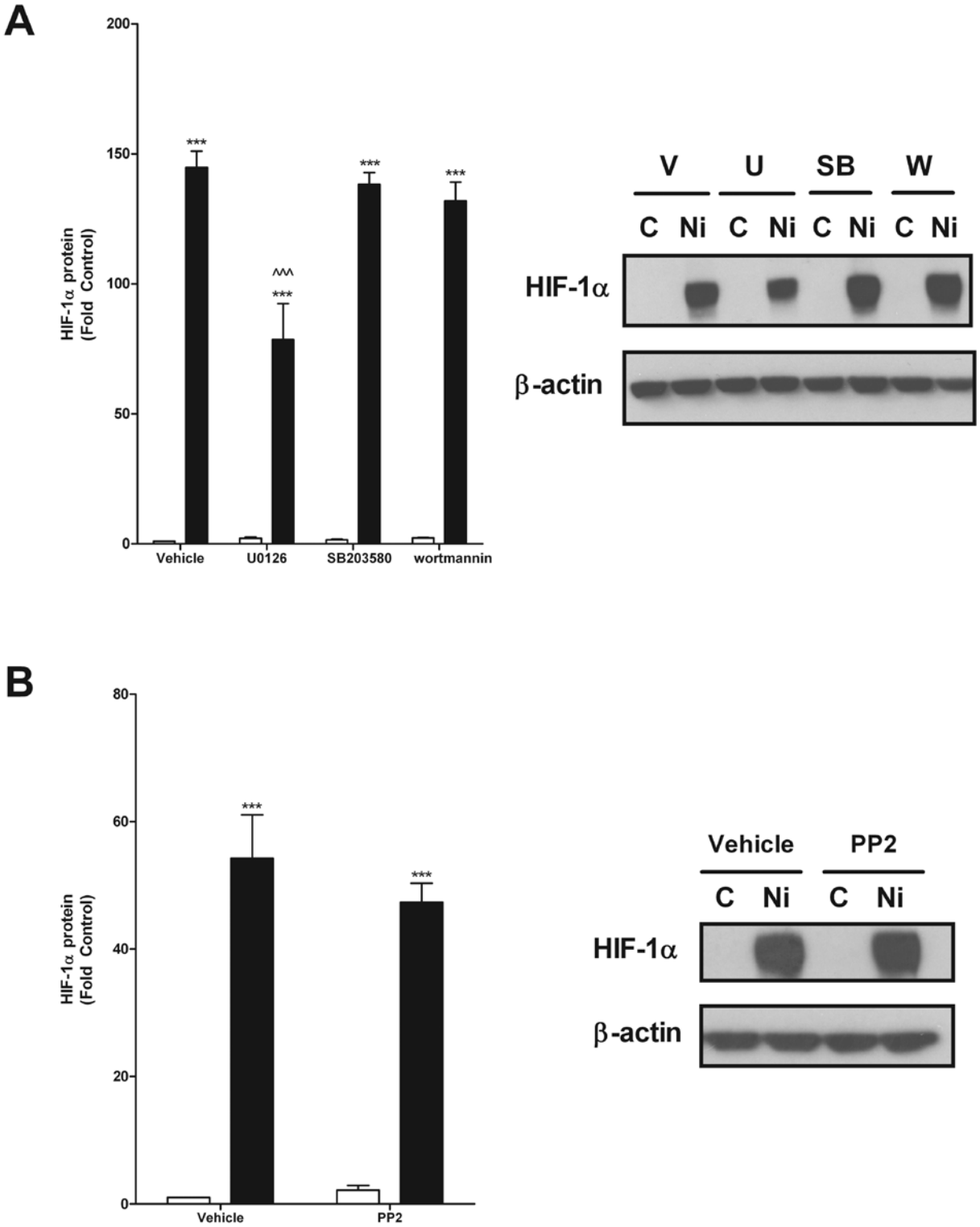

Figure 20. Ni-induced HIF-1α stabilization requires ERK.

BEAS-2B cells were pretreated with **A.** 10 μM U0126, 20 μM SB203580, or 1 μM wortmannin or **B.** 10 μM PP2 prior to adding vehicle (white bars) or 200 μM Ni (black bars) for 24 h. Total protein was isolated and HIF-1α and β-actin protein levels were determined by western analysis. ImageJ software was used to quantify the intensity of the bands. Data represent means ± SEM of fold control (n=3). *** designates $p<0.001$ compared to untreated cells (control); ^^^ designates $p<0.001$ compared to cells treated with Ni alone.

4.3.3 Cr(VI) inhibits Ni-activated ERK signaling

Exposure to Cr(VI) had no effect on the basal ERK or Src phosphorylation states (Figure 21), and Cr(VI) did not affect basal HIF-1α protein levels or the activity of a HRE-driven luciferase reporter construct (Figure 22). In contrast, Cr(VI) inhibited Ni-stimulated ERK and Src activation (Figure 21), HIF-1α protein expression (Figure 22A), and transactivation of the HRE reporter construct (Figure 22B). The pattern of inhibition is consistent with Cr(VI) preventing Ni from activating ERK, the upstream kinase of the divergent signaling pathways.

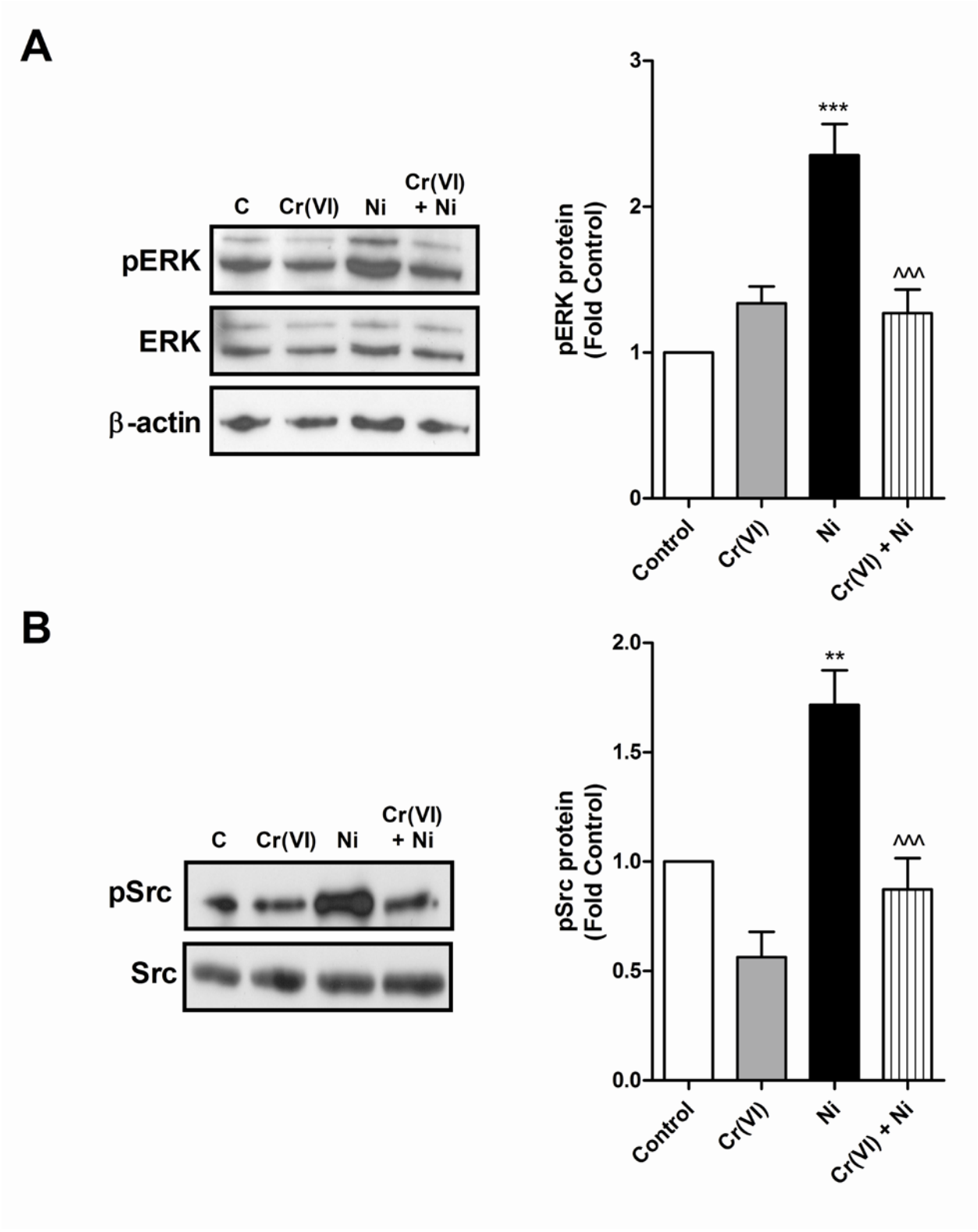

Figure 21. Cr(VI) abrogates Ni-stimulated ERK signaling.

A. BEAS-2B cells were exposed to 5 µM Cr(VI), 200 µM Ni, or Cr(VI) for 2h prior to adding 200 µM Ni for 5 min. Total protein was isolated and phosphorylated ERK (pERK), total ERK, and β-actin protein levels were determined by western analysis. **B.** BEAS-2B cells were exposed to 5 µM Cr(VI), 200 µM Ni, or Cr(VI) for 2h prior to adding 200 µM Ni for 30 min. Total Src was immunoprecipitated from whole cell lysates and immunoblotted for pSrc. ImageJ software was used to quantify the intensity of the bands and data represent means ± SEM of fold control (n=3). ** and *** designate $p<0.01$ and $p<0.001$, respectively compared to untreated cells (control); ^^^ designates $p<0.001$ compared to cells treated with Ni alone.

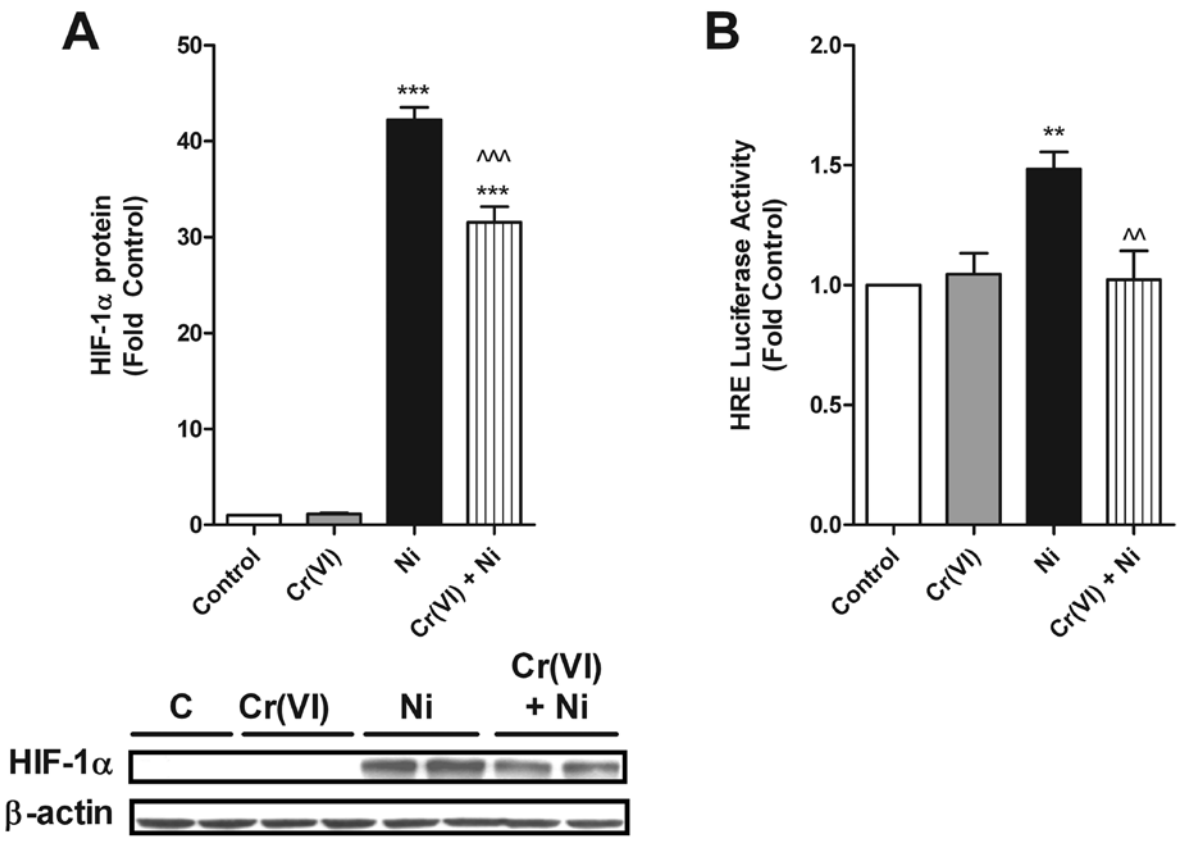

Figure 22. Cr(VI) partially inhibits Ni-induced HIF-1α stabilization and HRE transactivation.

A. BEAS-2B cells were exposed to 5 µM Cr(VI), 200 µM Ni, or Cr(VI) for 2 h prior to adding 200 µM Ni for 24 h. Total protein was isolated and HIF-1α and β-actin protein levels were determined by western analysis. ImageJ software was used to quantify the intensity of the bands. **B.** BEAS-2B cells were transiently transfected with HRE-luc and eGFP. After 24 h, cells were exposed to 5 µM Cr(VI), 200 µM Ni, or Cr(VI) for 2 h prior to adding 200 µM Ni for 8 h. Relative luciferase activity of HRE-luc was normalized to eGFP. Data represent means ± SEM of fold control (n=3). ** and *** designate $p<0.01$ and $p<0.001$, respectively, compared to untreated cells (control); ^^ and ^^^ designate $p<0.01$ and $p<0.001$, respectively, compared to cells treated with Ni alone.

4.3.4 STAT1 signaling is essential for Cr(VI) repression of VEGFA

STAT1 negatively regulates *VEGFA* induction (146) and transactivation by Sp1 (63). To investigate a role for Cr(VI)-stimulated STAT1 in repressing *VEGFA* inducibility, we generated BEAS-2B cell lines stably expressing either scrambled (shNC) or STAT1 (shSTAT1) shRNA. Western blot analysis in Figure 23A verifies STAT1 protein knockdown in shSTAT1 cells relative to shNC cells. In contrast to the response of parental BEAS-2B or the shNC cells, VEGFA mRNA levels increased in shSTAT1 cells within 4 h of Cr(VI) exposure (Figure 23C). In addition, a 2 h pretreatment of shSTAT1 cells with Cr(VI) enhanced VEGFA mRNA levels induced by Ni (Figure 23B) while the same treatment in shNC cells resulted in the same Cr(VI) inhibition of *VEGFA* inducibility observed in the parental BEAS-2B cells (Figure 18A and 23C). In addition, Cr(VI) had no effect on Ni-induced HIF-1α protein in the shSTAT1 cells relative to its effect in shNC cells (Figure 24A). Finally, Cr(VI) increased the activity of the Sp1-driven luciferase reporter construct in shSTAT1 cells, whereas there was no Cr(VI) effect on luciferase activity in the shNC cells (Figure 24B). The STAT1-containing complex, ISGF3, is known to indirectly inhibit IFN-β-inducible genes most likely by activating or increasing expression of an inhibitory protein (62,63). To examine this hypothesis that Cr(VI) stimulates ISGF3 induction of an inhibitor, parental BEAS-2B cells were exposed to Cr(VI) in the presence or absence of cycloheximide to inhibit protein synthesis. Data in Figure 23D confirm the effect of on basal VEGFA expression in control cells and demonstrates that Cr(VI) increased VEGFA mRNA levels when protein synthesis was inhibited. These data suggest that Cr(VI) signals through STAT1 to repress VEGF mRNA expression and that STAT1 may exert its inhibitory effects by increasing expression of protein repressor of *VEGFA* induction.

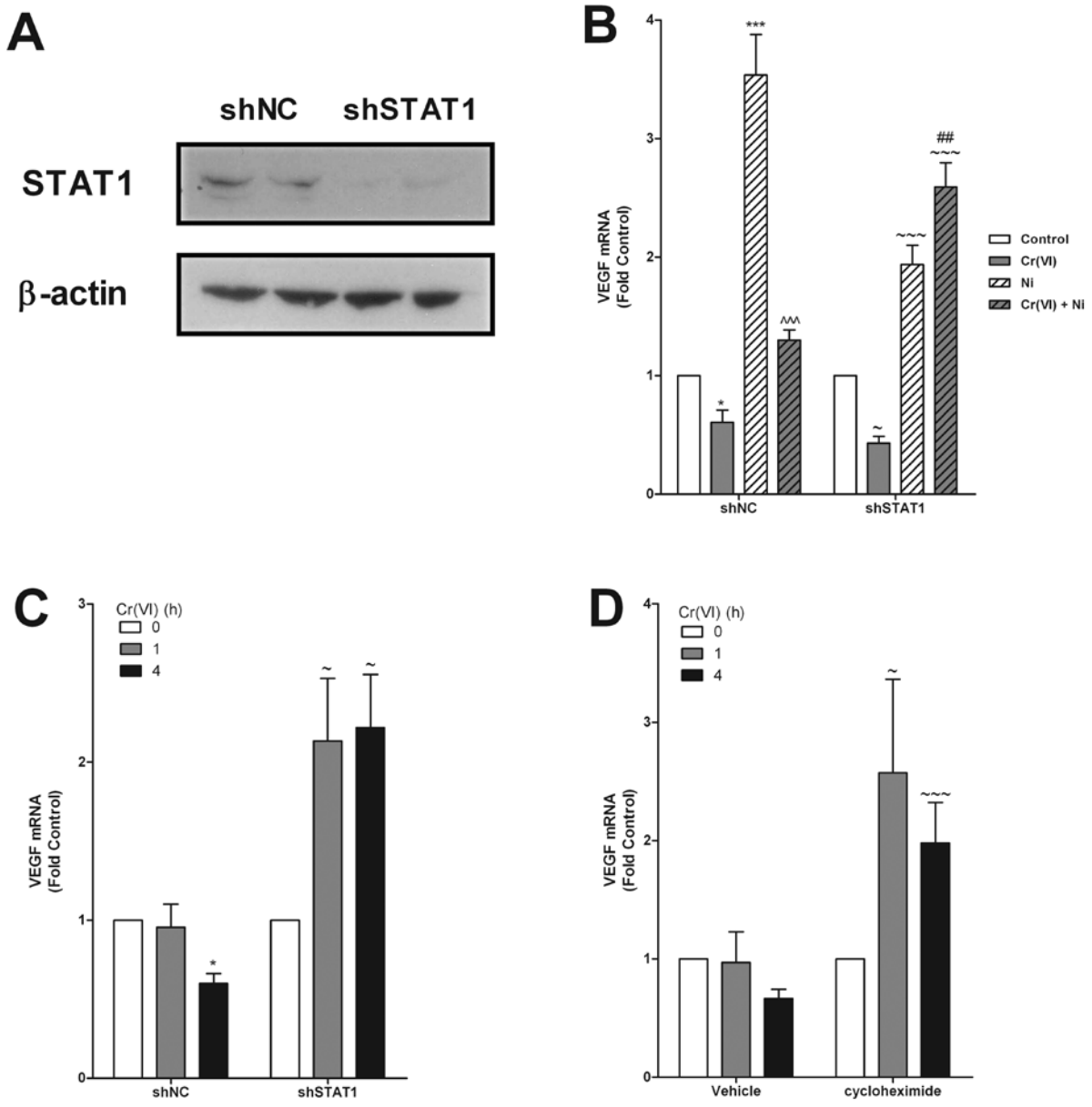

Figure 23. STAT1 is required for Cr(VI) suppression of VEGFA induction.

A. Total protein was isolated from BEAS-2B cell lines stably expressing either scrambled (shNC) or STAT1 (shSTAT1) shRNA and total STAT1 and β-actin protein levels were determined by western analysis. **B.** shNC and shSTAT1 cells were exposed to 5 µM Cr(VI), 200 µM Ni, or Cr(VI) for 2 h prior to adding 200 µM Ni for 24 h. **C.** shNC and shSTAT1 cells were exposed to 5 µM Cr(VI) for the indicated times. **D.** Parental BEAS-2B cells were pretreated with 10 µg/ml of cycloheximide for 5 min prior to exposure to 5 µM Cr(VI) for the indicated

times. Total RNA was isolated and VEGFA mRNA levels were measured by real-time PCR. Data represent mean ± SEM of fold control (n=3). * and ~ designate $p<0.05$, *** and ~~~ designate $p<0.001$ compared to respective untreated cells (control); ## and ^^^ designate $p<0.01$ and $p<0.001$, respectively, compared to respective cells treated with Ni alone.

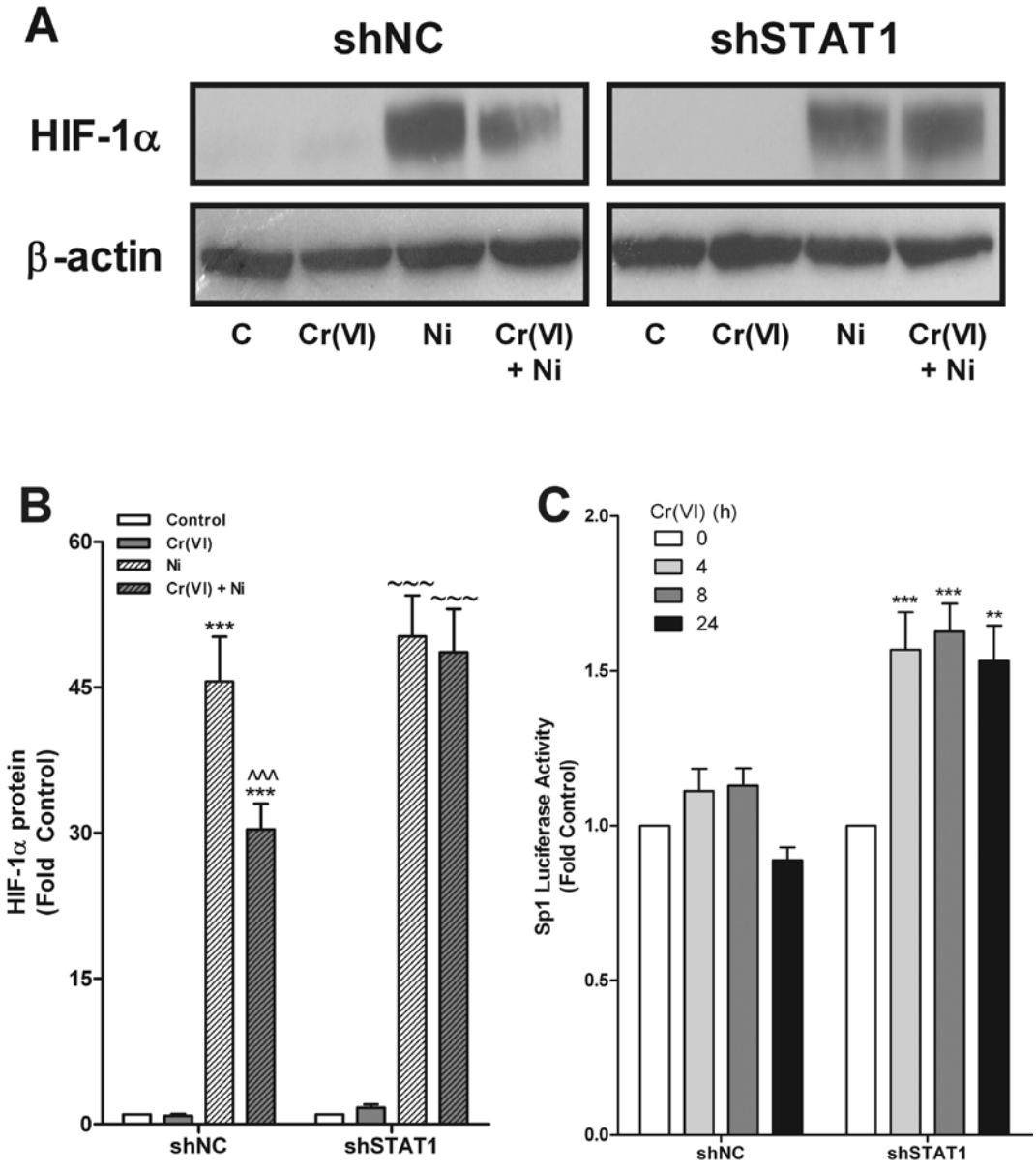

Figure 24. STAT1 represses HIF-1α protein stabilzation and Sp1 transactivation.

A. BEAS-2B cell lines stably expressing either scramble (shNC) or STAT1 (shSTAT1) shRNA were exposed to 5 μM Cr(VI), 200 μM Ni, or Cr(VI) for 2 h prior to adding 200 μM Ni for 24 h. Total protein was isolated and HIF-1α and β-actin protein levels were determined by western analysis. **B.** Density of the protein

bands from three separate experiments were quantified using ImageJ software and is presented as mean ± SEM of fold control (n=3). *** and ~~~ designate $p<0.001$ compared to the respective untreated cells (control). ^^^ designates $p<0.001$ compared to cells treated with Ni alone. **C.** shNC or shSTAT1 cells were transiently transfected with Sp1-luc and eGFP and exposed to 5 µM Cr(VI) for the indicated times. Relative luciferase activity of Sp1-luc was normalized to eGFP. Data represent means ± SEM of fold control (n=3). ** and *** designate $p<0.01$ and $p<0.001$, respectively, compared to untreated cells (control).

4.4 DISCUSSION

Environmental and occupational exposure to Cr(VI) and Ni cause pulmonary diseases (43,150) and although epidemiological studies associate exposure to metal mixtures with exacerbated lung injury (37,42,47-49), there are few studies investigating the molecular interaction of these metals. Cr(VI) readily enters airway cells through anion channels where it is rapidly reduced to Cr(III) (reviewed in (6)) and exerts effects on both cell signaling processes and DNA. Exposure to Cr(VI) rarely affects the expression of constitutive genes (15,24), but silences inducible gene expression *in vivo* and *in vitro* (15,19). While there are substantial amounts of data in the literature suggesting that Cr(VI)-induced DNA adducts and ROS generated through the reduction of Cr(VI) are responsible for gene silencing (5,16,17,20), there is also ample evidence suggesting that Cr(VI) exerts epigenetic effects in silencing gene induction through altering transcriptional complexes (19,24). In the present studies, we examined the effect of Cr(VI) on basal and Ni-induced signal transduction and VEGFA transcript levels in a pertinent lung target cell using concentrations relevant to occupational exposures. These concentrations are not cytotoxic in this cell model ((55) and data not shown), but promote both positive and negative signaling effects (19,55). These studies are the first to identify signaling through STAT1 as an essential

regulatory mechanism for Cr(VI)-stimulated gene suppression. These data may also explain the discrepancies observed in other studies where Cr(VI) induced *VEGFA* in cancer cells whose functional STAT1 signaling status is questionable (121) .

The major stimulus of Ni-induced VEGFA mRNA and protein is HIF-1α stabilization (6,118,119). However, HIF-1α signaling could not be the dominant or sole pathway for Ni-induced VEGFA in the BEAS-2B cell model, since inhibiting Src completely blocked VEGFA mRNA without affecting HIF-1α stability (Figures 19B and 20B). Although ERK, p38, PI3K, and Src have all been implicated as upstream kinases in VEGFA induction in response to a variety of stimuli (118,121,123), our data indicates Ni signals through ERK and Src to induce VEGFA (Figure 19A-B). Ni stimulated ERK phosphorylation within 5 min of exposure in contrast to Src phosphorylation which required a 30 min exposure to Ni (Fig. 19 and data not shown) indicating that ERK is upstream of Src although it is not directly phosphorylating Src. The signaling events leading to Src activation from ERK are unclear and beyond the scope of this paper. Furthermore, the upstream dominance of ERK was demonstrated by U0126 inhibiting both Src phosphorylation (Figure 19C) and HIF-1α stabilization (Figure 20A). HIF-1α cooperates with other transcription factors to transactivate a number of different promoters (119,125,156) and the data are consistent with cooperation with Sp1 for full ERK-mediated induction of *VEGFA* (129). While the data implicate ERK as the primary divergence point for the cooperating Ni-stimulated signaling pathways, these studies did not investigate the mechanism for Ni-stimulated phosphorylation of ERK or potential interactions of Ni and Cr(VI) signaling on upstream kinases. In addition, Ni activation of ERK may be dependent on cell type or cell culture conditions since others fail to observe Ni stimulation of ERK when basal levels are high or in transformed airway epithelium (157).

Cr(VI) completely blocked both Ni-induced ERK and Src phosphorylation and VEGFA mRNA expression (Figs. 18-19). We previously demonstrated that Cr(VI) had an inhibitory effect on both ERK and Src activities (22) and these data suggest that Cr(VI) interferes with their activation by Ni to prevent *VEGFA* induction. However, Cr(VI) only partially inhibits Ni-induced HIF-1α protein stabilization (Figure 22A), since Ni-induced HIF-1α stabilization mostly results from a direct inhibitory effect on the proline hydroxylases marking the protein for ubiquitination and degradation (122). However, Ni-stimulated activity of the HRE reporter construct was completely inhibited by Cr(VI) (Figure 22B). The HRE reporter construct does not contain additional *cis* elements that might cooperate with HIF-1α binding to the HRE sites. Thus, the data are consistent with previous observations that phosphorylation by ERK-mediated signaling cascades is required for full transactivation potential of Ni-activated HIF-1α (119). Moreover, Cr(VI) had a greater effect on Ni-activated ERK and Src compared to HIF-1α indicating that ERK-mediated Src signaling and Sp1 transactivation are more crucial for Ni-induced *VEGFA*.

STAT1 is a member of the STAT transcription factor family. Although STAT3 has been implicated as an upstream inducer of VEGFA (124), STAT1 is required for IFN-mediated inhibition of VEGFA (146). Cr(VI) activates STAT1 phosphorylation and nuclear translocation in parental BEAS-2B cells; although the mechanism of this activation remains uncharacterized (55). The current findings support the hypothesis that STAT1 activation is essential for Cr(VI) to repress gene expression. In addition, they also demonstrate that STAT1 activation blocks the Cr(VI) signals that induce *VEGFA* in shSTAT1 cells or that positively interact with Ni signaling (Figure 23B-C). It is likely that STAT1 suppresses the signaling for activation of factors that cooperate with HIF-1α or sequesters these factors by STAT1-induced protein complexes limit

Cr(VI) induction of *VEGFA* in the parental cells. Recent evidence suggests that IFN-β activated a STAT1-containing ISGF3 complex to inhibit Sp1 recruitment or binding of Sp1 and co-activators (e.g. CBP, p300) to inducible promoters (62,63). The exact mechanism of this inhibition is uncharacterized. Neither ISGF3 nor any of the individual protein components bind directly to the promoters to block transcription, but rather, it is possible that STAT1 stimulates an inhibitory protein that interferes with the binding of Sp1. In the absence of protein synthesis, Cr(VI)-induced VEGFA mRNA expression (Figure 23D); suggesting that a protein induced by STAT1 transcriptional complexes represses *VEGFA* induction. The identity of this protein remains unknown, but is being actively investigated. Since Cr(VI) stimulates Sp1 in the absence of STAT1 (Figure 24B) and Sp1 activation is essential for VEGFA expression, it is probably that the induced inhibitory protein represses Sp1-dependent transactivation and induction of the *VEGFA*.

The antiviral and anti-proliferative effects of IFN-α and IFN-β are limited or reversed to proliferative responses in cells that lack STAT1 (152). STAT1 is deleted in a number of cancers (146) and without STAT1 activation, IFN stimulation of STAT3 and 5 or their constitutive activation provides a cell survival advantage and can cause transformation (152). Others reported that Cr(VI) stabilizes HIF-1α protein and induces *VEGFA* in prostate cancer cells (121) and we show that Cr(VI) has opposite effects on HIF-1α protein and *VEGFA* in shNC and shSTAT1 cell lines (Figures 23B-C and 24A). Cr(VI) also has opposite effects on *HMOX1* inducibility in lung cell lines that differ in transformation status (19,158). Thus, an implication of these findings is that, as with IFN responses, Cr(VI) has opposite signaling effects and pathogenic actions in normal cells compared to transformed cells that lack functional STAT1. In the normal cells, Cr(VI) would limit inducibility of protective genes or genes involved in injury

repair. In transformed cells, Cr(VI) alone or in combination with other stimuli like Ni might promote proliferation and tumor growth by increasing VEGFA or other growth factor expression.

In summary, this study has identified STAT1 activation as an essential and pivotal mechanism in Cr(VI)-stimulated gene regulation. In normal cells exposed to metal mixtures, Cr(VI) interferes with Ni-stimulated ERK signaling to compromise the induction of protective genes which may exacerbate pulmonary diseases. Loss of STAT1-mediated transcriptional repression unmasks Cr(VI)-stimulated gene induction and enhancement of the Ni response. Thus, the data support the conclusion that pathogenic actions of Cr(VI) signaling in lung cells and interaction of this signaling with that of other metals in mixtures depend on the STAT1 status of the airway cells.

5.0 NICKEL MOBILIZES INTRACELLULAR ZINC TO INDUCE METALLOTHIONEIN IN HUMAN AIRWAY EPITHELIAL CELLS

The data presented in this chapter is published in

Am J Respir Cell Mol Biol 2008 Dec 18 [Epub ahead of print].

Antonia A. Nemec, George D. Leikauf, Bruce R. Pitt, Karla J. Wasserloos, and Aaron Barchowsky

Department of Environmental and Occupational Health

University of Pittsburgh

Bridgeside Point Building

100 Technology Dr., Ste. 350

Pittsburgh, PA 15219

5.1 ABSTRACT

We recently reported that induction of MT was critical in limiting Ni-induced lung injury in intact mice. Nonetheless, the mechanism by which Ni induces MT expression is unclear. We hypothesized that the ability of Ni to mobilize Zn may contribute to such regulation and therefore, we examined the mechanism for Ni-induced MT2A expression in human airway epithelial (BEAS-2B) cells. Ni induced MT2A transcript levels and protein expression by 4 h. Ni also increased the activity of a MRE promoter luciferase reporter construct suggesting that Ni induces MRE binding of the MTF-1. Exposure to Ni resulted in the nuclear translocation of MTF-1 and Ni failed to induce MT in MEFs lacking MTF-1. As Zn is the only metal known to directly bind MTF-1, we then showed that Ni increased a labile pool of intracellular Zn in cells as revealed by FACS using the Zn-sensitive fluorophore, FluoZin-3. Ni-induced increases in MT2A mRNA and MRE-luciferase activity were sensitive to the Zn chelator, TPEN, supporting an important role for Zn in mediating the effect of Ni. Although neither the source of labile Zn nor the mechanism by which Ni liberates labile Zn was apparent, it was noteworthy that Ni increased intracellular ROS. Although both NAC and AA decreased Ni-induced increases in ROS, only NAC prevented Ni-induced increases in MT2A mRNA suggesting a special role for interactions of Ni, thiols, and Zn release.

5.2 INTRODUCTION

Ni is a well-known environmental and occupational hazard present in air pollution (33), cigarette smoke (35), diesel exhaust (36), and welding fumes (37,38). Ni is a common component of alloy metals and is used in electroplating, stainless steel, coins, and jewelry (37,42,159). Inhalation of Ni has been associated with lung and nasal cancers (38,48,160,161), fibrosis, and various other cardiopulmonary diseases (33,38), including acute lung injury (37,45).

MT are highly conserved, small molecular weight, cysteine-rich proteins. In humans, the MT-gene family contains more than 10 members of which MT2A is most commonly expressed (reviewed in (75)). MT sequesters metals and thus maintains Zn homeostasis and protects cells from metal toxicity (76,79,80). MT also appears to be important in limiting injury due to reactive oxygen and nitrogen species (84). MT transcripts increase during hyperoxic lung injury (86), in response to LPS and diesel exhaust particles ((85), and in ovalbumin-induced airway inflammation (87). Furthermore, MT transgenic mice are resistant to Ni- (44) and Cd- induced toxicity (75), whereas MT null mice are more susceptible to injury from exposure to Ni (44), Cd (75), or LPS (83). Thus, MT is protective against lung injury (162) and may even serve as a therapeutic target in airway diseases (87).

MT is induced by and capable of binding 18 different metals including Zn and Ni (reviewed in (81)), but the precise mechanism of its induction is only known for Zn. Zn-induced MT2A is primarily transcriptionally regulated by Zn causing the MTF-1 to bind multiple copies of the MRE in the promoter region (75,90). The interaction of Zn with MTF-1 is unique since this Zn finger protein is directly activated only by Zn relative to other metals (163). Since MT plays an essential role in protecting the lung from Ni-induced injury, we investigated the hypothesis that Ni increases MT2A transcript levels in human bronchial airway epithelial cells

by mobilizing Zn. These data support a role for intracellular Zn in the signaling pathway for Ni-induced increases in MT.

5.3 RESULTS

5.3.1 Ni increases MT expression and MRE transactivation

Exposure to Ni is known to induce MT expression in hepatocytes (79) and in mouse lung (82). To examine the effects of Ni on MT2A mRNA levels in airway epithelial cells, BEAS-2B cells were exposed to 200 μM Ni (up to 48 h). Ni increased MT2A transcript levels significantly by 2 h and remained elevated at 24 h with maximal induction occurring at 4 h after exposure (Figure 25A). This induction was time-dependent as determined by linear trend analysis. Moreover, Ni increased MT protein after 4 h as shown by western blotting (Figure 25C). It is well understood that MT expression is regulated at the level of transcription (90). Although there are numerous cis-elements in the promoter region of MT2A, MTF-1 transactivation of MRE is essential for both basal and inducible MT expression (90). Therefore, we tested the hypothesis that Ni stimulates the transactivation of MREs to induce MT2A mRNA levels. pLucMRE luciferase activity increased in cells exposed to 200 μM Ni for 4 h or 8 h (Figure 25B). These data suggest that the induction of MT2A by Ni is transcriptionally regulated.

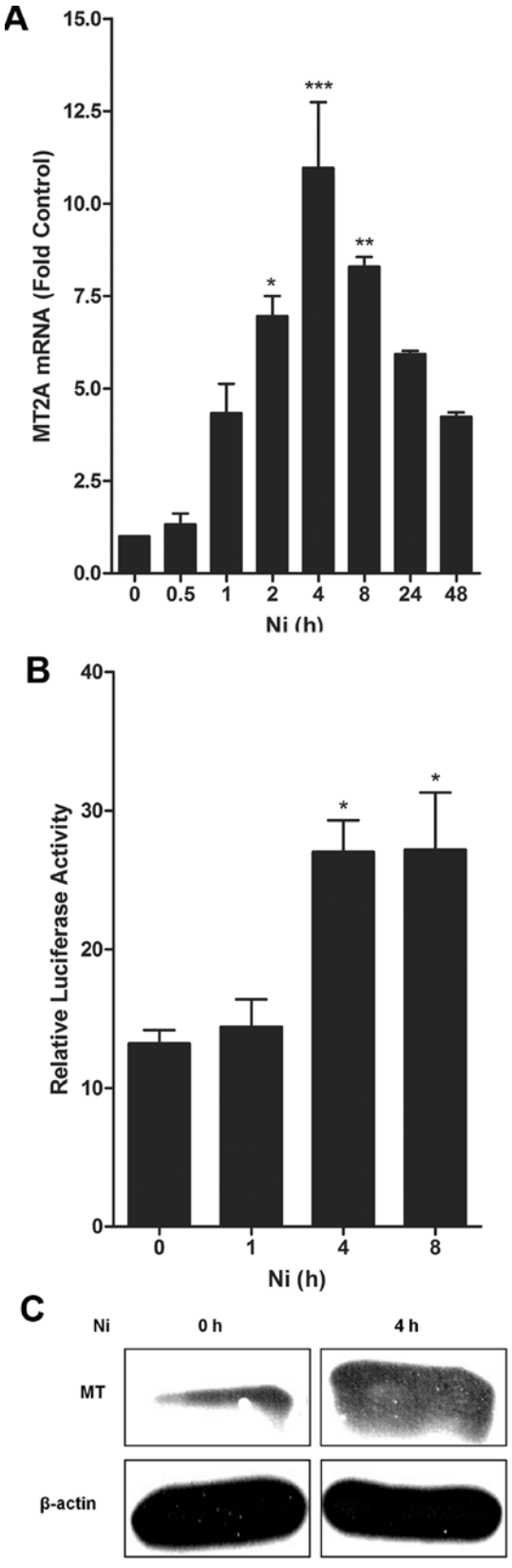

Figure 25. Ni increase MT expression and MRE transactivation

A. BEAS-2B cells were exposed to 200 µM Ni for the indicated times and total RNA was isolated. MT2A mRNA levels were measured by real-time PCR and were normalized to the housekeeping gene RPL13A. Data represent means ± SEM of fold control (n=3). B. BEAS-2B cells were transiently transfected with pLucMRE. Twenty-four hours after transfection, cells were exposed to 200 µM Ni for the indicated times. Cells were lysed and luciferase assays were performed. Data represent means ± SEM (n=3). *, **, and *** designate $p<0.05$, $p<0.01$, and $p<0.001$, respectively, compared to untreated cells. C. BEAS-2B cells were left untreated or exposed to Ni for 4 h. Total protein was isolated and western analysis for MT was performed. The data are representative of duplicate samples from 3 separate experiments.

5.3.2 Nickel stimulates the transactivation of MRE and induces MT2A through a Zn-dependent pathway

Zn increases the binding activity of MTF-1 to induce MT2A (80), but the mechanism for other metals, especially Ni, is poorly resolved. Therefore, we exposed the cells to Ni in the presence or absence of TPEN, a Zn chelator, to examine whether Ni activates MREs to induce MT2A transcripts by increasing free intracellular Zn. Cells that were transiently transfected with pLucMRE and exposed to TPEN and Ni had decreased luciferase expression compared to cells exposed to Ni alone (Figure 26A). Likewise, the data in Figure 26B show that TPEN pretreatment inhibited both Ni and Zn-induced MT2A mRNA levels. These data indicated that the Ni induction of MT2A required free intracellular Zn.

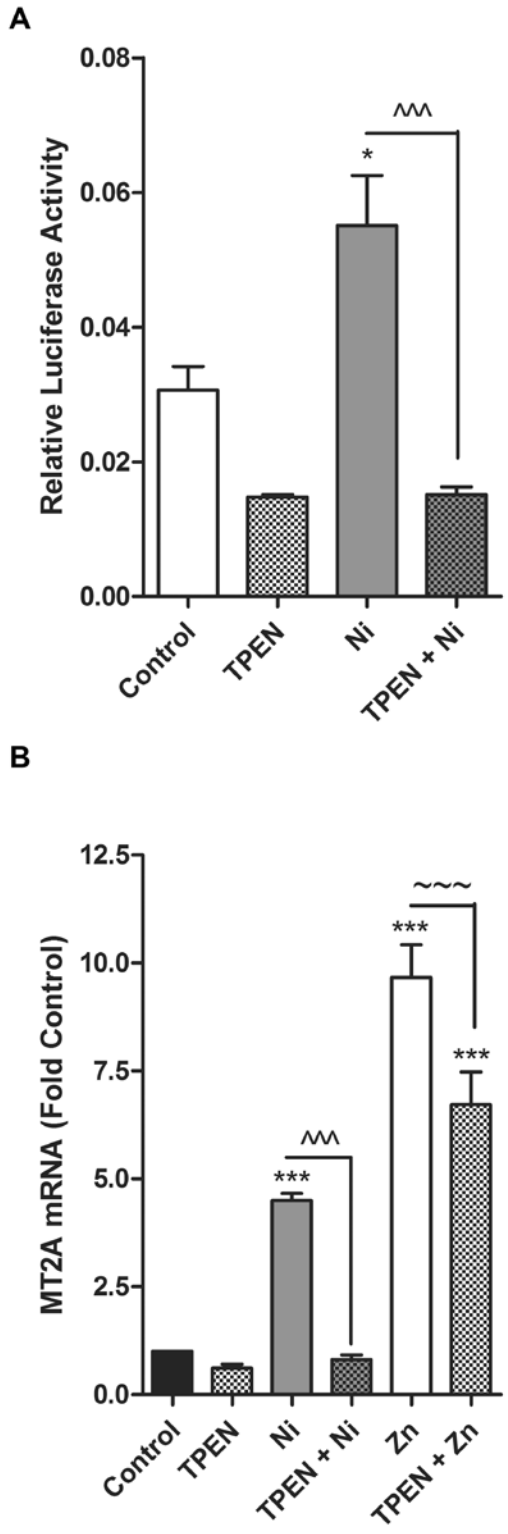

Figure 26. TPEN prevents Ni-induced MRE transactivation and MT2A mRNA expression

A. BEAS-2B cells were transiently transfected with pLucMRE. Twenty-four hours after transfection, cells were pretreated with 5 µM TPEN for 30 min prior to exposure to 200 µM Ni for 4 h. Cells were lysed and

luciferase assays were performed. Data represent means ± SEM (n=3). B. BEAS-2B cells were pretreated with 5 µM TPEN prior to exposure to 200 µM Ni or 100 µM Zn for 2 h. Total RNA was isolated and MT2A mRNA levels were measured by real-time PCR and normalized to the housekeeping gene RPL13A. Data represent means ± SEM of fold control (n=3). * and *** designate $p<0.05$ and $p<0.001$, respectively, compared to untreated cells; ^^^ designates $p<0.001$ compared to cells treated with Ni alone; ~~~ designates $p<0.001$ compared to cells treated with Zn alone.

5.3.3 Ni activates MTF-1 to induce MT

To examine the effects of Ni on MTF-1 nuclear localization, we transiently transfected BEAS-2B cells with eGFP-MTF-1, a reporter molecule with eGFP fused to MTF-1 (139). After 24 h, cells were left untreated or exposed to Ni from 1 h to 4 h. Exposure to Ni increased MTF-1 protein in the nucleus (Figure 27A-B). The requirement of MTF-1 for Ni-induced MT expression was also demonstrated using MEFs deficient in MTF-1 (dko7). Wild-type and dko7 cells were exposed to Ni for up to 4 h and Mt1 transcript levels were measured. The data in Figure 27C show that in the absence of MTF-1, Ni fails to induce Mt1 transcripts indicating that MTF-1 is essential in Ni stimulation of MT.

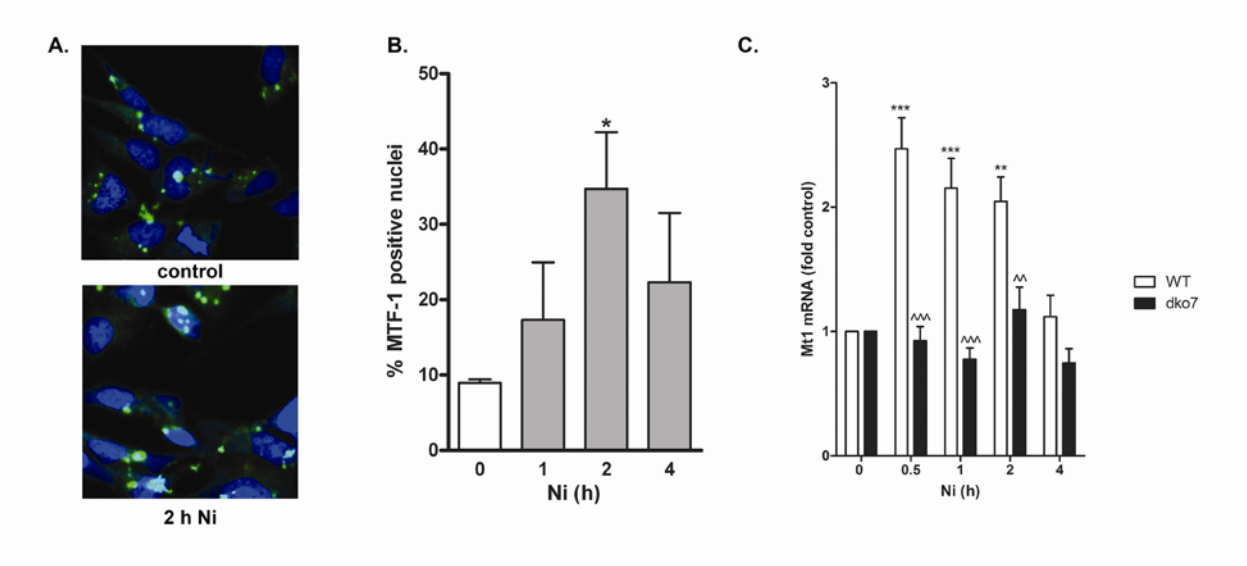

Figure 27. Ni activates MTF-1 to induce MT expression

A. BEAS-2B cells were transiently transfected with eGFP-MTF-1. Twenty-four hours after transfection, cells were replated on chamber slides and exposed to 200 µM Ni for 1 to 4 h or 100 µM Zn for 2 h. Cells were fixed with 4% paraformaldehyde and nuclei were stained with DRAQ5™. The representative images were captured at 60X with an Olympus Fluoview 500 confocal microscope. B. Quantitative analysis of eGFP-MTF-1 positive nuclei is presented as means ± SEM. * designates $p<0.05$ compared to untreated cells. C. MEF and dko7 cells were exposed to 200 µM Ni for the indicated times. Total RNA was isolated and Mt1 mRNA levels were measured by real-time PCR and normalized to the housekeeping gene β-actin. Data represent means ± SEM of fold control (n=3). ** and *** designate $p<0.01$ and $p<0.001$, respectively compared to untreated cells (0 h). ^^ and ^^^ designate $p<0.01$ and $p<0.001$, respectively compared to wild-type MEF cells (WT) at the corresponding time.

5.3.4 Ni increases ROS, but Ni-induced MT2A expression does not require intracellular ROS production

We previously demonstrated that particulate Ni increases intracellular oxidant production using the fluorescent intracellular oxidant indicator CM-H_2DCFDA in BEAS-2B cells (119). The data in Figure 28 demonstrated that soluble Ni also increases intracellular ROS in BEAS-2B cells.

Increasing the intracellular reduced thiol pool by incubating the cells with 2 mM NAC for 18 h or increasing the levels of the antioxidant by incubating the cells with 2 mM ascorbic acid for 30 min inhibited Ni stimulated ROS production. However, only treatment with NAC blocked Ni-induced increases in MT2A transcript levels; suggesting that MT2A is induced by Ni through a thiol-dependent, but not ROS-dependent pathway (Figure 29).

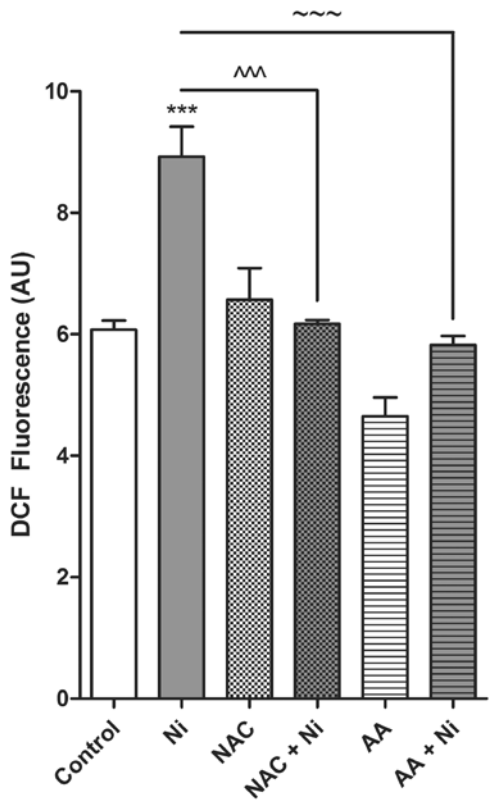

Figure 28. Ni-induced intracellular ROS production is prevented by antioxidants

BEAS-2B cells were pretreated with 2 mM NAC for 18 h or 2 mM L-Ascorbic acid (AA) for 30 min prior to loading cells with 20 µM CM-H_2DCFDA for 10 min. Cells were then exposed to 200 µM Ni for 10 min. Fluorescence was measured with a fluorescent plate reader with excitation at 485 nm and emission at 530 nm. Data represent means ± SEM (n=3). *** designates $p<0.001$ compared to untreated cells; ^^^ and ~~~ designate $p<0.001$ compared to cells treated with Ni alone.

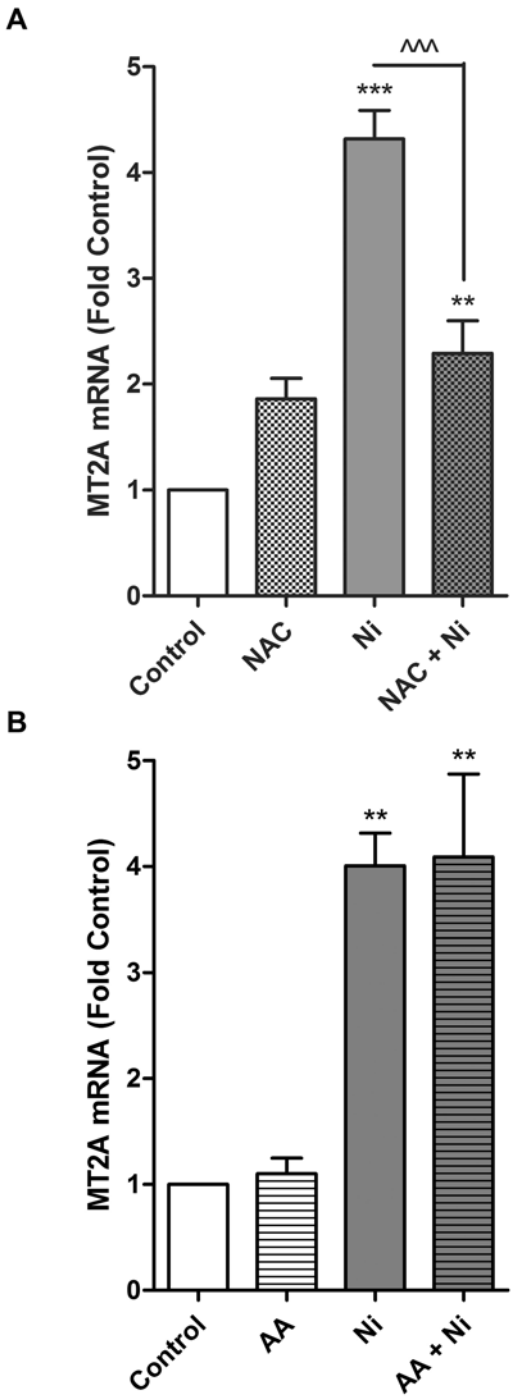

Figure 29. NAC, but not AA, prevents Ni-induced MT2A mRNA levels

BEAS-2B cells were pretreated with A. 2 mM NAC for 18 h or B. 2 mM L-Ascorbic acid (AA) for 30 min prior to exposure to 200 µM Ni for 2 h. Total RNA was isolated and MT2A mRNA levels were measured by real-time PCR and were normalized to the housekeeping gene RPL13A. Data represent means ± SEM of fold control

(n=3). ** and *** designate $p<0.01$ and $p<0.001$, respectively, compared to untreated cells; ^^^ designates $p<0.001$ compared to cells treated with Ni alone.

5.3.5 Nickel increases intracellular free zinc levels

To investigate whether Ni signals by increasing free intracellular Zn levels, we performed flow cytometry on live cells loaded with the Zn-sensitive fluorophore FluoZin-3. The data in Figure 30A demonstrated that exposure to Ni or Zn increased FluoZin-3 fluorescence from 0.2% to 42.1% and 93.8% of total cells, respectively. The addition of TPEN attenuated the Ni-induced increase in FluoZin-3 (42.1% to 12.0% of total cells) fluorescence suggesting that Ni mobilized intracellular Zn. These experiments used the ionophore, pyrithione, to facilitate the entry of Zn and Ni into the cells. We found that exposure to 20 µM or 200 µM Ni in the presence of ionophore mobilized the same amount of labile Zn. The data in Figure 30B demonstrate that exposure to 20 µM Ni in combination with 5 µM pyrithione had a similar induction of MT2A mRNA levels after 4 h compared to 200 µM Ni without ionophore.

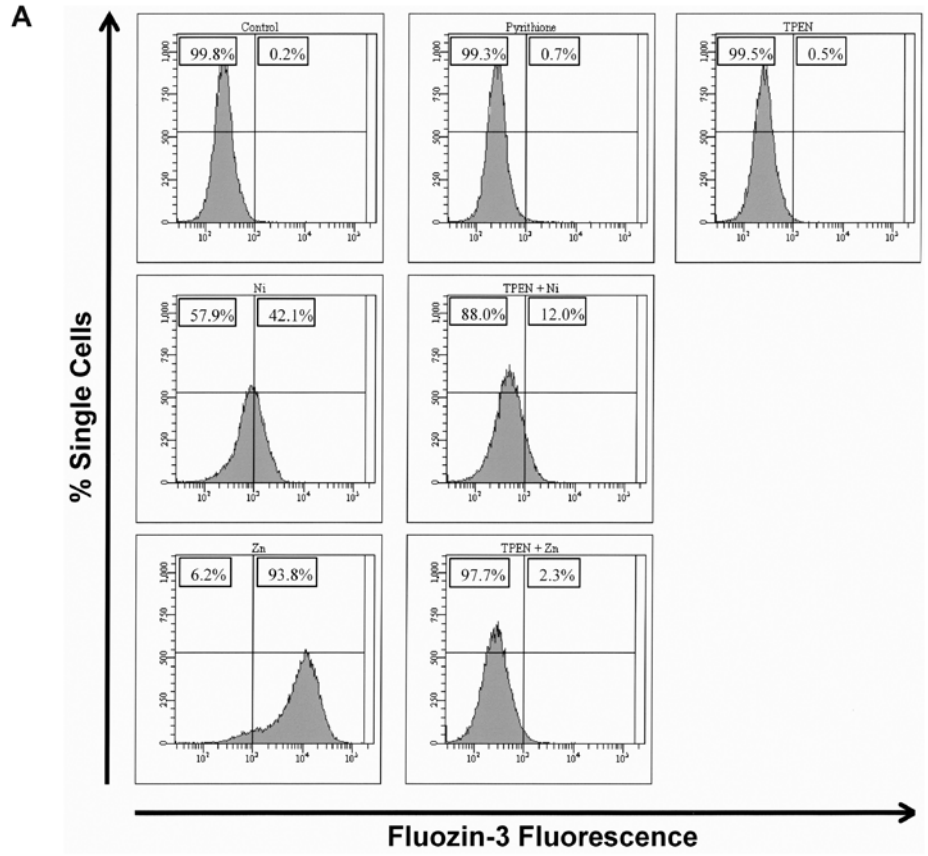

Figure 30. Ni increases free intracellular zinc

A. BEAS-2B cells were loaded with 5 μM FluoZin-3 AM ester with Pluronic F-127. Cells were exposed to 20 μM Ni or 10 μM Zn in the presence of 5 μM pyrithione for 30 min. TPEN was added for 5 min before harvesting to chelate the Zn. FluoZin-3 fluorescence was measured by flow cytometry. Data represent the results of 3 separate experiments. The percentages on the left and right sides of the histograms represent negative and positive Fluozin-3 fluorescence, respectively. B. BEAS-2B cells were exposed to 20 μM Ni in combination with 5 μM pyrithione or 200 μM Ni alone. Total RNA was isolated and MT2A mRNA levels were measured by real-time PCR and were normalized to the housekeeping gene RPL13A. Data represent means ± SEM of fold control (n=3). *** designates $p<0.001$ compared to untreated cells.

5.4 DISCUSSION

Ni is a major component of ambient air particulate matter (33,34) that is associated with inappropriate immune responses (34,41), airway hyperresponsiveness (42,43), and increased cardiopulmonary disease (33). Mechanisms of action for inhaled Ni that are independent of its antigenicity remain poorly defined. It is evident, however, that without induction of protective or adaptive genes, such as increasing MT in airway epithelium, the pathogenic responses to inhaled Ni are greatly enhanced (44,82). These studies used the BEAS-2B cells to model the terminal bronchiolar epithelial responses to Ni. While these cells are SV40 immortalized, we have demonstrated that their responses to metals are nearly identical to primary normal human bronchiolar epithelial cells cultured on an air/liquid interface (55) and mouse bronchiolar epithelium *in vivo* (19). Induction of MT following Ni exposure in these cells closely matches responses observed in mouse lungs (82) and thus, the mechanisms for this induction in BEAS-2B cells are likely to be broadly applicable. As indicated, MT induction by Ni and other toxic metals is a protective response. However, since only Zn has been shown to directly induce the

gene, it remains unclear how Ni and other metals signal for indirect gene activation. The current studies indicate that Ni transcriptionally activates MT2A by first mobilizing intracellular Zn to bind with MTF-1. Ni does not elicit ROS generation to mobilize labile Zn pools, but may displace Zn from thiols or interact with regulatory reduced thiols to stimulate MTF-1 transactivation.

MT regulates Zn homeostasis and is induced by various stressors including metals (76,79,80). We demonstrated that Ni exacerbated acute lung injury in MT null mice (44) acknowledging its protective function in the lung. MT is basally expressed in the airway epithelium (164) and inducible by exogenous chemicals (165,166). Our data in Figure 25A corroborates previous findings that Ni induces MT2A mRNA (79,82). This induction was rapid and time-dependent with the highest expression after 4 h of Ni exposure. Ni also increased MT protein levels after 4 h of Ni exposure (Figure 25C). There are multiple transcription factors that drive MT2A gene expression, but the activation of MTF-1 has an essential role by binding to MREs present in the promoter region of MT2A (90). Ni increased transactivation of MRE (Figure 24B), which occurred through the increased binding activity of MTF-1. Exposure to Ni facilitated the translocation of MTF-1 to the nucleus (Figure 27A-B). Also, Ni did not induce MT in cells deficient in MTF-1 (Figure 27C). However, since only Zn can directly activate and increase DNA binding of MTF-1 (90,91), the data support the hypothesis that Ni-induced MT2A is caused by redistributed Zn stimulating MTF-1 DNA binding.

Soluble Ni increased intracellular ROS (Figure 28) which is consistent with our previous report using particulate Ni_3S_2 (119). Likewise, NAC and AA prevented Ni-increased intracellular ROS levels. However, in the previous report, neither antioxidant affected transcriptional induction of SERPINE1 following Ni exposures (119). In contrast, in the current

study, only NAC prevented Ni-induced MT2A transcript levels (Figure 29). Thus, production of ROS may not be involved in Ni-induced MT2A, but free thiols may regulate the ability of Ni to induce certain genes. NAC acts as an antioxidant by increasing the intracellular free thiol pool and increasing synthesis of glutathione (GSH) (167). GSH and oxidized gluthothione (GSSG) are key regulators of the release of Zn from MT (168,169). GSSG interacts with MT to facilitate the transfer of Zn from MT (169). However in reducing conditions, when GSH concentrations are high, Zn remains bound to MT (168). The data from Figure 29 suggest that adding NAC pushed the thiol balance towards enhanced Zn binding to MT and prevented its mobilization to interact with MTF-1. Exposure to high levels of Ni has been shown to reduce the intracellular GSH content and increase the GSSG/GSH ratio (170,171). Hence it is possible that in our system Ni decreased the GSH content of the cell to facilitate Zn mobilization. However, this is unlikely given the low level of oxidant generation in response to Ni and the overwhelming amount of intracellular GSH relative to the amount of Ni added.

Transcriptional activation of MT2A by Ni required Zn mobilization, since pretreatment with TPEN, a Zn chelator, abrogated Ni-induced MRE transactivation and increased MT2A transcripts (Figure 26). Although TPEN is often used as a Zn-specific chelator, it has affinities for other divalent metals including Ni (76). However, the stochiometry of TPEN metal chelation is such that the low concentration used in the present study was sufficient to bind only 5% of the added Ni. Furthermore, the ability of Zn, but not Ni, to rescue the response observed (Figure 26B) indicates that the added TPEN predominantly bound the intracellular Zn released by Ni to inhibit Ni-stimulated MT induction. This inhibition did not result from toxicity since TPEN was added at a concentration that did not cause cell death (data not shown). Thus, the observed results consistently support a role for mobilization of endogenous Zn in Ni-stimulated signaling.

Moreover, increased FluoZin-3 fluorescence after Ni exposure (Figure 30) established that Ni increases free intracellular Zn levels as was previously demonstrated in hepatocytes (172). In summary, we demonstrated that Ni increases free intracellular Zn levels to induce MT2A transcript levels. This was not at the level of MT itself, since Ni has a low affinity for MT, relative to Zn, and cannot displace Zn from MT (76). The precise mechanism of how Ni is redistributing Zn has not been investigated fully, but remains an area of interest. However, this study elucidates the mechanism of Ni-induced MT2A and provides a better understanding of how metals other than Zn produce this adaptive response. This understanding may offer insight for developing protective strategies to reduce pathogenic airway responses to inhaled metals.

6.0 CONCLUSIONS

6.1 CHROMIUM AND PULMONARY DISEASE

Chronic exposure to Cr(VI) causes lung diseases including asthma, chronic bronchitis, airway hypersensitivities, and lung cancer (13). These diseases occur more frequently in workers in the industries where levels of Cr(VI) are highest. The data presented in this dissertation proposes a possible mechanism that may explain the association between inhalation of Cr(VI) with pulmonary diseases. This mechanism involves the selective activation of the SFK, Fyn, leading to the stimulation of STAT1 and the repression of the protective genes, MT and VEGFA, induced by Ni in the lung. Studies using mice deficient in STAT1 are required to verify that this pathway is involved in the pathogenesis of Cr(VI)-induced pulmonary diseases. The confirmation of this pathway will provide insight into how to better protect people from these diseases.

6.2 METAL MIXTURES

Epidemiological studies associate exposure to metal mixtures with increased incidence of pulmonary diseases. Despite this association, few studies have examined how metals may interact to promote diseases. In this dissertation, cell signaling mechanisms of Cr(VI) and Ni

were examined both separately and in combination. These two metals were studied because they are often found together in industry, are present in over half of the NPL toxic waste sites, and have been shown to positively interact in causing lung disease (42,46-49). The data in Chapters 4 and 5 demonstrated that following exposure to Ni, MT and VEGFA were induced in BEAS-2B cells. However, in cells pretreated with Cr(VI), this induction was inhibited (Figures 18 and 32) which was mediated by the activation of STAT1 signaling. These data suggest that exposure to metal mixtures results in a worsened outcome compared to exposure to either one individually. Further studies are needed to verify that exposure to both metals result in exacerbated lung diseases compared to the individual metal.

6.3 MECHANISM OF CR(VI)-ACTIVATED STAT1 SIGNALING

STAT1 plays an important role in the innate immune response and promotes antiproliferative and antiviral effects (67,68). STAT1 is specifically activated in the bronchial epithelial cells of asthmatic patients and its aberrant expression may be vital to the development of inflammatory pulmonary diseases (1). The ability of Cr(VI) to activate STAT1 was demonstrated in Chapter 3. In BEAS-2B cells, Cr(VI) stimulated STAT1 phosphorylation leading to the dimerization with STAT2, transactivation of ISRE, and the induction of IRF7 mRNA. The STAT1-STAT2 dimer binds IRF9 to form the ISGF3 complex. This complex is of biological relevance because studies have shown that ISGF3 activation silences IFNβ-induced genes (62,63). Although the precise mechanism of this repression is unknown, all three protein components are needed. Surprisingly, the proteins do not bind directly to the promoters of these genes, but instead may activate an

inhibitory protein that either sequesters the necessary transcription factors in the nucleus, or binds to the promoter and blocks its binding (62,63).

Histone modifications are an important method for gene regulation. Typically, histone deacetylation is associated with gene repression and acetylation with gene activation (173). However, in unique cases, histone deacetylation is required for gene induction. Specifically, this modification is needed for activation of ISRE-driven genes, but not GAS-driven genes (60,61). HDAC is required for the recruitment of transcriptional machinery to the promoters of these genes (61). Cr(VI) has been shown to prevent the liberation of HDAC from the promoters of PAH-inducible genes resulting in the prevention of RNA polymerase II recruitment and the silencing of the gene induction (24). It was demonstrated in Figure 13 that Cr(VI) induction of IRF7 mRNA required HDAC activity since pretreatment with the HDAC inhibitor, NaB, prevented the induction. However, NaB pretreatment had no effect on Ni-induced VEGFA mRNA expression (Figure 37) indicating that Cr(VI) is not silencing this gene through a HDAC-dependent mechanism.

STAT1 was initially discovered as a downstream effector of IFN signaling (52). Although treatment with an IFNAR neutralizing antibody prevented IFN-induced IRF7 mRNA expression, it had no effect on Cr(VI)-induced IRF7 suggesting that Cr(VI) activates STAT1 through an IFN-independent mechanism. Furthermore, preincubating cells with IFN-α2 prior to Ni exposure had no effect on MT2A or VEGF mRNA expression (Figures 35-36). These data indicate that while STAT1 is required for Cr(VI) repression of Ni-induced genes, it is not through the stimulation of IFN. These data further indicate that STAT1 is indirectly affecting gene induction through the induction of an inhibitory protein.

It has been previously shown that Cr(VI) directly activates affinity purified Fyn *in vitro* (22). There are critical cysteine residues in regulatory domain of Fyn that regulates substrate phosphorylation (174). This domain is highly conserved among SFKs with the two cysteines flanking eleven amino acids. These cysteines are targets of oxidant (174) and metal (74,175,176) effects on substrate recognition. However, it is not known whether Cr(VI) can directly bind this motif to activate Fyn. Although Fyn is the initial target of Cr(VI) signaling, it might not be directly phosphorylating STAT1. c-Abl is a NRTK that is ubiquitously expressed and activated by various factors including SFKs (177). Specifically, Src and Fyn phosphorylate c-Abl and increase its kinase activity (147). Gleevec, a specific inhibitor of c-Abl, can be used to examine the requirement of c-Abl for Fyn-mediated activation of STAT1. Csk is a soluble PTK that regulates SFKs by phosphorylating an inhibitory tyrosine residue in the C-terminus (178). Mg ions are required for this reaction and other metal ions (Mn, Co, Ni, Zn) are capable of binding to the Mg binding site and altering the activity of Csk (175). Currently there is no evidence that Cr(VI) can bind this site or if it can compete with Mg ions, but it remains a possibility of how Cr(VI) may activate STAT1 signaling.

Cr(VI) is well known for its negative effect on the gene inducibility. The overall hypothesis of this dissertation is that Cr(VI)-activated STAT1 signaling is responsible for the repression of genes and the data presented supports the idea that STAT1 acts as a master regulator of Cr(VI)-induced gene regulation. The data in Chapter 4 and Appendix A demonstrated that in STAT1-deficient cells, Cr(VI) induced VEGFA and MT2A. Moreover, Cr(VI) positively interacted with Ni signaling to further increase the transcription of these genes. Functional STAT1 is often lacking in cancers (146), which can explain the differential effects of Cr(VI) on expression of the same gene in different cell lines. Contrary to the data in Chapter 4, Cr(VI) stabilized HIF-1α and induced VEGFA mRNA in prostate cancer cells (121) and also had opposite effects on HO-1 mRNA expression in normal

cell lines compared to cancerous cell lines (19,158). Therefore, the pathogenic actions of Cr(VI) signaling in lung cells and interactions with other metals may depend on the STAT1 status of the airway cells.

6.4 TRANSCRIPTIONAL REGULATION OF *VEGFA* BY CHROMIUM AND NICKEL

VEGFA is most known for its role in angiogenesis and vascularization. Although its role in the lung and the airway epithelial cells remains controversial and largely unknown, VEGFA is an important mediator of wound healing and repair (113,115). In cancers, hypoxic conditions stabilize HIF-1α to induce VEGFA expression and although hypoxia is the main inducer of HIF-1α, metals, including Ni, can also stabilize HIF-1α (118,119,122,141). The exact mechanism of this stabilization is unknown, but it is hypothesized that Ni may interfere with the proteins involved in the degradation or the transcriptional activation of HIF-1α (e.g. prolyl hydroxylase domain (PHD), asparagine hydroxylases, respectively). PHDs hydroxylate HIF-1α prolines to promote binding to the VHL ubiquination complex allowing it to be degraded. Ni decreases the binding of VHL to HIF-1α and that stabilization of HIF-1α was a persistent response indicated by its presence for up to 72 h after Ni was removed from the media of cells in culture (122). However, the function of HIF-1α was not examined in these studies. The PHD enzymes require iron, ascorbic acid, and oxygen for proper function (179). Previous studies from our laboratory showed that preincubation of cells with antioxidants had no effect on Ni-induced HIF-1α stabilization or transactivation suggesting that Ni stabilization of HIF-1α may be due to Ni displacing iron from the PHDs rendering them inactive (119). In addition to the PHDs,

hydroxylation of an asparagine residue in the C-terminal transactivation domain is required for the interaction of HIF-1α with co-activators (e.g. p300). *In vitro* assays using purified HIF-1α fragments showed that the hydroxylation of asparagine is directly inhibited by metals (e.g. Co and Zn) (180) thereby suggesting that this may be a mechanism of Ni-induced HIF-1α stabilization.

There is growing evidence that upstream kinases are involved in mediating HIF-1α phosphorylation and transactivation. In the studies in Chapter 4, it was demonstrated that Ni-activated ERK was partially responsible for HIF-1α stabilization knocking it down by 54% (Figure 20A). The partial inhibition could result from either the activation of other upstream kinases not examined or more likely, through altering the degradation pathway by interfering with PHDs or inhibiting asparagine hydroxylases activity. However, it is important to note that not all of HIF-1α protein that is stabilized by Ni is functional. Ni robustly increases HIF-1α protein stabilization (Figure 22A), but the transactivation of HRE was increased only about 2 fold in response to Ni (Figure 22B). Although this observation could be due to the lack of sensitivity of the HRE luciferase assay, it strongly suggests that while Ni may increase the stability of the protein, it is not transcriptionally active. Further analysis of the phosphorylation status and nuclear localization of HIF-1α is required to address this hypothesis.

As stated above, there is evidence of kinase involvement in the induction of VEGFA. Specifically in cancer cells and tumors, Src and STAT3 appear to be essential mediators of VEGFA expression (124). In other systems, different kinases including MAPKs and PI3K are involved in the signaling pathway (118,119). The precise signaling is dependent on the cell type and stimuli. In BEAS-2B cells exposed to Ni, ERK was activated and was upstream of HIF-1α transactivation and Src-mediated Sp1 transactivation (Figures 19C, 20A, and 31). p38 and PI3K

had no role in either the induction of *VEGFA* or HIF-1α stabilization (Figures 19A and 20A). ERK activation was determined to be upstream of Src, since inhibiting ERK prevented Ni-stimulated Src phosphorylation (Figure 19C). Inhibiting Src prevented Ni-induced VEGFA mRNA expression without affecting HIF-1α stabilization (Figures 19B and 20B) indicating that both HIF-1α dependent and independent signaling is required for *VEGFA* induction. However, the mechanism by which Ni activates ERK remains unknown. Ni may be activating MEK1/2 to phosphorylate ERK, and this activation could be direct or mediated through receptors (e.g. GPCRs).

Sp1 phophorylation is required for full induction of *VEGFA* (129). Although Sp1 phosphorylation status was not examined, Ni stimulated increased binding to Sp1 as shown by luciferase assays. It is likely that the phosphorylation is mediated by ERK and Src, but other kinases have also been implicated in the activation of Sp1 (e.g. DNA-PK, CDKs, PI-3K). Sp1 can be phosphorylated on 5 different Ser/Thr residues with the biological response being dependent on the specific site. ERK-mediated Sp1 activation of VEGFA is dependent on the phosphorylation of Thr453 and Thr739 (131). Due to the lack of available antibodies specific to each phosphorylation site, site-directed mutagenesis will need to be employed to determine which residue(s) is important for Ni-induced VEGFA expression. To determine the requirement of ERK and Src, electrophoretic mobility shift assays for Sp1 DNA binding can be performed after preincubation of cells with the specific inhibitors to each kinase prior to Ni exposure.

When Cr(VI) was added to the cells prior to Ni exposure, Ni-activation of ERK, Src, HIF-1α, and VEGFA was inhibited (Figures 21-22). The effect of Cr(VI) on HIF-1α stabilization was only partial, but completely blocked HRE transactivation (Figure 22) once again suggesting that not all of the protein stabilized by Ni is functional. Cr(VI) is known to

prevent the recruitment of co-activators to promoters (26) so it is possible Cr(VI) may be repressing HIF-1α transactivation through interfering with the asparagine hydroxylase and needs to be investigated further. Also, the mechanism of the inhibitory effect of Cr(VI) on ERK remains unknown. Previous reports demonstrated that Cr(VI) decreases basal ERK phosphorylation (22) but whether this effect is direct or through altering the upstream signaling events needs to be studies.

STAT1 signaling is required for Cr(VI) effects on VEGFA repression. In shSTAT1 cells, Cr(VI) induced VEGFA mRNA levels (Figure 23C) and further increased the Ni response (Figure 23B). HIF-1α cooperates with other transcription factors and it is probable that STAT1 or the STAT1-containing complex sequesters these transcription factors or prevents them from binding the *VEGFA* promoter through the induction of an inhibitory protein. In the absence of protein synthesis, Cr(VI) induces VEGFA mRNA expression (Figure 23D) in the same time frame as in shSTAT1 cells (Figure 23C) suggesting that a protein activated by STAT1 transcriptional complexes repress *VEGFA* induction. The identification of this inhibitory protein is vital to understanding the development of Cr(VI)-induced pulmonary diseases. Since Cr(VI) activates STAT1 (55) and induces *VEGFA* in the absence of STAT1 (Figure 23C) and protein synthesis (Figure 23D) within one hour, this inhibitroy protein must be present within 1 h of Cr(VI) treatment. Also, the ISGF3 complex interferes with Sp1 recruitment to inducible promoters (62) and Cr(VI) stimulates Sp1 transactivation in the absence of STAT1 (Figure 24B). Therefore it is possible that the inhibitory protein is interacting with Sp1 and preventing its transactivation. One approach to identifying this protein is to immunoprecipitate Sp1 from whole cell lysate after Cr(VI) exposure. The immunoprecipitate can be separated by SDS-PAGE and the proteins can be identified by mass spectrometry. Also, the shNC and shSTAT1 cells can

be exposed to Cr(VI) and proteins separated by SDS-PAGE. Proteins present in the shNC cells, but not in the shSTAT1 cells will be identified by mass spectrometry.

6.5 TRANSCRIPTIONAL REGULATION OF *MT2A* BY CHROMIUM AND NICKEL

MT is well known for its role in metal detoxification and protection against environmental insults. It has been demonstrated that exposure to Ni rapidly induced MT expression and is crucial in protecting against Ni-induced lung injury (44). However, only the mechanism for Zn-induced MT is known. The data in Chapter 5 demonstrated that exposure to Ni caused the redistribution of Zn which directly activated MTF-1 to transcribe MT2A, the major human isoform of MT. The precise mechanism for how Ni mobilizes Zn remains unknown since Ni cannot displace Zn from MT or other Zn-binding proteins (76). Ni increases in labile Zn did not arise from the production of ROS. Exposure to Ni modestly increased intracellular ROS production (Figure 28), but preincubation with ascorbic acid had no effect on Ni-induced MT2A (Figure 29B). In contrast, increasing intracellular free thiols through the addition of NAC prevented Ni-induced MT2A mRNA expression (Figure 29A). NAC is a precursor to GSH and when GSH concentrations are high, Zn remains tightly bound to MT (168). Although Ni can decrease the GSH content of cells, it requires higher concentrations of Ni than used in these studies (170,171). Thus, the mechanism of Ni mobilized Zn requires further examination.

MT2A is primarily transcriptionally regulated through the binding of MTF-1 to MREs in the *MT2A* promoter (90). Ni increased MT mRNA, protein, and MRE transactivation (Figure 25). Exposure to Ni activated MTF-1 nuclear localization and Ni did not induce MT transcripts in MTF-1-null cells (Figure 27). Zn directly activated MTF-1 and TPEN treatment prevented

MT2A induction indicating the requirement of Zn for this response (Figure 26). Furthermore, exposure to Ni caused an increase in a Zn-specific fluorophore (Figure 30). In addition to Zn-dependent mechanisms for the activation of MTF-1, its phosphorylation is also critical for its activity (90-92). Ni activation of p38, PI-3K, and SFKs were determined to be necessary for the prolonged induction of MT2A mRNA which was demonstrated by the loss of Ni-induced MT2A transcripts in the presence of the specific inhibitors (Figure 33).

Cr(VI) has been shown to inhibit Zn- and Cd-induced MT expression by interfering with the transactivation potential of MTF-1 (23) and preventing RNA polymerase II recruitment to the promoter (25). Cr(VI) has no effect on Ni-induced MT2A transcripts until after 8 h of exposure (Figure 32) suggesting that Cr(VI) has no effect on the redistribution of Zn, but may affect the upstream kinases activated by Ni. Interestingly, in cells deficient in STAT1, Cr(VI) modestly induces MT2A mRNA expression and greatly increases MT2A in the presence of Ni (Figure 34). It remains unknown how Cr(VI)-activated STAT1 may interfere with *MT2A* induction, but MTF-1 also cooperates with other transcription factors including HIF-1α and Sp1 (93-96) and Cr(VI) interferes with their transactivation (Figures 22B and 24B).

6.6 SUMMARY

In conclusion, these studies demonstrated that exposure to occupationally relevant concentrations of Cr(VI) activates STAT1-dependent signaling to alter the transactivation of basal and Ni-induced protective genes in airway epithelial cells (Figure 31). Cr(VI) directly activates the SFK, Fyn, to initiate this signaling cascade. More importantly, the stimulation of STAT1 phosphorylation appears to be the determining factor of Cr(VI) effects on VEGFA and MT2A

induction. The exact mechanism of Cr(VI) repression is unresolved. However, these studies provide evidence that STAT1 is crucial in the regulation of genes by Cr(VI). Definitive experiments can be designed that will provide support for the hypothesis that Cr(VI)-activated STAT1 is an essential mediator of Cr(VI)-induced pulmonary diseases.

Future directions of this work include investigating the effects of Cr(VI) and Ni exposure both acutely and chronically *in vivo*, identifying the mechanism by which Cr(VI) activates Fyn, and investigating how STAT1 disrupts the transcriptional complexes required to drive inducible gene expression. The mechanism revealed by this research is necessary for understanding the toxic effects of inhaled metals and metal mixtures and for improving the prevention and treatment of metal-induced pulmonary diseases.

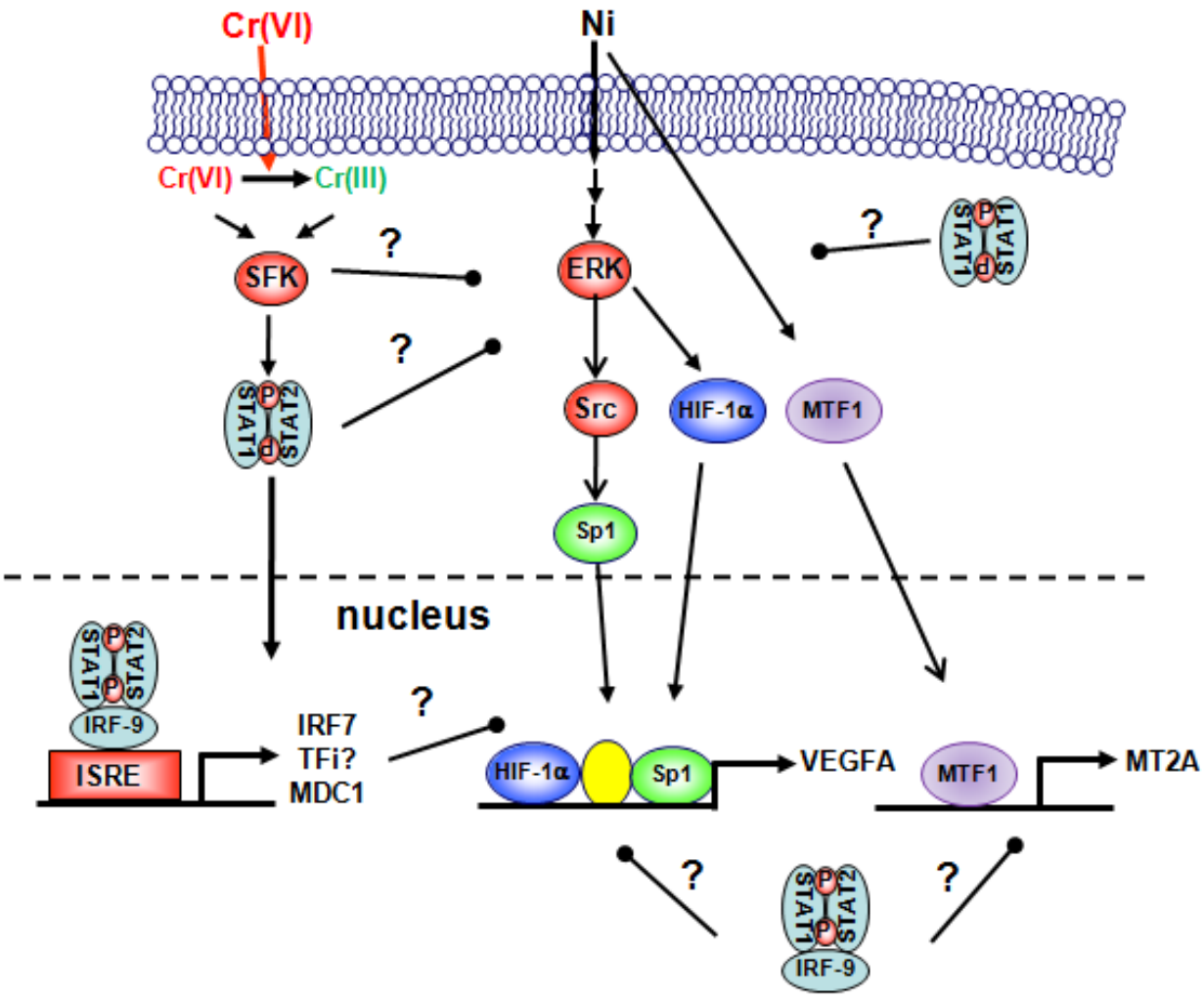

Figure 31. Proposed signaling scheme for the role of STAT1 in Cr(VI) signaling for repressed gene induction.

APPENDIX A

SUPPLEMENTAL FIGURES

THE EFFECT OF CR(VI) ON NI-INDUCED MT2A

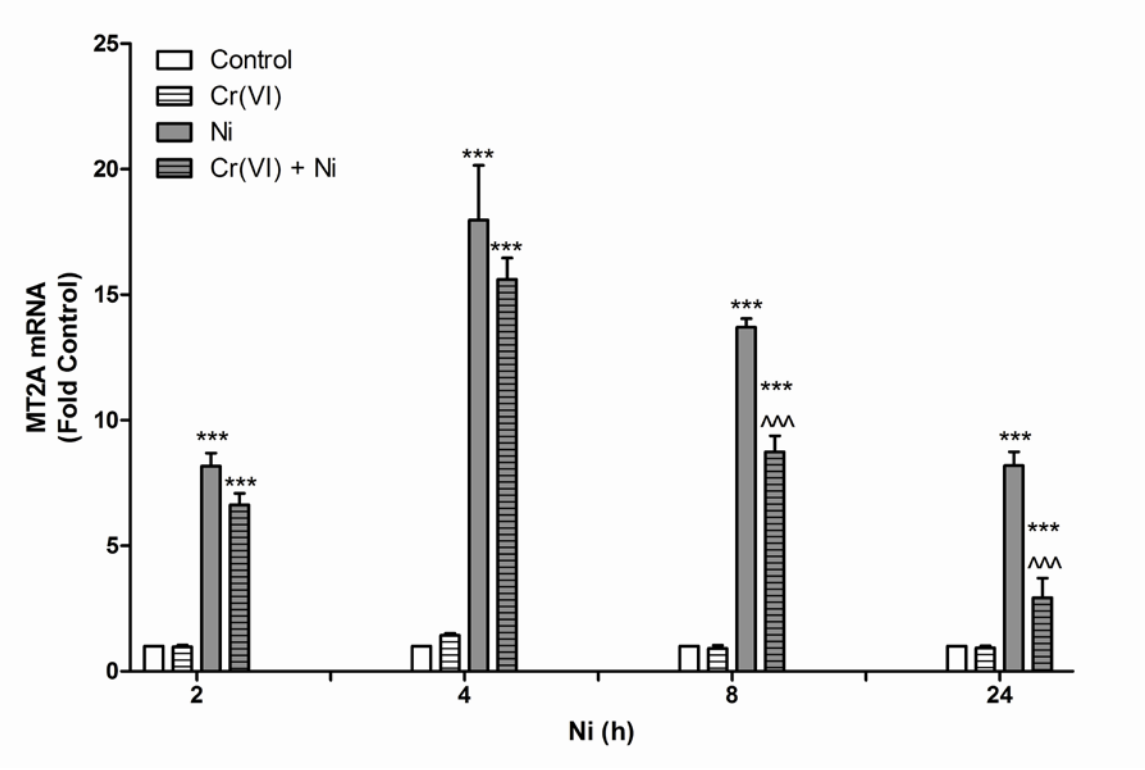

Figure 32. Cr(VI) effects on Ni-induced MT2A mRNA levels.

BEAS-2B cells were exposed to 5μM Cr(VI), 200 μM Ni, Cr(VI) for 30 min prior to 200 μM Ni for the indicated times. Total RNA was isolated. MT2A mRNA levels were measured by real-time PCR and normalized to the housekeeping gene, RPL13A. Data represent mean ± SEM of fold control. *** designates $p<0.001$ compared to respective control; ^^^ designates $p<0.001$ compared to Ni alone.

THE EFFECT OF KINASE INHIBITORS ON NI-INDUCED MT2A

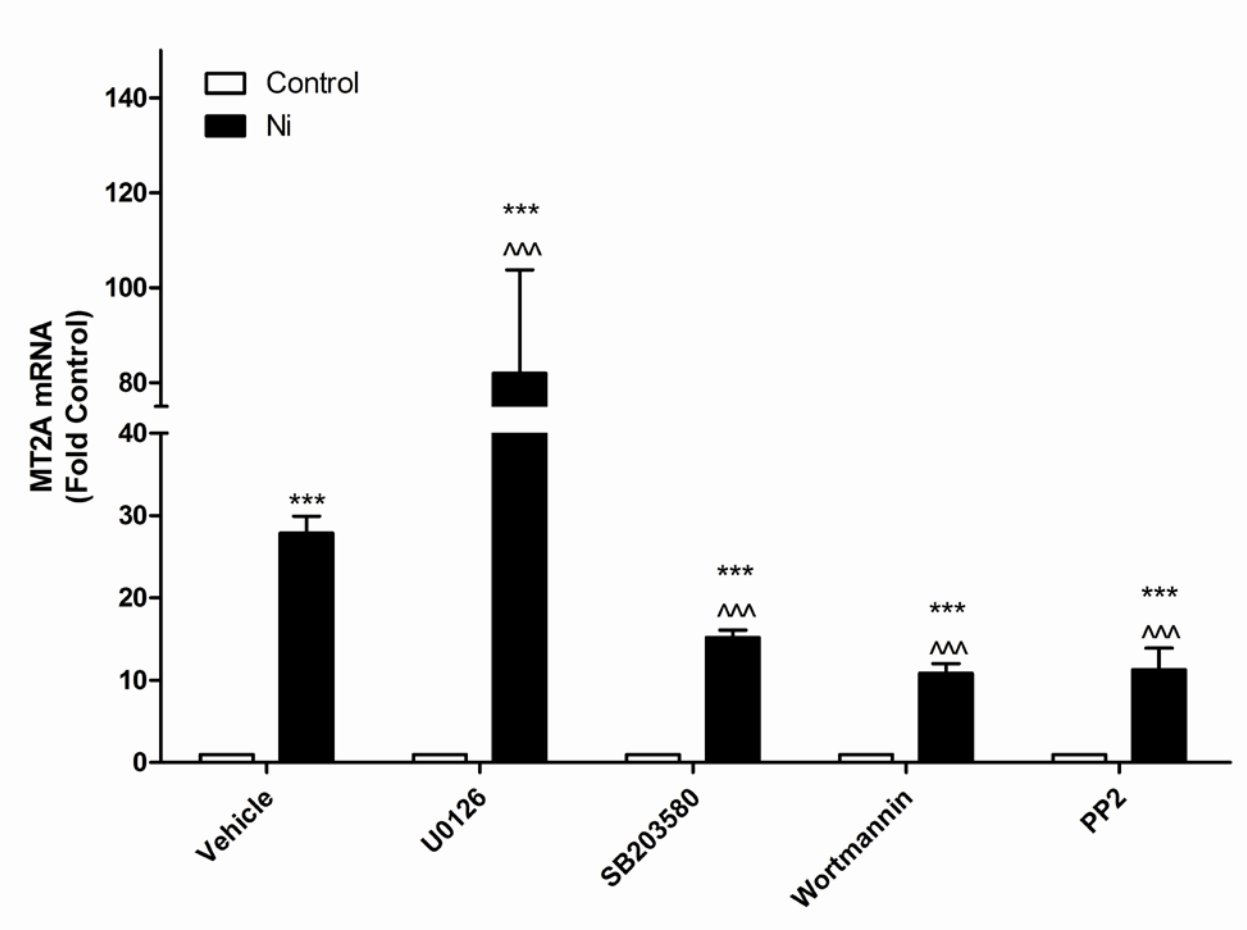

Figure 33. The role of kinase signaling in Ni-induced MT2A mRNA levels.

BEAS-2B cells were pretreated with 10 µM U0126, 20 µM SB203580, 1 µM wortmannin, or 10 µM PP2 prior to adding vehicle (open bars) or 200 µM Ni (closed bars) for 24 h. Total RNA was isolated. MT2A mRNA levels were measured by real-time PCR and normalized to the housekeeping gene RPL13A. Data represent mean ± SEM. *** designates $p<0.001$ compared to respective control; ^^^ designates $p<0.001$ compared to Ni alone.

STAT1 IS REQUIRED FOR CR(VI) SILENCING OF NI-INDUCED MT2A

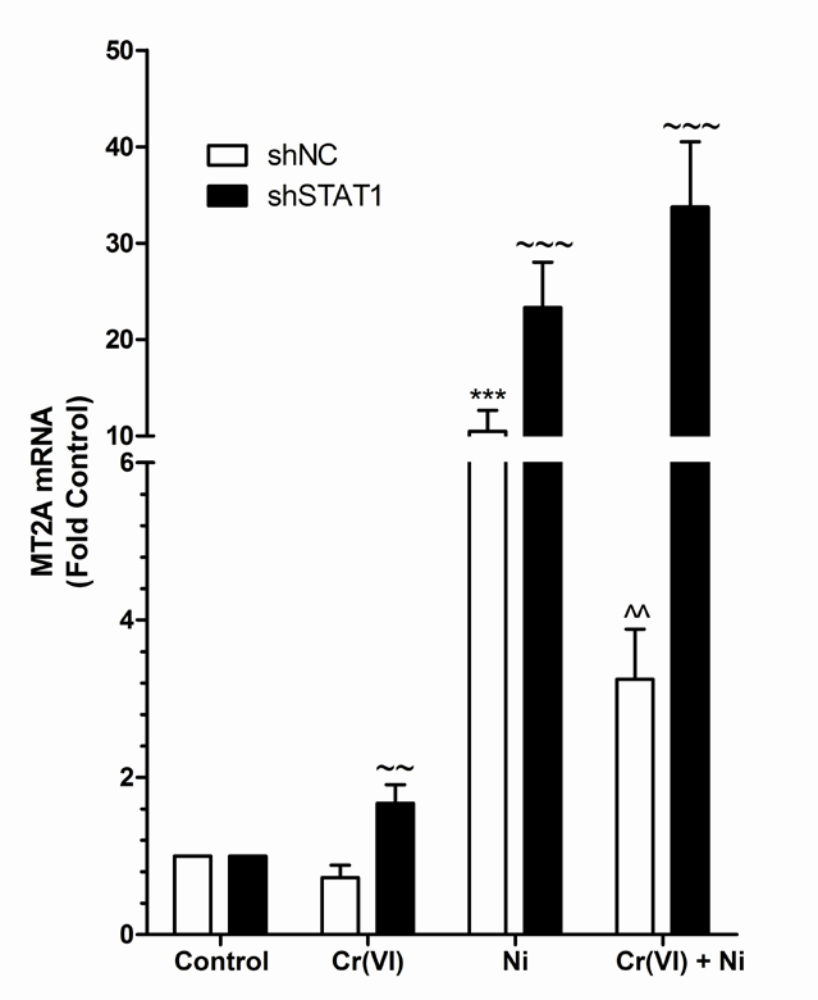

Figure 34. STAT1 is required for Cr(VI) suppression of MT2A induction.

BEAS-2B cells stably expressing either random (shNC) or STAT1 (shSTAT1) shRNA were exposed to 5 µM Cr(VI), 200 µM Ni, or 5 µM Cr(VI) for 2 h prior to the addition of 200 µM Ni for 24 h. Total RNA was isolated. MT2A mRNA levels were measured by real-time PCR. Data represent mean ± SEM of fold control. *** deginates $p<0.001$; ~~ and ~~~ designate $p<0.01$ and 0.001 compared to respective control cells. ^^ designates $p<0.01$ compared to cells treated with Ni alone.

THE EFFECT OF IFN-A2 ON NI-INDUCED MT2A

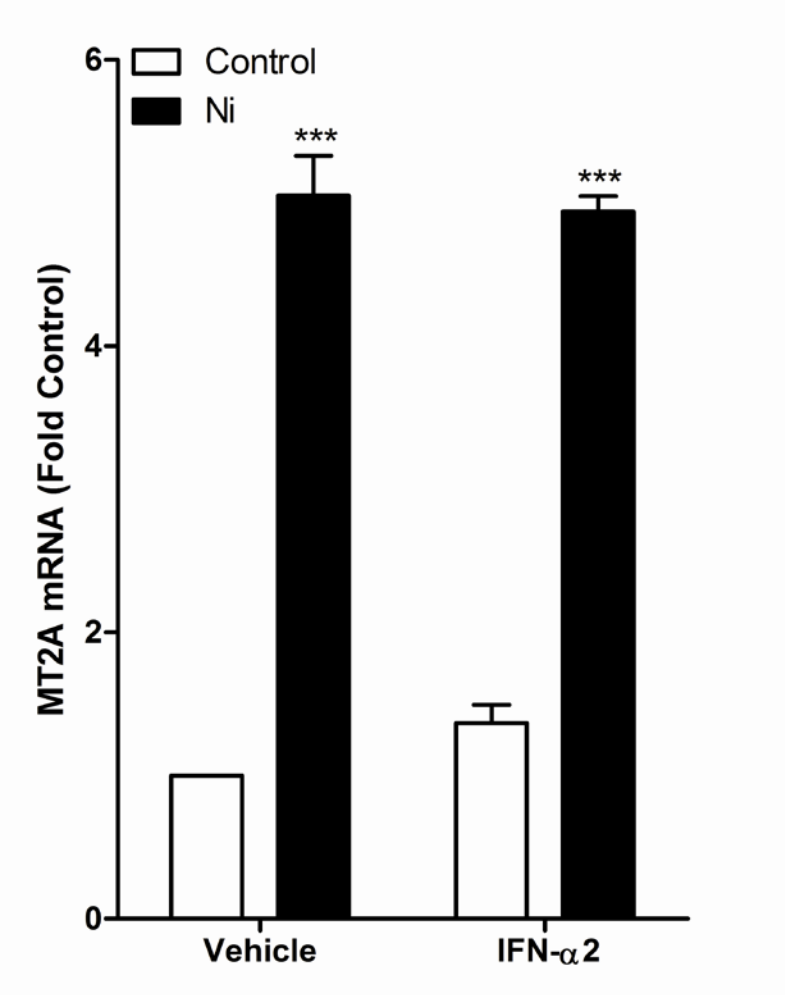

Figure 35. IFN-α2 has no effect on Ni-induced MT2A mRNA levels.

BEAS-2B cells were preincubated with 100 U/ml IFN-α2 for 2 h prior to exposure to vehicle (open bars) or 200 µM Ni (closed bars) for 24h. Total RNA was isolated and MT2A mRNA levels were measured by real-time PCR. Data represent mean ± SEM of fold control. *** designates $p<0.001$ compared to the respective control.

THE EFFECT OF IFN-A2 ON NI-INDUCED VEGFA

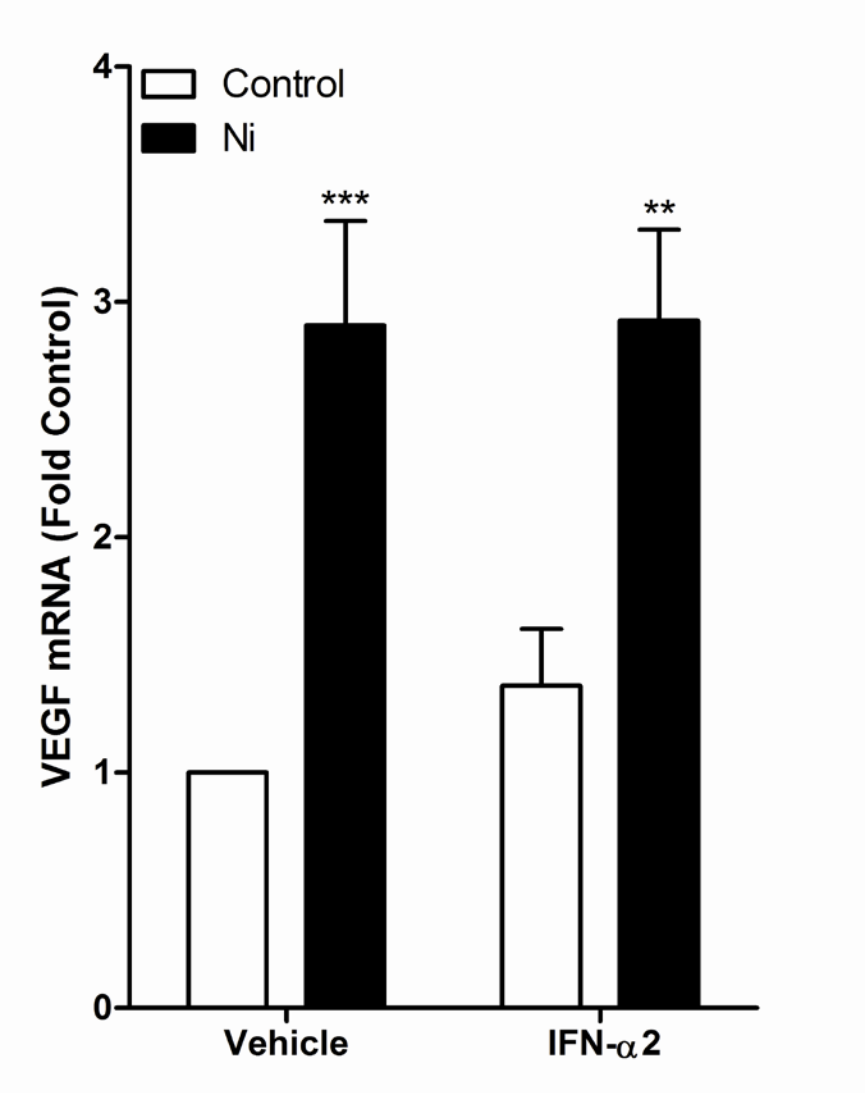

Figure 36. IFN-α2 has no effect on Ni-induced VEGFA mRNA levels.

BEAS-2B cells were preincubated with 100 U/ml IFN-α2 for 2 h prior to exposure to vehicle (open bars) or 200 µM Ni (closed bars) for 24h. Total RNA was isolated and VEGFA mRNA levels were measured by real-time PCR. Data represent mean ± SEM of fold control. ** and *** designate $p<0.01$ and 0.001, respectively, compared to the respective control.

THE EFFECT OF HDAC ON NI-INDUCED VEGFA

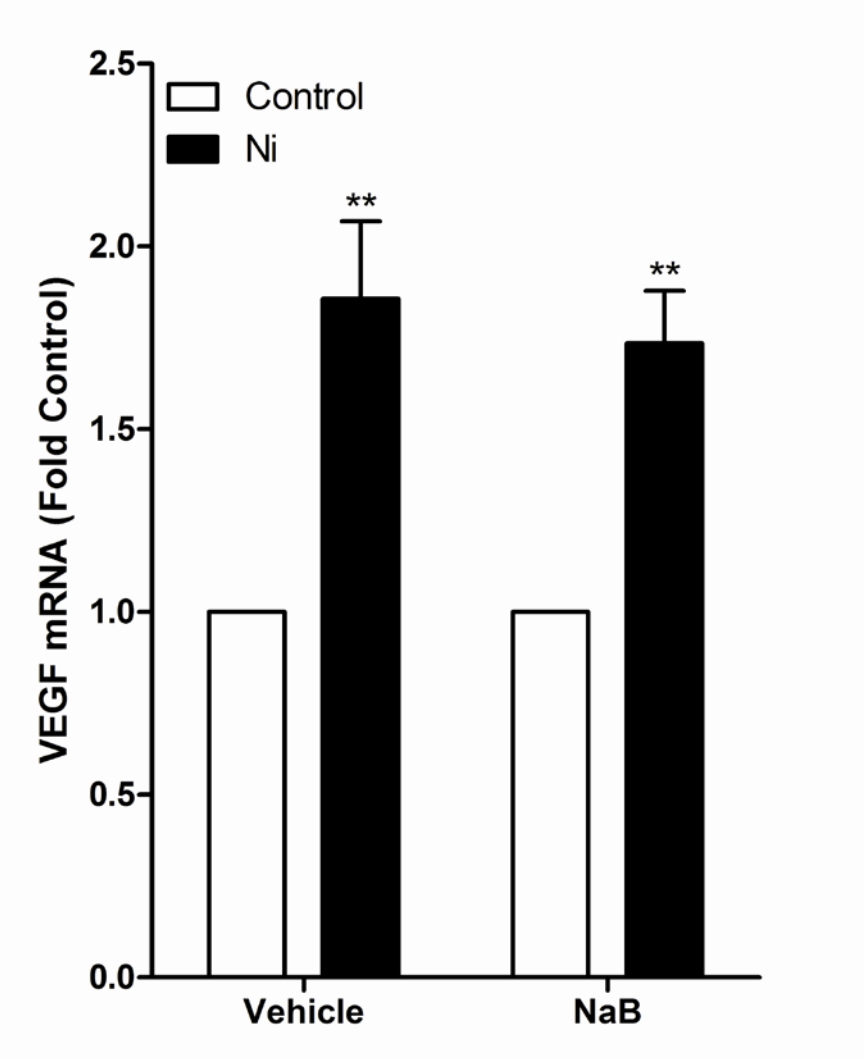

Figure 37. HDAC activity is not required for repression of Ni-induced VEGFA mRNA expression.

BEAS-2B cells were preincubated with 2 mM NaB for 16 h prior to exposure to vehicle (open bars) or 200 µM Ni (closed bars) for 24h. Total RNA was isolated and VEGFA mRNA levels were measured by real-time PCR. Data represent mean ± SEM of fold control. ** designates $p<0.01$ compared to the respective control.

BIBLIOGRAPHY

1. Sampath, D., Castro, M., Look, D. C., and Holtzman, M. J. (1999) *J. Clin. Invest* **103,** 1353-1361

2. Barnhart, J. (1997) *Regul. Toxicol. Pharmacol.* **26,** S3-S7

3. Vitale, R. J., Mussoline, G. R., and Rinehimer, K. A. (1997) *Regul. Toxicol. Pharmacol.* **26,** S80-S85

4. Agency for Toxic Substances and Disease Registry (ATSDR) (2008) Toxicological profile for Chromium (*Draft for Public Comment*). Atlanta GA: U.S. Department of Health and Human Services, Public Health Service.

5. O'Brien, T. J., Ceryak, S., and Patierno, S. R. (2003) *Mutat. Res.* **533,** 3-36

6. Salnikow, K. and Zhitkovich, A. (2008) *Chem. Res. Toxicol.* **21,** 28-44

7. Chen, G., Liu, P., Pattar, G. R., Tackett, L., Bhonagiri, P., Strawbridge, A. B., and Elmendorf, J. S. (2006) *Mol. Endocrinol.* **20,** 857-870

8. Pattar, G. R., Tackett, L., Liu, P., and Elmendorf, J. S. (2006) *Mutat. Res.* **610,** 93-100

9. Alcedo, J. A. and Wetterhahn, K. E. (1990) *Int. Rev. Exp. Pathol.* **31,** 85-108

10. De Flora, S., Serra, D., Camoirano, A., and Zanacchi, P. (1989) *Biol. Trace Elem. Res.* **21,** 179-187

11. De Flora, S. (2000) *Carcinogenesis* **21,** 533-541

12. Wetterhahn, K. E., Hamilton, J. W., Aiyar, J., Borges, K. M., and Floyd, R. (1989) *Biol Trace Elem Res* **21,** 405-411

13. Agency for Toxic Substances and Disease Registry (ATSDR) (2005) Toxicological profile for Chromium. Atlanta GA: U.S. Department fo Health and Human Services, Public Health Service.

14. Costa, M. (1997) *Crit. Rev. Toxicol.* **27,** 431-442

15. Hamilton, J. W. and Wetterhahn, K. E. (1989) *Mol. Carcinog.* **2,** 274-286

16. Wetterhahn, K. E. and Hamilton, J. W. (1989) *Sci Total Environ* **86,** 113-129

17. Hamilton, J. W., Kaltreider, R. C., Bajenova, O. V., Ihnat, M. A., McCaffrey, J., Turpie, B. W., Rowell, E. E., Oh, J., Nemeth, M. J., Pesce, C. A., and Lariviere, J. P. (1998) *Environ Health Perspect* **106 Suppl 4,** 1005-1015

18. Alcedo, J. A., Misra, M., Hamilton, J. W., and Wetterhahn, K. E. (1994) *Carcinogenesis* **15,** 1089-1092

19. O'Hara, K. A., Nemec, A. A., Alam, J., Klei, L. R., Mossman, B. T., and Barchowsky, A. (2006) *J. Cell Physiol* **209,** 113-121

20. Reynolds, M., Peterson, E., Quievryn, G., and Zhitkovich, A. (2004) *J. Biol Chem.* **279,** 30419-30424

21. Shi, X. L. and Dalal, N. S. (1990) *Arch. Biochem. Biophys.* **281,** 90-95

22. O'Hara, K. A., Klei, L. R., and Barchowsky, A. (2003) *Toxicol. Appl. Pharmacol.* **190,** 214-223

23. Majumder, S., Ghoshal, K., Summers, D., Bai, S., Datta, J., and Jacob, S. T. (2003) *J. Biol. Chem.* **278,** 26216-26226

24. Wei, Y. D., Tepperman, K., Huang, M. Y., Sartor, M. A., and Puga, A. (2004) *J. Biol. Chem.* **279,** 4110-4119

25. Kimura, T., Li, Y., Okumura, F., Itoh, N., Nakanishi, T., Sone, T., Isobe, M., and Andrews, G. K. (2008) *Biochem. J.* **415,** 477-482

26. Shumilla, J. A., Broderick, R. J., Wang, Y., and Barchowsky, A. (1999) *J Biol. Chem.* **274,** 36207-36212

27. Wakeman, T. P., Wyczechowska, D., and Xu, B. (2005) *Mol. Cell Biochem.* **279,** 69-73

28. Ceryak, S., Zingariello, C., O'Brien, T., and Patierno, S. R. (2004) *Mol. Cell Biochem.* **255,** 139-149

29. Ha, L., Ceryak, S., and Patierno, S. R. (2004) *Carcinogenesis* **25,** 2265-2274

30. Agency for Toxic Substances and Disease Registry (ATSDR) (2005) Toxicological profile for Nickel. Atlanta GA: U.S. Department of Health and Human Services, Public Health Service.

31. Snow, E. T. (1992) Metal carcinogenesis: mechanistic implications.

32. WHO Regional Office for Europe, C. D. (2009) Air Quality Guidelines- Second Edition.

33. Lippmann, M., Ito, K., Hwang, J. S., Maciejczyk, P., and Chen, L. C. (2006) *Environ. Health Perspect.* **114,** 1662-1669

34. Salnikow, K., Li, X., and Lippmann, M. (2004) *Toxicol. Appl. Pharmacol.* **196,** 258-265

35. Stojanovic, D., Nikic, D., and Lazarevic, K. (2004) *Cent. Eur. J. Public Health* **12,** 187-189

36. Gavett, S. H., Madison, S. L., Dreher, K. L., Winsett, D. W., McGee, J. K., and Costa, D. L. (1997) *Environ. Res.* **72,** 162-172

37. Antonini, J. M., Taylor, M. D., Zimmer, A. T., and Roberts, J. R. (2004) *J. Toxicol Environ. Health A* **67,** 233-249

38. Luo, J. C., Hsu, K. H., and Shen, W. S. (2006) *Am. J. Ind. Med.* **49,** 407-416

39. Dreher, K. L., Jaskot, R. H., Lehmann, J. R., Richards, J. H., McGee, J. K., Ghio, A. J., and Costa, D. L. (1997) *Journal of Toxicology & Environmental Health* **50,** 285-305

40. Salnikow, K., Li, X., and Lippmann, M. (2004) *Toxicol Appl. Pharmacol.* **196,** 258-265

41. Gao, F., Barchowsky, A., Nemec, A. A., and Fabisiak, J. P. (2004) *Toxicol Sci* **81,** 467-479

42. Bright, P., Burge, P. S., O'Hickey, S. P., Gannon, P. F. G., Robertson, A. S., and Boran, A. (1997) *Thorax* **52,** 28-32

43. Leikauf, G. D. (2002) *Environ. Health Perspect.* **110 Suppl 4,** 505-526

44. Wesselkamper, S. C., McDowell, S. A., Medvedovic, M., Dalton, T. P., Deshmukh, H. S., Sartor, M. A., Case, L. M., Henning, L. N., Borchers, M. T., Tomlinson, C. R., Prows, D. R., and Leikauf, G. D. (2006) *Am. J. Respir. Cell Mol. Biol.* **34,** 73-82

45. Leikauf, G. D., McDowell, S. A., Wesselkamper, S. C., Hardie, W. D., Leikauf, J. E., Korfhagen, T. R., and Prows, D. R. (2002) *Chest* **121,** 70S-75S

46. Novey, H. S., Habib, M., and Wells, I. D. (1983) *J. Allergy Clin. Immunol.* **72,** 407-412

47. Takemoto, K., Kawai, H., Kuwahara, T., Nishina, M., and Adachi, S. (1991) *Int. Arch. Occup. Environ. Health* **62,** 579-586

48. Kuo, C. Y., Wong, R. H., Lin, J. Y., Lai, J. C., and Lee, H. (2006) *J. Toxicol. Environ. Health A* **69,** 1337-1344

49. Hisatomi, K., Ishii, H., Hashiguchi, K., Seki, M., Ide, M., Sugiyama, K., Ishimoto, H., Nakayama, S., Mukae, H., and Kohno, S. (2006) *Respirology.* **11,** 814-817

50. Ortmann, R. A., Cheng, T., Visconti, R., Frucht, D. M., and O'Shea, J. J. (2000) *Arthritis Res.* **2,** 16-32

51. Levy, D. E. and Darnell, J. E., Jr. (2002) *Nat. Rev. Mol Cell Biol* **3,** 651-662

52. Darnell, J. E., Jr. (1997) *Science* **277,** 1630-1635

53. Ihle, J. N. and Kerr, I. M. (1995) *Trends Genet.* **11,** 69-74

54. Kypta, R. M., Goldberg, Y., Ulug, E. T., and Courtneidge, S. A. (1990) *Cell* **62,** 481-492

55. O'Hara, K. A., Vaghjiani, R. J., Nemec, A. A., Klei, L. R., and Barchowsky, A. (2007) *Biochem. J.* **402,** 261-269

56. Chaturvedi, P., Reddy, M. V., and Reddy, E. P. (1998) *Oncogene* **16,** 1749-1758

57. Darnell, J. E., Jr., Kerr, I. M., and Stark, G. R. (1994) *Science* **264,** 1415-1421

58. Shuai, K. (2000) *Oncogene* **19,** 2638-2644

59. Platanias, L. C. (2005) *Nat. Rev. Immunol.* **5,** 375-386

60. Nusinzon, I. and Horvath, C. M. (2003) *Proc. Natl. Acad. Sci. U. S. A* **100,** 14742-14747

61. Sakamoto, S., Potla, R., and Larner, A. C. (2004) *J. Biol Chem.* **279,** 40362-40367

62. Zhao, X., Nozell, S., Ma, Z., and Benveniste, E. N. (2007) *FEBS J.* **274,** 6456-6468

63. Laver, T., Nozell, S. E., and Benveniste, E. N. (2008) *J. Interferon Cytokine Res.* **28,** 13-23

64. Stephanou, A. (2004) *J. Cell Mol. Med.* **8,** 519-525

65. Dudley, A. C., Thomas, D., Best, J., and Jenkins, A. (2004) *Cell Commun. Signal.* **2,** 8

66. Laskin, D. L., Fakhrzadeh, L., Heck, D. E., Gerecke, D., and Laskin, J. D. (2002) *Mol. Cell Biochem.* **234-235,** 91-98

67. Tanabe, Y., Nishibori, T., Su, L., Arduini, R. M., Baker, D. P., and David, M. (2005) *J. Immunol.* **174,** 609-613

68. Gimeno, R., Lee, C. K., Schindler, C., and Levy, D. E. (2005) *Mol. Cell Biol.* **25,** 5456-5465

69. Townsend, P. A., Scarabelli, T. M., Davidson, S. M., Knight, R. A., Latchman, D. S., and Stephanou, A. (2004) *J. Biol. Chem.* **279,** 5811-5820

70. Severgnini, M., Takahashi, S., Rozo, L. M., Homer, R. J., Kuhn, C., Jhung, J. W., Perides, G., Steer, M., Hassoun, P. M., Fanburg, B. L., Cochran, B. H., and Simon, A. R. (2004) *Am. J. Physiol Lung Cell Mol. Physiol* **286,** L1282-L1292

71. Thomas, S. M. and Brugge, J. S. (1997) *Annu. Rev. Cell Dev. Biol.* **13,** 513-609

72. Engen, J. R., Wales, T. E., Hochrein, J. M., Meyn, M. A., III, Banu, O. S., Bahar, I., and Smithgall, T. E. (2008) *Cell Mol. Life Sci.* **65,** 3058-3073

73. Kanda, S., Miyata, Y., Kanetake, H., and Smithgall, T. E. (2007) *Int. J Mol. Med.* **20,** 113-121

74. Ahmadibeni, Y., Hanley, M., White, M., Ayrapetov, M., Lin, X., Sun, G., and Parang, K. (2007) *Chembiochem.* **8,** 1592-1605

75. Klaassen, C. D., Liu, J., and Choudhuri, S. (1999) *Annu. Rev. Pharmacol. Toxicol.* **39,** 267-294

76. Coyle, P., Philcox, J. C., Carey, L. C., and Rofe, A. M. (2002) *Cell Mol. Life Sci.* **59,** 627-647

77. Masters, B. A., Quaife, C. J., Erickson, J. C., Kelly, E. J., Froelick, G. J., Zambrowicz, B. P., Brinster, R. L., and Palmiter, R. D. (1994) *J. Neurosci.* **14,** 5844-5857

78. Quaife, C. J., Findley, S. D., Erickson, J. C., Froelick, G. J., Kelly, E. J., Zambrowicz, B. P., and Palmiter, R. D. (1994) *Biochemistry* **33,** 7250-7259

79. Bauman, J. W., Liu, J., and Klaassen, C. D. (1993) *Fundam. Appl. Toxicol.* **21,** 15-22

80. Palmiter, R. D. (1994) *Proc. Natl. Acad. Sci. U. S. A* **91,** 1219-1223

81. Laity, J. H. and Andrews, G. K. (2007) *Arch. Biochem. Biophys.* **463,** 201-210

82. McDowell, S. A., Gammon, K., Bachurski, C. J., Wiest, J. S., Leikauf, J. E., Prows, D. R., and Leikauf, G. D. (2000) *Am. J. Respir. Cell Mol. Biol.* **23,** 466-474

83. Takano, H., Inoue, K., Yanagisawa, R., Sato, M., Shimada, A., Morita, T., Sawada, M., Nakamura, K., Sanbongi, C., and Yoshikawa, T. (2004) *Thorax* **59,** 1057-1062

84. Sato, M. and Bremner, I. (1993) *Free Radic. Biol. Med.* **14,** 325-337

85. Yanagisawa, R., Takano, H., Inoue, K., Ichinose, T., Yoshida, S., Sadakane, K., Takeda, K., Yoshino, S., Yamaki, K., Kumagai, Y., and Yoshikawa, T. (2004) *Exp. Biol. Med. (Maywood.)* **229,** 1081-1087

86. Perkowski, S., Sun, J., Singhal, S., Santiago, J., Leikauf, G. D., and Albelda, S. M. (2003) *Am. J. Respir. Cell Mol. Biol.* **28,** 682-696

87. Inoue, K., Takano, H., Yanagisawa, R., Sakurai, M., Ichinose, T., Sadakane, K., Hiyoshi, K., Sato, M., Shimada, A., Inoue, M., and Yoshikawa, T. (2005) *Exp. Biol. Med. (Maywood.)* **230,** 75-81

88. Gunes, C., Heuchel, R., Georgiev, O., Muller, K. H., Lichtlen, P., Bluthmann, H., Marino, S., Aguzzi, A., and Schaffner, W. (1998) *EMBO J.* **17,** 2846-2854

89. Smirnova, I. V., Bittel, D. C., Ravindra, R., Jiang, H., and Andrews, G. K. (2000) *J. Biol. Chem.* **275,** 9377-9384

90. Heuchel, R., Radtke, F., Georgiev, O., Stark, G., Aguet, M., and Schaffner, W. (1994) *EMBO J.* **13,** 2870-2875

91. Bittel, D., Dalton, T., Samson, S. L., Gedamu, L., and Andrews, G. K. (1998) *J. Biol. Chem.* **273,** 7127-7133

92. LaRochelle, O., Gagne, V., Charron, J., Soh, J. W., and Seguin, C. (2001) *J. Biol. Chem.* **276,** 41879-41888

93. Murphy, B. J., Sato, B. G., Dalton, T. P., and Laderoute, K. R. (2005) *Biochem. Biophys. Res. Commun.* **337,** 860-867

94. Murphy, B. J., Kimura, T., Sato, B. G., Shi, Y., and Andrews, G. K. (2008) *Mol. Cancer Res.* **6,** 483-490

95. Li, Y., Kimura, T., Huyck, R. W., Laity, J. H., and Andrews, G. K. (2008) *Mol. Cell Biol.* **28,** 4275-4284

96. Ogra, Y., Suzuki, K., Gong, P., Otsuka, F., and Koizumi, S. (2001) *J. Biol. Chem.* **276,** 16534-16539

97. Olsson, A. K., Dimberg, A., Kreuger, J., and Claesson-Welsh, L. (2006) *Nat. Rev. Mol. Cell Biol.* **7,** 359-371

98. Robinson, C. J. and Stringer, S. E. (2001) *J. Cell Sci* **114,** 853-865

99. Acarregui, M. J., Penisten, S. T., Goss, K. L., Ramirez, K., and Snyder, J. M. (1999) *Am. J. Respir. Cell Mol. Biol.* **20,** 14-23

100. Zeng, X., Wert, S. E., Federici, R., Peters, K. G., and Whitsett, J. A. (1998) *Dev. Dyn.* **211,** 215-227

101. Christou, H., Yoshida, A., Arthur, V., Morita, T., and Kourembanas, S. (1998) *Am. J. Respir. Cell Mol. Biol.* **18,** 768-776

102. Brown, K. R., England, K. M., Goss, K. L., Snyder, J. M., and Acarregui, M. J. (2001) *Am. J. Physiol Lung Cell Mol. Physiol* **281,** L1001-L1010

103. Tang, K., Rossiter, H. B., Wagner, P. D., and Breen, E. C. (2004) *J. Appl. Physiol* **97,** 1559-1566

104. McColley, S. A., Stellmach, V., Boas, S. R., Jain, M., and Crawford, S. E. (2000) *Am. J Respir. Crit Care Med.* **161,** 1877-1880

105. Kanazawa, H., Asai, K., Hirata, K., and Yoshikawa, J. (2003) *Am J Med* **114,** 354-358

106. Mura, M., dos Santos, C. C., Stewart, D., and Liu, M. (2004) *J. Appl. Physiol* **97,** 1605-1617

107. Lassus, P., Ristimaki, A., Ylikorkala, O., Viinikka, L., and Andersson, S. (1999) *Am. J. Respir. Crit Care Med.* **159,** 1429-1433

108. Fehrenbach, A., Pufe, T., Wittwer, T., Nagib, R., Dreyer, N., Pech, T., Petersen, W., Fehrenbach, H., Wahlers, T., and Richter, J. (2003) *J. Heart Lung Transplant.* **22,** 967-978

109. Partovian, C., Adnot, S., Raffestin, B., Louzier, V., Levame, M., Mavier, I. M., Lemarchand, P., and Eddahibi, S. (2000) *Am. J. Respir. Cell Mol. Biol.* **23,** 762-771

110. Kunig, A. M., Balasubramaniam, V., Markham, N. E., Seedorf, G., Gien, J., and Abman, S. H. (2006) *Am. J. Physiol Lung Cell Mol. Physiol* **291,** L1068-L1078

111. Hanaoka, M., Droma, Y., Naramoto, A., Honda, T., Kobayashi, T., and Kubo, K. (2003) *J. Appl. Physiol* **94,** 1836-1840

112. Boussat, S., Eddahibi, S., Coste, A., Fataccioli, V., Gouge, M., Housset, B., Adnot, S., and Maitre, B. (2000) *Am. J. Physiol Lung Cell Mol. Physiol* **279,** L371-L378

113. Roberts, J. R., Perkins, G. D., Fujisawa, T., Pettigrew, K. A., Gao, F., Ahmed, A., and Thickett, D. R. (2007) *Crit Care Med.* **35,** 2164-2170

114. Thickett, D. R., Armstrong, L., and Millar, A. B. (2002) *Am. J. Respir. Crit Care Med.* **166,** 1332-1337

115. Frank, S., Hubner, G., Breier, G., Longaker, M. T., Greenhalgh, D. G., and Werner, S. (1995) *J. Biol. Chem.* **270,** 12607-12613

116. Semenza, G. L. (2000) *Biochem. Pharmacol.* **59,** 47-53

117. Semenza, G. L. (1999) *Annu. Rev. Cell Dev. Biol.* **15,** 551-578

118. Ouyang, W., Li, J., Shi, X., Costa, M., and Huang, C. (2005) *Mol. Cell Biochem.* **279,** 35-43

119. Andrew, A. S., Klei, L. R., and Barchowsky, A. (2001) *Am J Physiol* **281,** L607-L615

120. Duyndam, M. C., Hulscher, S. T., van der, W. E., Pinedo, H. M., and Boven, E. (2003) *J Biol Chem.* **278,** 6885-6895

121. Gao, N., Jiang, B. H., Leonard, S. S., Corum, L., Zhang, Z., Roberts, J. R., Antonini, J., Zheng, J. Z., Flynn, D. C., Castranova, V., and Shi, X. (2002) *J Biol Chem.* **277,** 45041-45048

122. Davidson, T. L., Chen, H., Di Toro, D. M., D'Angelo, G., and Costa, M. (2006) *Mol. Carcinog.* **45,** 479-489

123. Eliceiri, B. P., Paul, R., Schwartzberg, P. L., Hood, J. D., Leng, J., and Cheresh, D. A. (1999) *Mol. Cell* **4,** 915-924

124. Gray, M. J., Zhang, J., Ellis, L. M., Semenza, G. L., Evans, D. B., Watowich, S. S., and Gallick, G. E. (2005) *Oncogene* **24,** 3110-3120

125. Salnikow, K., Kluz, T., Costa, M., Piquemal, D., Demidenko, Z. N., Xie, K., and Blagosklonny, M. V. (2002) *Mol. Cell Biol.* **22,** 1734-1741

126. Richard, D. E., Berra, E., Gothie, E., Roux, D., and Pouyssegur, J. (1999) *J Biol. Chem.* **274,** 32631-32637

127. Arany, Z., Foo, S. Y., Ma, Y., Ruas, J. L., Bommi-Reddy, A., Girnun, G., Cooper, M., Laznik, D., Chinsomboon, J., Rangwala, S. M., Baek, K. H., Rosenzweig, A., and Spiegelman, B. M. (2008) **451,** 1008-1012

128. Mizukami, Y., Li, J., Zhang, X., Zimmer, M. A., Iliopoulos, O., and Chung, D. C. (2004) *Cancer Res.* **64,** 1765-1772

129. Pages, G. and Pouyssegur, J. (2005) *Cardiovasc. Res.* **65,** 564-573

130. Shi, Q., Le, X., Abbruzzese, J. L., Peng, Z., Qian, C. N., Tang, H., Xiong, Q., Wang, B., Li, X. C., and Xie, K. (2001) *Cancer Res.* **61,** 4143-4154

131. Chu, S. and Ferro, T. J. (2005) *Gene* **348,** 1-11

132. Antonini, J. M. and Roberts, J. R. (2007) *J. Immunotoxicol.* **4,** 117-127

133. Antonini, J. M., Stone, S., Roberts, J. R., Chen, B., Schwegler-Berry, D., Afshari, A. A., and Frazer, D. G. (2007) *Toxicol. Appl. Pharmacol.* **223,** 234-245

134. Antonini, J. M., Roberts, J. R., Stone, S., Chen, B. T., Schwegler-Berry, D., and Frazer, D. G. (2009) *Inhal. Toxicol.* **21,** 182-192

135. Gimeno, R., Lee, C. K., Schindler, C., and Levy, D. E. (2005) *Mol. Cell Biol* **25,** 5456-5465

136. Tanabe, Y., Nishibori, T., Su, L., Arduini, R. M., Baker, D. P., and David, M. (2005) *J. Immunol.* **174,** 609-613

137. Stephanou, A. and Latchman, D. S. (2005) *Growth Factors* **23,** 177-182

138. Ivanov, S. V., Salnikow, K., Ivanova, A. V., Bai, L., and Lerman, M. I. (2006) *Oncogene*

139. Stitt, M. S., Wasserloos, K. J., Tang, X., Liu, X., Pitt, B. R., and St Croix, C. M. (2006) *Vascul. Pharmacol.* **44,** 149-155

140. Chen, X., Zhang, B., Harmon, P. M., Schaffner, W., Peterson, D. O., and Giedroc, D. P. (2004) *J. Biol. Chem.* **279,** 4515-4522

141. Salnikow, K., An, W. G., Melillo, G., Blagosklonny, M. V., and Costa, M. (1999) *Carcinogenesis* **20,** 1819-1823

142. Yu, C. L., Jove, R., and Burakoff, S. J. (1997) *J Immunol* **159,** 5206-5210

143. Xi, S., Zhang, Q., Dyer, K. F., Lerner, E. C., Smithgall, T. E., Gooding, W. E., Kamens, J., and Grandis, J. R. (2003) *J. Biol. Chem.* **278,** 31574-31583

144. Deb, D. K., Sassano, A., Lekmine, F., Majchrzak, B., Verma, A., Kambhampati, S., Uddin, S., Rahman, A., Fish, E. N., and Platanias, L. C. (2003) *J Immunol.* **171,** 267-273

145. Klampfer, L., Huang, J., Swaby, L. A., and Augenlicht, L. (2004) *J. Biol. Chem.* **279,** 30358-30368

146. Battle, T. E., Lynch, R. A., and Frank, D. A. (2006) *Cancer Res.* **66,** 3649-3657

147. Plattner, R., Kadlec, L., DeMali, K. A., Kazlauskas, A., and Pendergast, A. M. (1999) *Genes Dev.* **13,** 2400-2411

148. Carlesso, N., Frank, D. A., and Griffin, J. D. (1996) *J. Exp. Med.* **183,** 811-820

149. Danial, N. N. and Rothman, P. (2000) *Oncogene* **19,** 2523-2531

150. Rice, T. M., Clarke, R. W., Godleski, J. J., Al Mutairi, E., Jiang, N. F., Hauser, R., and Paulauskis, J. D. (2001) *Toxicol. Appl. Pharmacol.* **177,** 46-53

151. Namiki, A., Brogi, E., Kearney, M., Kim, E. A., Wu, T., Couffinhal, T., Varticovski, L., and Isner, J. M. (1995) *J. Biol. Chem.* **270,** 31189-31195

152. Huang, S., Bucana, C. D., Van, A. M., and Fidler, I. J. (2002) *Oncogene* **21,** 2504-2512

153. Duyndam, M. C., Hulscher, T. M., Fontijn, D., Pinedo, H. M., and Boven, E. (2001) *J. Biol. Chem.* **276,** 48066-48076

154. Reisinger, K., Kaufmann, R., and Gille, J. (2003) *J. Cell Sci.* **116,** 225-238

155. Curry, J. M., Eubank, T. D., Roberts, R. D., Wang, Y., Pore, N., Maity, A., and Marsh, C. B. (2008) *PLoS. ONE.* **3,** e3405

156. Barchowsky, A., Soucy, N. V., O'Hara, K. A., Hwa, J., Noreault, T. L., and Andrew, A. S. (2002) *J Biol. Chem.* **277,** 24225-24231

157. Ke, Q., Li, Q., Ellen, T. P., Sun, H., and Costa, M. (2008) *Carcinogenesis* **29,** 1276-1281

158. Dubrovskaya, V. A. and Wetterhahn, K. E. (1998) *Carcinogenesis* **19,** 1401-1407

159. Larsson-Stymne, B. and Widstrom, L. (1985) *Contact Dermatitis* **13,** 289-293

160. Grimsrud, T. K. and Peto, J. (2006) *Occup. Environ. Med.* **63,** 365-366

161. Anttila, A., Pukkala, E., Aitio, A., Rantanen, T., and Karjalainen, S. (1998) *Int. Arch. Occup. Environ. Health* **71,** 245-250

162. St Croix, C. M., Leelavaninchkul, K., Watkins, S. C., Kagan, V. E., and Pitt, B. R. (2005) *Proc. Am. Thorac. Soc.* **2,** 236-242

163. Bittel, D., Dalton, T., Samson, S. L., Gedamu, L., and Andrews, G. K. (1998) *J. Biol. Chem.* **273,** 7127-7133

164. Courtade, M., Carrera, G., Paternain, J. L., Martel, S., Carre, P. C., Folch, J., and Pipy, B. (1998) *Chest* **113,** 371-378

165. Mango, G. W., Johnston, C. J., Reynolds, S. D., Finkelstein, J. N., Plopper, C. G., and Stripp, B. R. (1998) *Am. J. Physiol* **275,** L348-L356

166. Sarafian, T., Habib, N., Mao, J. T., Tsu, I. H., Yamamoto, M. L., Hsu, E., Tashkin, D. P., and Roth, M. D. (2005) *Toxicol. Lett.* **158,** 95-107

167. Shattuck, K. E., Rassin, D. K., and Grinnell, C. D. (1998) *JPEN J. Parenter. Enteral Nutr.* **22,** 228-233

168. Maret, W. (1994) *Proc. Natl. Acad. Sci. U. S. A* **91,** 237-241

169. Jiang, L. J., Maret, W., and Vallee, B. L. (1998) *Proc. Natl. Acad. Sci. U. S. A* **95,** 3483-3488

170. Misra, M., Rodriguez, R. E., and Kasprzak, K. S. (1990) *Toxicology* **64,** 1-17

171. Kaur, S., Zilmer, M., Eisen, M., Rehema, A., Kullisaar, T., Vihalemm, T., and Zilmer, K. (2004) *Arch. Dermatol. Res.* **295,** 517-520

172. Kleineke, J. W. and Brand, I. A. (1997) *J. Pharmacol. Toxicol. Methods* **38,** 181-187

173. Struhl, K. (1998) *Genes Dev.* **12,** 599-606

174. Veillette, A., Dumont, S., and Fournel, M. (1993) *J. Biol. Chem.* **268,** 17547-17553

175. Sun, G. and Budde, R. J. (1999) *Biochemistry* **38,** 5659-5665

176. Grace, M. R., Walsh, C. T., and Cole, P. A. (1997) *Biochemistry* **36,** 1874-1881

177. Levav-Cohen, Y., Goldberg, Z., Zuckerman, V., Grossman, T., Haupt, S., and Haupt, Y. (2005) *Biochem. Biophys. Res. Commun.* **331,** 737-749

178. Roskoski, R., Jr. (2004) *Biochem. Biophys. Res. Commun.* **324,** 1155-1164

179. Jaakkola, P., Mole, D. R., Tian, Y. M., Wilson, M. I., Gielbert, J., Gaskell, S. J., Kriegsheim, A., Hebestreit, H. F., Mukherji, M., Schofield, C. J., Maxwell, P. H., Pugh, C. W., and Ratcliffe, P. J. (2001) *Science* **292,** 468-472

180. Hewitson, K. S., McNeill, L. A., Riordan, M. V., Tian, Y. M., Bullock, A. N., Welford, R. W., Elkins, J. M., Oldham, N. J., Bhattacharya, S., Gleadle, J. M., Ratcliffe, P. J., Pugh, C. W., and Schofield, C. J. (2002) *J. Biol. Chem.* **277,** 26351-26355